Understanding vented gas explosions

Risto Lautkaski

VTT Energy

VTT

ABSTRACT

The report is an introduction to vented gas explosions for nonspecialists, particularly designers of plants for flammable gases and liquids. The phenomena leading to pressure generation in vented gas explosions in empty and congested rooms are reviewed. The four peak model of vented gas explosions is presented with simple methods to predict the values of the individual peaks. Experimental data on the external explosion of dust and gas explosions is discussed. The empirical equation by Wirkner-Bott et al. relating the internal and external peak pressures in vented dust explosions is shown to be valid for gas explosion tests in 30 m^3 and 550 m^3 chambers. However, the difficulty of predicting the internal peak pressure in large chambers remains. Methods of explosion relief panel design and principles of vent and equipment layout to reduce explosion overpressures are reviewed.

CONTENTS

LIST OF SYMBOLS

$\underline{A}$ projected area of on object normal to flow direction [m^2]

A   scaled vent size of the Bradley Mitcheson method

A_f actual flame area [m^2]

A_n area of an idealized (laminar) flame [m^2]

A_s area of cross section of a room in the plane of vent [m^2]

A_v vent size or total area of vents [m^2]

C_d discharge coefficient of a vent

C_D drag coefficient of an object

C_L lower flammability limit [%]

C_R parameter of Runes' method [bar$^{1/2}$]

C_s theoretical steady state concentration [%]

$C(x,y)$ average concentration at a point x,y [%]

C_0 initial concentration of gas [%]

c_0 velocity of sound in the unburned mixture [m/s]

D   (hydraulic) diameter of a duct [m]

D_m diffusion coefficient of a vapour in air [m^2/s]

D_r hydraulic diameter of a room [m]

d_0 diameter of a orifice [m]

E   expansion factor

F_D drag force [N]

f(t)   overpressure loading [N]

f_{max} static loading [N]

H_r height of a room perpendicular to air flow [m]

H_{st} heat of reaction per unit volume of stoichiometric mixture [MJ/m^3]

I   moment of inertia [kgm^2]

K   vent coefficient, $K = V^{2/3}/A_v$

K_{av} effective overall vent coefficient

K_i vent coefficient of an explosion vent panel/door

k   stiffness constant of a spring [N/m]

K_g constant of the cube root law for a gas [bar·m/s]

K_{St} constant of the cube root law for a dust [bar·m/s]

K_1 constant [bar]

k_1 experimental constant, $k_1 = 5$

k_2 experimental constant, $k_2 = 57.3$

L   length/characteristic dimension [m]

l   distance between vent and ignition source [m]

L_f maximum flame length [m]

L_{max} the longest dimension of a room [m]

L_{min} the shortest dimension of a room [m]

L_1 the largest dimension of a room [m]

L_2 the second largest dimension of a room [m]

N_i number of moles in the unburned mixture [mol]

N_f number of moles in the combustion products [mol]

P   internal pressure [kPa]

P_a atmospheric pressure, $P_a = 101.3$ kPa

5

P_f	final pressure in a confined explosion [kPa]
P_{em}	maximum pressure of the external explosion [kPa]
P_{ext}	peak pressure of the external explosion [kPa]
P_i	initial pressure in a vessel [kPa]
P_l	maximum explosion pressure for a flammable layer [kPa]
P_p	partial pressure of a vapour in air [kPa]
P_{red}	maximum internal overpressure of a vented explosion [kPa]
P_s	saturated vapour pressure of a liquid [kPa]
P_v	opening pressure of a vent [kPa]
P_1	first peak of the internal pressure [kPa]
P_2	second peak of the internal pressure [kPa]
P_3	third peak of the internal pressure [kPa]
P_2	fourth peak of the internal pressure [kPa]
ΔP	pressure difference across a vent [kPa]
ΔP_s	peak pressure generated in a congested volume [bar]
Q_a	air flow rate through a room [m^3/h]
Q_g	gas release rate [m^3/h]
Q_v	evaporation rate [m^3/s]
r	distance from the blast centre [m]
R_b	distance of the blast centre from a vent [m]
Re	Reynolds number
Re_p	Reynolds number of a pool
Re_r	Reynolds number of a room
R_f	final radius of the equivalent hemisphere [m]
r_f	radius of flame front [m]
$R(y)$	resistance function of a spring [N]
R_0	radius of the equivalent hemisphere [m]
S_f	flame speed [m/s]
$\underline{S}_0$	laminar burning velocity [m/s]
S_0	scaled flame speed of the Bradley Mitcheson method
t	time [s]
t_d	duration of loading [s]
T_f	adiabatic flame temperature [K]
T_i	initial temperature [K]
T_n	natural period of vibration [s]
u	flow velocity [m/s]
V	volume [m^3]
V_i	initial volume [m^3]
V_f	final volume [m^3]
V_l	volume of flammable layer [m^3]
V^*	volume into which gas is mixed [m^3]
y	displacement of the centre of mass [m]
y_{fail}	failure point [m]
y_{max}	maximum deflection [m]
y_{yield}	yield point [m]
W	width of pool perpendicular to air flow [m]
W_r	width of room perpendicular to air flow [m]
w	mass per unit area of vent cover [kg/m^2]

μ	ductility ratio
ν	kinematic viscosity of fluid [m^2/s]
ρ	density of the gases flowing to vent [kg/m^3]
ρ_a	density of air [kg/m^3]
ρ_0	initial density of gas [kg/m^3]

INDEX OF TERMS WITH FINNISH EQUIVALENTS

1 INTRODUCTION

This report is an introduction to vented gas explosions for nonspecialists, particularly designers of plants handling flammable gases and liquids. The starting point of the presentation is provided by the well-known textbook "The investigation and control of gas explosions in buildings and heating plant" by Harris (1983). Although this book is an excellent presentation of the basic explosion phenomena it has to be supplemented with more recent findings.

An extensive research on gas explosions on offshore platforms started around 1980 and has contributed significantly to the understanding of the physical processes involved. In 1987, it was shown that the internal pressure of a vented gas explosion as a function of time can be described by four distinct pressure peaks which can (but do not have to) occur (the four peak model). Each peak is produced by different physical processes at successive stages during a vented explosion.

Methods used to predict the pressure peak(s) of vented gas explosions (venting guidelines) are based on tests in room-sized or smaller chambers. It was not at all straightforward to apply these methods to rooms of industrial scale.

British Gas (1990) performed a critical evaluation of venting guidelines using data of the explosion tests performed in the 1980's and interpreting the earlier explosion tests in the light of the four peak model. The conclusion was that some venting guidelines gave satisfactory predictions for rooms having volumes up to 300 m³, while others predicted too small or too large pressures, or were based on incorrect assumptions.

Simultaneous research on the mechanisms of pressure generation in vapour cloud explosions revealed that high peak pressures were caused by acceleration of the flame front by repeated obstacles. Repeated obstacles (pipes, vessels etc.) occur also in indoor process installation and high explosion pressures can be expected because of this effect. In spite of the complexity of the coupled physical and chemical phenomena leading to flame acceleration, some simple design rules have emerged by which it is often possible to reduce explosion damage.

In 1987, it was shown that the strongest distant blast effects of a vented explosion were caused by the external explosion. The external explosion happens in the jet of unburned mixture pushed out of the room through the explosion relief vent and is ignited by flames emerging from the vent. The external and internal overpressures interact in a complicated way. However, an empirical equation relating the internal and external peak pressures has been derived from dust explosion tests.

2 BASIC CONCEPTS

The basic concepts related to gas explosions are reviewed.

Explosion can be defined eg. as a sudden release of energy leading to a rapid increase of pressure. The energy can be either physical or chemical.

Physical explosion is an explosion caused by a release of physical energy: eg. nuclear explosion, bursting of a pressure vessel, steam explosion caused eg. by the contact of molten metal and water.

Chemical explosion is an explosion caused by a release of chemical energy: eg. detonation of a high explosive, runaway reaction, combustion of gas, vapour, mist or dust in air or other oxidizers.

Simultaneous explosion is an explosion in which the energy is released (practically) simultaneously in the material: eg. nuclear explosion, runaway reaction.

Propagating explosion is an explosion in which the energy is released in a thin front propagating through the material: detonation of a high explosive, combustion of gas, vapour, mist or dust in air or other oxidizers.

Lower flammability limit is the lowest concentration of a gas (vapour, mist or dust) in air (or other oxidizer) that can be ignited (by a spark in a test apparatus).

Upper flammability limit is the highest concentration of gas (vapour or mist) in air (or other oxidizer) that can be ignited (by a spark in a test apparatus).

Flammable mixture is a mixture of a fuel and air (or other oxidizer) whose concentration is in the **flammability range** ie. between the lower flammability limit and the upper flammability limit.

Deflagration is the combustion of gas, vapour, mist or dust in air or other oxidizer, the reaction zone propagating at a speed that is less than the sound velocity in the unreacted medium. Depending on the conditions, the speed may increase and again decrease during the process.

Detonation is an explosion at which the reaction zone propagates at a constant speed that is greater than the sound velocity in the unreacted medium and is typical of the exploding system.

Confined explosion is an explosion in a pipe or vessel capable of withstanding the pressure created.

Vented explosion is an explosion in which the overpressure generated in a vessel or room is relieved through vents in the walls. The vents may be permanent, made by the opening explosion relief panels or doors, or caused by walls breaking from the

overpressure.

Flash fire is the deflagration of an unconfined gas or vapour cloud in which only a negligible overpressure is generated.

Laminar flow is a flow of fluid in layers with parallel streamlines and no mixing (Fig. 2.1).

Turbulent flow is characterized by an irregular random fluctuation imposed on the mean (time-averaged) flow velocity. The fluctuation is caused by eddies in the flow. The eddies result in effective mixing of the fluid (Fig. 2.1).

Laminar   Turbulent

Figure 2.1. Laminar and turbulent flow (Bjerketvedt et al. 1993).

The **Reynolds number** is a dimensionless parameter characterizing whether the flow is laminar or turbulent. The Reynolds number Re is defined by

$$Re = \frac{uL}{\nu} \tag{1}$$

where
u   is the flow velocity [m/s]
L   is characteristic dimension of the geometry [m]
ν is the kinematic viscosity of the fluid [m²/s].

Figure 2.2 shows the flow field around a cylinder in a cross flow for different values of Re. The characteristic dimension L for this geometry is the diameter of the cylinder. For a low flow velocity u, Re is small and the flow is laminar. For higher values of u and, consequently, Re, vortices develop in the wake of the cylinder and the flow will be turbulent.

13

Re ≈ 1   Re < 200 000   Re > 400 000
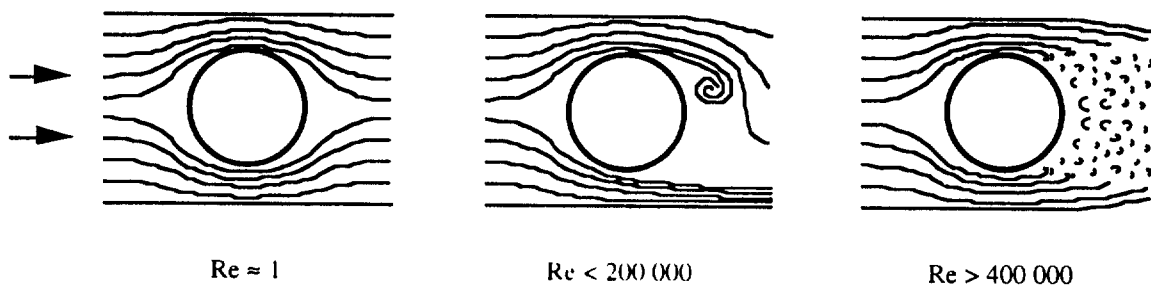
Figure 2.2. Cylinder in a crossflow for different values of Re (Bjerketvedt et al. 1993).

Vapour cloud explosion is the deflagration of a partially confined gas or vapour cloud usually involving turbulence generating obstacles. The speed of the reaction zone or **flame front** is accelerated and a blast wave is generated in the atmosphere.

Jet ignition is the ignition of a gas or vapour cloud by a jet of hot combustion products emerging from a vented explosion. A vapour cloud explosion may follow even if there are no turbulence generating obstacles in the cloud.

External explosion is the combustion of the jet of unreacted mixture formed outside an explosion vent in a vented explosion. The jet is ignited by the flame front emerging from the vent.

Blast wave is the air wave set in motion by an explosion. A blast wave is characterized by the value and time dependence of pressure. Blast waves can be divided eg. in shock and pressure waves.

Shock wave is a blast wave whose overpressure reaches its maximum value instantly and decays gradually. The positive (overpressure) phase is followed by a negative (underpressure) phase (Fig. 2.3a). A strong shock wave propagates in the atmosphere at supersonic speed. A shock wave is created eg. by a bursting pressure vessel or a detonation.

Pressure wave is a blast wave whose overpressure both reaches its maximum value and decays gradually. The positive (overpressure) phase is followed by a negative (underpressure) phase (Fig. 2.3b). A pressure wave propagates in the atmosphere at sound velocity. A pressure wave is created by a deflagration eg. vented explosion or vapour cloud explosion.

Explosion damage is caused by the primary and secondary effects of explosion. The **primary effects** are overpressure in enclosed spaces, blast wave and flame. If the explosion relief panels close after a vented explosion the underpressure generated by the cooling of the combustion products may damage the walls. Sometimes the negative phase of the blast wave may break the windows that have survived the positive phase. The **secondary effects** are missiles (flying debris and objects set in motion by the explosion) and fires ignited by the flame.
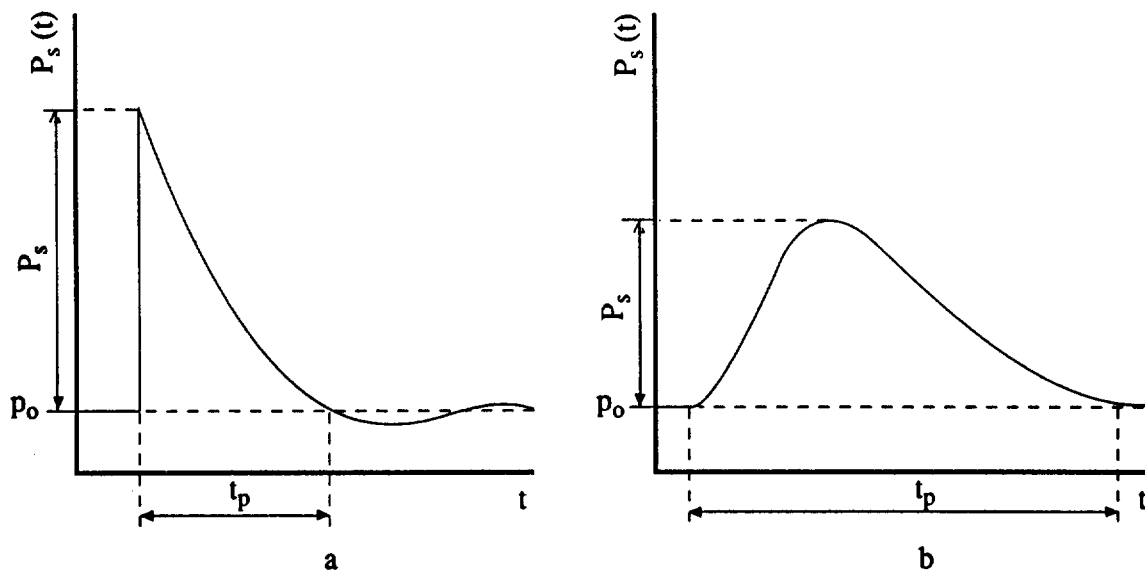
Figure 2.3. a) Shock wave, b) pressure wave (CPR 1989).

The limitation of damages from gas and vapour explosions can in principle be accomplished with measures performed at several stages:

1. Preventing releases that may form flammable mixtures: high standards of maintenance, safety training and small inventories of flammable materials. Early detection and closing of leaks.

2. Preventing flammable mixtures from being formed. Efficient ventilation of enclosed spaces. The ventilation rate may be increased when a leak is detected. Confining spills of flammable liquids.

3. Removing potential ignition sources. Using explosion protected electrical equipment and eliminating static charges by grounding,

4. Suppressing the explosion by injecting water spray or other suppressant automatically when the ignition has been detected.

5. Reducing the explosion overpressure by an appropriate layout of pipes, vessels etc. and designing explosion relief panels or explosion relief doors to have an area large enough, open early and fast, and relieve the pressure effectively. The area outside the explosion vents should be open enough.

6. Limiting the explosion damage by placing other buildings at a distance and, possibly, equipping them with blast resistant windows.

In this report, the measures pertaining to the stages 4 to 6 are discussed. This does not mean that the measures of the stages 1 to 3 are less effective or less important, rather on the contrary. To be able to design a plant in a way to reduce the overpressure in a gas explosion has been the goal of extensive research sponsored by the offshore industry in the 1980's and the 1990's. New methods and tools have been developed many of which, however, require significant experimental and computational resources and expertise. Also previous simple methods have been evaluated on the basis of the new research.

3 COMBUSTION PROPERTIES OF GAS-AIR MIXTURES

The burning of a gas in air is a chemical reaction in which the fuel is oxidized releasing heat and often light. The chemical products of the complete combustion of a hydrocarbon fuel are mainly carbon dioxide CO_2 and water vapour H_2O. Combustion of methane in air can be described by the reaction

$$CH_4 + 2(O_2 + 3.76N_2) -> CO_2 + 2 H_2O + 2(3.76N_2) + heat$$
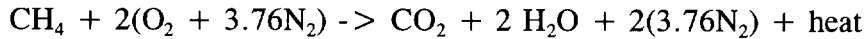
Note that the atmospheric nitrogen N_2 does not participate in the reaction. Actually, this is the net reaction of a number of chemical reactions involving intermediate reaction products some of which (the free radicals) are extremely reactive.

A flammable fuel-air mixture is usually ignited by spark, open flame or a hot surface. The **ignition energy** of a mixture depends on fuel concentration and type of fuel, and is measured in a test apparatus. For most fuels, the minimum ignition energy in air ranges 0.1 to 0.3 mJ. However, hydrogen, acetylene and carbon disulphide have one order of magnitude lower minimum ignition energy ie. 0.02 mJ (Table 3.2). The minimum ignition energy is relevant particularly to the control of static electricity.

Another useful quantity is the **autoignition temperature** which is the lowest temperature of a hot surface able to ignite a fuel-air mixture. Also this quantity depends on fuel concentration and type of fuel, and is measured in a test apparatus. For most hydrocarbons, the autoignition temperature lies between 210 °C (decane) and 540 °C (methane) (Table 3.2). Carbon disulphide has an exceptionally low autoignition temperature: 100 °C.

Actually a gas in air can burn in two ways. If the concentration of the gas when released in air is above upper flammability limit (the mixture is overrich) the burning occurs as the fuel and oxygen are mixed during the combustion process. This phenomenon is called **diffusion flame.** Due to lack of oxygen, the combustion is incomplete producing soot which makes the flame red or orange.

A flammable mixture burns generally faster than an overrich one since no mixing of air is required. This phenomenon is called a **premixed flame.** The combustion is usually complete producing only gaseous combustion products. The flame is blue indicating a higher combustion temperature than that of a diffusion flame.

A flammable mixture is called **stoichiometric mixture** if the concentration of gas matches the atmospheric concentration of oxygen so that all the gas is burned using up all the oxygen. The gas concentration of a stoichiometric mixture is calculated easily from the combustion reaction. For example 1 mole of methane requires $2x4.76 = 9.52$ moles of air for complete combustion. Hence the concentration of a stoichiometric mixture is $1/(1+9.52) = 9.5 \%$.

If the concentration is lower the flammable mixture is **lean** and if it is higher the mixture is **rich**.

The temperature of a premixed flame can be calculated from the (lower) heat of combustion of the gas and the specific heats of the combustion products. The flame temperature is highest for a stoichiometric mixture. This temperature is called the **adiabatic flame temperature** since it is calculated assuming the combustion to be an adiabatic process (no heat losses to the environment). Table 3.1 presents the adiabatic flame temperatures T_f [K] of some hydrocarbon gases and hydrogen in air.

The adiabatic flame temperature T_f [K] can be used to calculate the volume of a stoichiometric mixture after the combustion has occurred. It follows from the ideal gas law PV = NRT that

$$\frac{V_f}{V_i} = \frac{N_f T_f}{N_i T_i} \tag{2}$$

where
V_i is the initial volume [m^3]
V_f is the final volume [m^3]
N_i is the number of moles in the unburned mixture [mol]
N_f is the number of moles in the combustion products [mol]
T_i is the initial temperature [K].

At high temperatures the combustion products are partly broken down into atoms and free radicals such as H, O, and OH. This phenomenon, called **dissociation**, increases N_f. However, the adiabatic flame temperatures of most hydrocarbons are not high enough to cause any significant dissociation of the combustion products. Thus, dissociation can be neglected in the calculation of N_f.

For methane, the number of moles is conserved ie. $N_i = N_f = 10.52$. Generally, the number of moles may decrease or increase during combustion. Consider hydrogen:

$$H_2 + 0.5(O_2 + 3.76N_2) \rightarrow H_2O + 1.88N_2 + heat$$
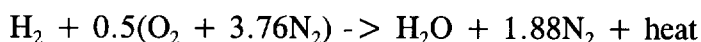
The mole number ratio is 2.88/3.88 = 0.85. Eg. for butane the opposite is valid:

$$C_5H_{12} + 8(O_2 + 3.76N_2) \rightarrow 6H_2O + 5CO_2 + 30.08N_2 + heat$$
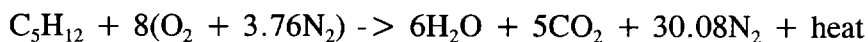
The mole number ratio is 41.08/39.08 = 1.05.

The ratio $E = V_f/V_i$ is called the **expansion factor** of a gas. Values of the expansion factor E are given for hydrocarbon gases and hydrogen in Table 3.1. For most hydrocarbon fuels, to a first approximation the mole number ratio N_f/N_i can be taken as 1. The expansion factor can then be equated to the ratio of temperatures T_f/T_i.

In combustion technology, the heat of combustion is given as energy per unit mass of fuel (J/kg) or energy per unit volume of gas (J/m^3 at standard temperature and

17

pressure). Regarding gas explosions, this may be misleading. The heat of reaction per unit volume of stoichiometric mixture H_{st} [MJ/m^3] shows little variation between different gases (Table 3.1). A high adiabatic flame temperature follows from a high value of this quantity and/or a low value of mole number ratio.

Table 3.1. Combustion properties of some hydrocarbon gases and hydrogen in air (Harris 1983).

fuel	flamm. range %	stoich. mixt. %	T_f K	E	H_{st} MJ/m^3
hydrogen	4 - 75	30	2318	8.0	3.06
methane	5 - 15	9.5	2148	7.4	3.23
ethane	3 - 12.5	5.6	2168	7.5	3.39
propane	2.2 - 9.5	4.0	2198	7.6	3.46
butane	1.9 - 8.5	3.1	2168	7.5	3.48
pentane	1.5 - 7.8	2.6	2232	7.7	3.59
hexane	1.2 - 7.5	2.2	2221	7.7	3.62
heptane	1.2 - 6.7	1.9	2196	7.6	3.62
acetylene	2.5 - 80	7.7	2598	9.0	3.93
ethylene	3.1 - 32	6.5	2248	7.8	3.64
propylene	2.4 - 10.3	4.4	2208	7.7	3.59
butylene	1.7 - 9.5	3.4	2203	7.6	3.64
benzene	1.4 - 7.1	2.7	2287	7.9	3.62
cyclohexane	1.3 - 8.0	2.3	2232	7.8	3.85

A basic quantity of premixed gas flames is the **burning velocity** S_0 [m/s]. This is the velocity at which the flame front (thin reaction zone) travels in a laminar flow with respect to the unburned mixture immediately ahead of it. The burning velocity is measured in a test apparatus in which the flow velocity of the mixture is adjusted so that the flame front is stationary. The flame front is stationary also in a burner for premixed gas (Fig. 3.1).

The value of burning velocity is determined by molecular transport processes, such as heat and mass transfer within the flame front. The burning velocity is a function of gas concentration, reaching a maximum just on the fuel rich side of the stoichiometric concentration (Fig. 3.2). This maximum value and the corresponding concentration are given in Table 3.2 for the gases in Table 3.1. It is seen that the maximum laminar burning velocity of most hydrocarbon fuels is close to 0.5 m/s. Hydrogen has an 0exceptionally large laminar burning velocity 3.5 m/s.

burnt gases

burning velocity
acts in opposite
direction to flow
of unburnt gases

thin reaction zone/
flame front

reaction zone
remains stationary
at mouth of burner

unburnt gases

burner tube

gas–air mixture

B Propagating or explosion flame

burnt gases

burning velocity
acts in same
direction as flow of
unburnt gases

point of ignition

thin reaction zone/
flame front travels
through unburnt
gas–air mixture

unburnt gases

Figure 3.1. Stationary and propagating flames (Harris 1983).

19
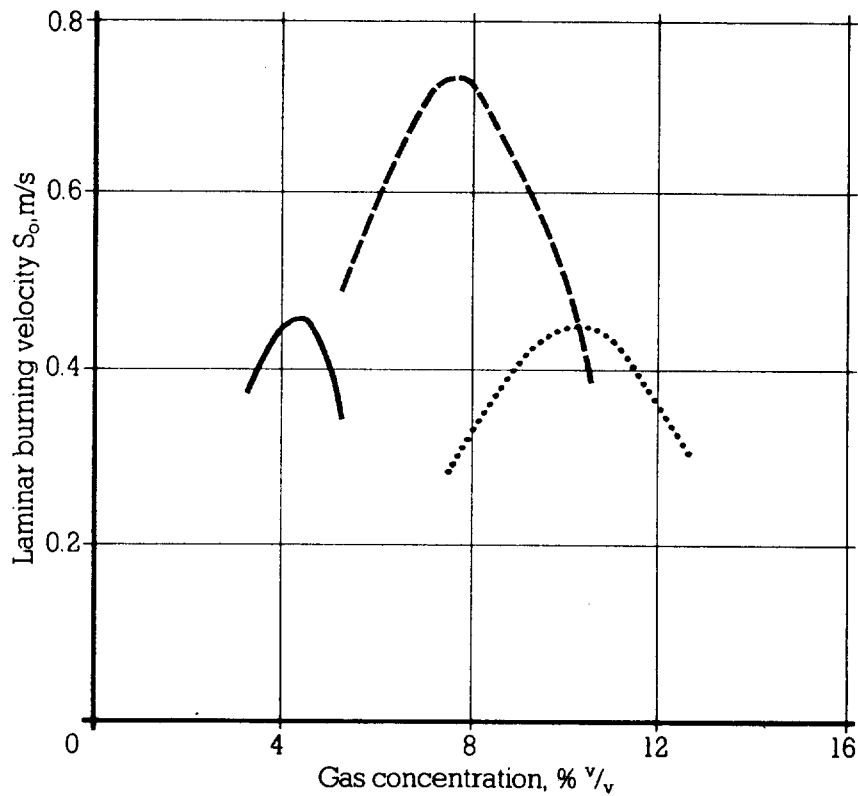
Figure 3.2. Effect of gas concentration on burning velocity. Solid line = propane, dashed line = ethylene, dotted line = methane (Harris 1983).

Table 3.2. Combustion properties of some hydrocarbon gases and hydrogen in air (Harris 1983).

fuel	max S_0 at %	max S_0 m/s	max S_f m/s	AIT K	min. ign. energy mJ
hydrogen	54	3.5	28	847	0.02
methane	10	0.45	3.5	813	0.29
ethane	6.3	0.53	4.0	788	0.24
propane	4.5	0.52	4.0	723	0.25
butane	3.5	0.50	3.7	678	0.25
pentane	2.9	0.52	4.0	533	0.25
hexane	2.5	0.52	4.0	498	0.25
heptane	2.3	0.52	4.0	488	0.25
acetylene	9.3	1.58	14.2	578	0.02
ethylene	7.4	0.83	6.5	763	0.12
propylene	5.0	0.66	5.1	733	0.28
butylene	3.9	0.57	4.3	658	0.28
benzene	3.3	0.62	4.9	833	0.22
cyclohexane	2.7	0.52	4.1	518	0.24

In a flash fire or gas explosion, the situation is different. The flame front is travelling away from the ignition point in a moving gas-air mixture. For central ignition, the expansion of the combustion products acts as a piston pushing the unburned mixture away from the point of ignition (Fig. 3.1). It is helpful to think the piston as porous one permitting the unburned mixture to flow through. The velocity of the flame front with respect to some fixed position is the sum of the flow and burning velocities. This velocity is called **flame speed.**

Assuming that the gas cloud is initially at rest, the flow is laminar, the flame surface is smooth and that the burned gases are at all times trapped behind the expanding flame front, the relationship between the flame speed and burning velocity can be expressed as (Harris 1983):

$$S_f = E S_0 \tag{3}$$

Eq. (3) is also valid in other geometries than the one in Fig. 3.1 (spherical symmetry) where the assumptions made in the derivation are valid (Fig. 3.3):

-       in a tube closed at one end and ignited at that end
-       between two parallel planes (cylindrical symmetry)
-       hemisphere eg. a gas cloud bordering on ground.
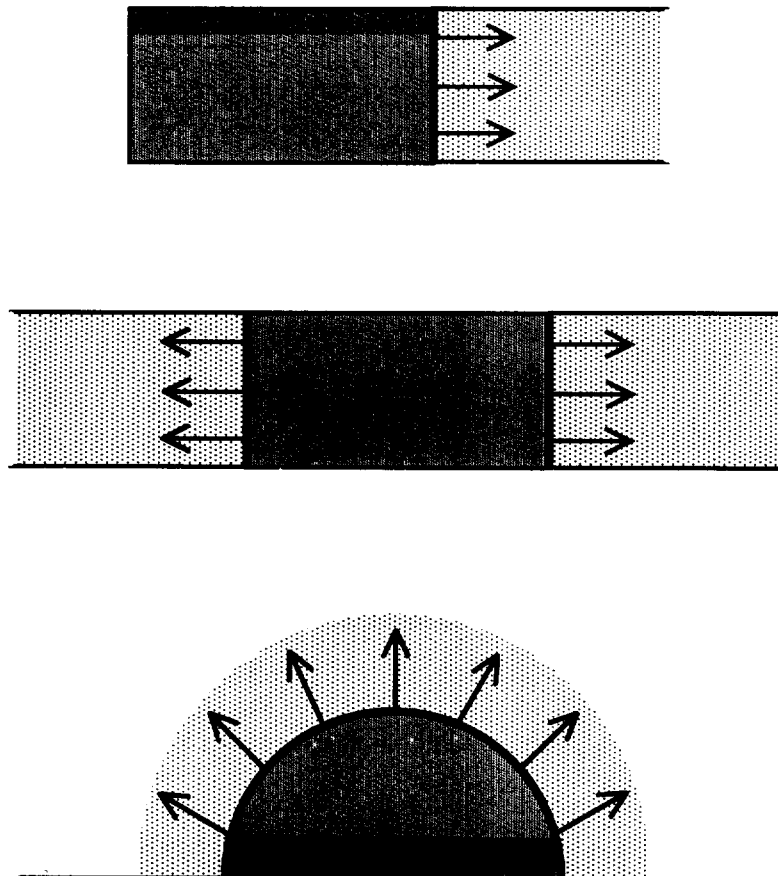
Figure 3.3. Different geometries.

21

Note that Eq. (3) is not valid if the burned gases are not trapped behind the flame front. This is the case if the gas mixture is ignited at the edge. The burned gas is expanding at the edge of the gas cloud and thus not pushing the unburned mixture, which remains almost stationary in front of the flame front (Fig. 3.4).
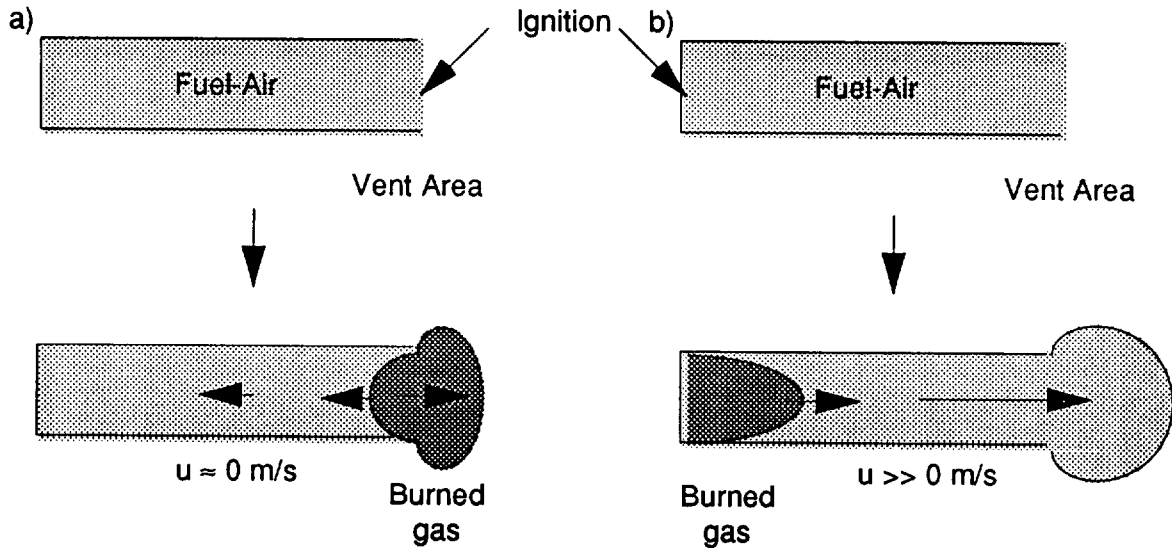
Figure 3.4. The effect of ignition location (Bjerketvedt et al. 1993).

Maximum values of the laminar flame speed S_f have been calculated using Eq. (3) and are given in Table 3.2. The adiabatic flame temperature T_f and hence the expansion factor E depend on the concentration, having a maximum at the stoichiometric mixture. It is concluded from Eq. (3) that the laminar flame speed S_f has a maximum close to the concentration at which the maximum burning velocity is measured.

In reality, when a flame front propagates in any geometry it can develop a cellular structure showing peaks and troughs, often collectively called wrinkles. These deviations from smooth surface can occur already when the flame radius is a few tens of centimetres. The volume production of burned gases, which expand to drive the flame front forward, is proportional to the actual surface area of the flame. This effect can be considered by adding an area correction term to Eq. (3) (Harris 1983):

$$S_f = E\frac{A_f}{A_n}S_0 \tag{4}$$

where
A_f is the actual flame area [m^2]
A_n is the area of the idealized (laminar) flame [m^2].

Unfortunately, there is no simple method to predict the actual flame area A_f. It is to be stressed that the burning velocity is a fundamental property of any gas-air mixture, but the flame speed is not such. The flame speed, however, is a useful concept and the laminar flame speed is a lower limit to the real (turbulent) flame speed.

In gas explosions, there are other effects which may increase the flame speed S_f even considerably. The most important one is turbulence which can be generated by factors such as

- wall friction (especially effective in a tube explosion)
- high flow velocities eg. near an explosion relief vent
- obstacles throttling the flow and generating vortices in their wakes.

The flame speed of a front propagating in a turbulent flow is affected by the turbulence in two ways (Fig. 3.5):

- the large turbulent eddies increase the flame area
- the small turbulent eddies increase the diffusion of heat and mass.

Increased flame surface   Increased diffusion of
                                              heat and mass
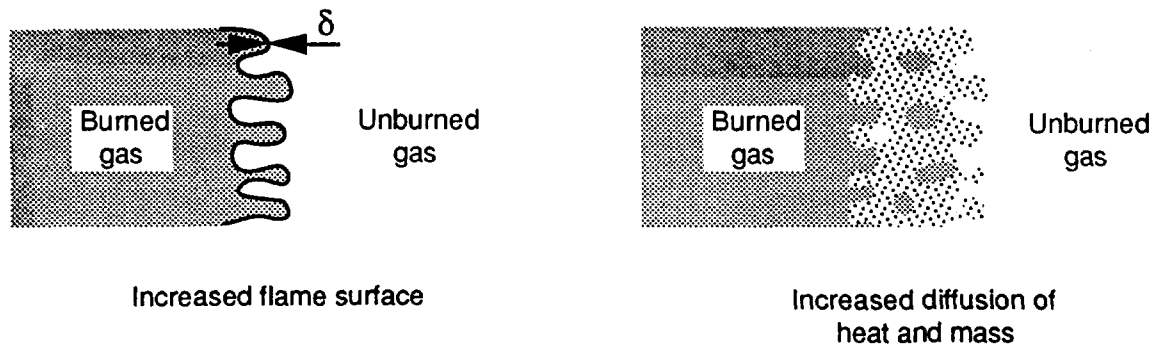
Figure 3.5: The effect of large and small eddies on flame front propagation (Bjerketvedt et al. 1993).

Both effects increase the flame speed S_f; the large eddies by increasing the area ratio A_f/A_i and the small ones by increasing the burning velocity from the laminar one S_0 in Eq. (4).

In a vented gas explosion, there are additional factors which may increase the flame area by creating a hydrodynamic instability of the interface between the unburned and the burned gases (Fig. 3.6):

- external explosion which momentarily reverses the flow through the vent
- flow of mixture towards the vent.

For the sake of simplicity, only one vent is assumed in Fig. 3.6. In Fig. 3.6a the mixture is ignited in the centre of the room. The flow of unburned mixture towards the vent gives the flame front a pear shape. The instability is triggered by the momentary reversal of the flow through the vent. This pushes the burned gases against unburned mixture opposite to the vent resulting in a hydrodynamic instability (Taylor instability) of this part of the interface (Fig. 3.6a) (Kees van Wingerden, Christian Michelsen Research, private communication).

In Fig. 3.6b the mixture is ignited at the rear wall. Also in this case the flame is stretched towards the vent. The hydrodynamic instability in Fig. 3.6b develops close to the vent. The cause of this (Helmholz-Kelvin) instability is the strong turbulence due to the large difference in flow velocities over this region (Solberg et al. 1981).

23
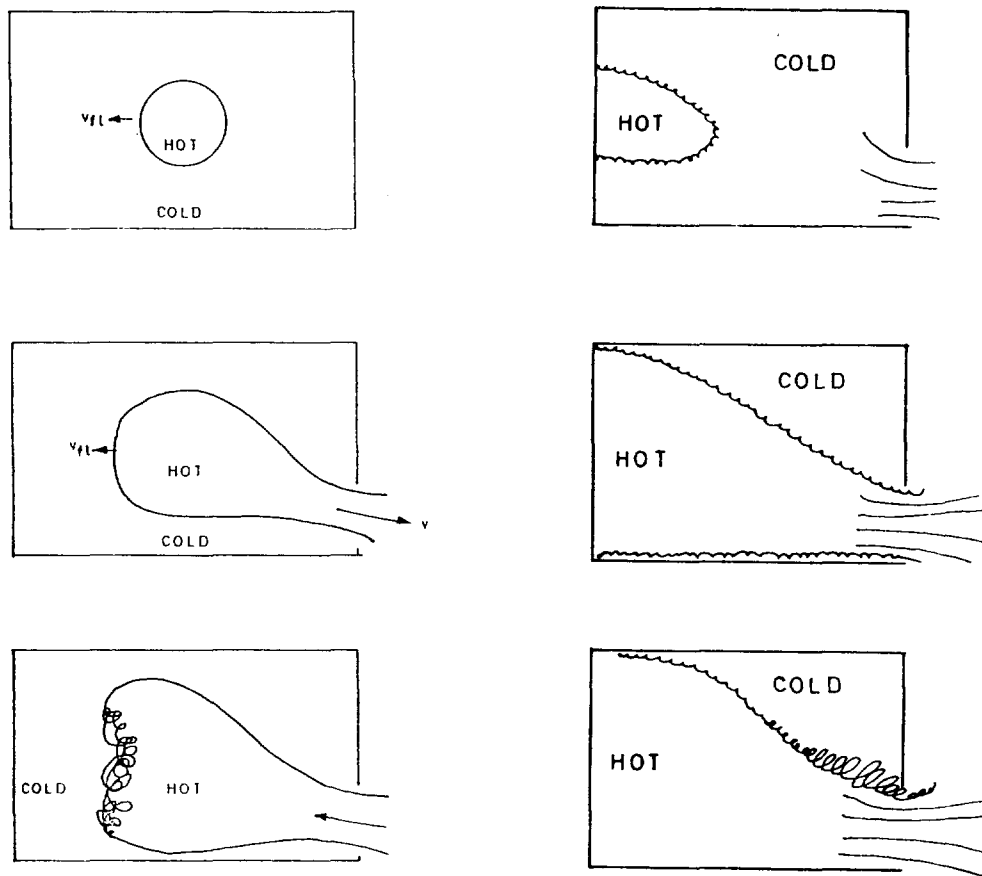
Figure 3.6. Additional factors increasing the flame area. a) Central ignition and Taylor instability (left). b) Rear ignition and Helmholz-Kelvin instability (right) (Solberg et al. 1981, modified).

Hydrodynamic instabilities are also caused by the standing acoustic wave which is formed in an empty, cubical or nearly cubical room towards the end of the explosion (after parts of the flame front have reached the walls). The pressure fluctuations of the acoustic wave are coupled with oscillating cellular instabilities of the flame front and, consequently, with the combustion rate. The resonance can amplify the acoustic wave and increase the combustion rate considerably.

4   GAS ACCUMULATION IN ENCLOSED SPACES

A flammable mixture may be formed as a consequence of a gas or liquid leak. A gas release forms a turbulent momentum jet in which the gas is diluted due to the entrainment of air. A spill of flammable liquid forms an evaporating pool. The pool evaporation rate and dilution of vapour are determined by the vapour pressure of the liquid and air flow velocity above the pool. Thus the two sources have quite different characteristics (Fig. 4.1).
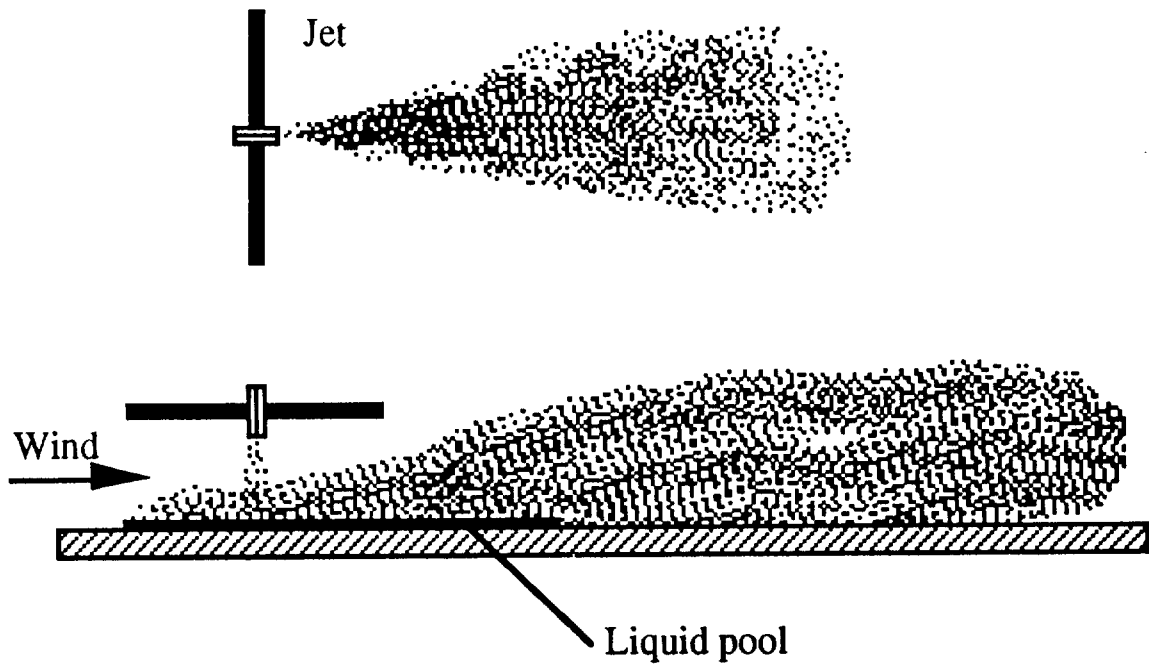
Figure 4.1. Jet release and evaporating pool (Bjerketvedt et al. 1993).

The momentum jet has the form of a cone whose axis is along the direction of release. If the x axis is aligned along the axis of the cone the average concentration at a point x,y C(x,y) [%] is given by the simple formula (Harris 1983)

$$\frac{C(x,y)}{C_0} = k_1 \left[\frac{\rho_a}{\rho_0}\right]^{\frac{1}{2}} \frac{d_0}{x} \exp\left(-k_2 \frac{y^2}{x^2}\right) \tag{5}$$

where

C_0 is the initial concentration of gas [%], usually $C_0 = 100$ %
k_1 is an experimental constant, $k_1 = 5$
ρ_a is density of air [kg/m^3]
ρ_0 is the initial density of gas [kg/m^3]
d_0 is the diameter of the orifice [m]
k_2 is an experimental constant, $k_2 = 57.3$.

It is seen from Eq. (5) that the concentration on the jet axis $C(x,0)$ is inversely proportional to distance x. In the direction perpendicular to the jet axis (ie. y axis), the concentration follows Gaussian distribution. Eq. (5) can be used to calculate the maximum distance at which an initially undiluted gas ($C_0 = 100$ %) will reach the lower flammability limit C_L. For methane ($C_L = 5$ %) this distance is $130d_0$ and for propane ($C_L = 2.1$ %) the distance is $190d_0$.

The derivation of Eq. (5) assumes that the jet is free ie. it does not collide against any object, nor there are any objects limiting the flow of ambient air into the jet. The flow velocity in the jet decreases as more air is entrained in the jet. The jet is usually assumed to end at a distance at which the flow velocity has reached that of the ambient air (outdoors this is the wind velocity). Outdoors these assumptions are often met and the flammable mixture produced by the gas leak is confined to the jet.

However, the situation is different indoors and in other enclosed spaces. The jet flow and eventual density difference between the gas mixture and air, create a circulating flow in the room. After a delay (whose length depends on the gas flow rate and the size of the room), it will no longer be air that is entrained in the jet, but a gas-air mixture. The concentration in the room will increase until it reaches a steady state value determined by the gas flow rate and the ventilation rate of the room.

If the jet impacts against an obstacle the nature of the flow is changed. Fig. 4.2a shows a free jet colliding at a perpendicular wall or other obstacle. If there are no other obstacles affecting the flow the dilution will go on in the "wall jet". If the release occurs between two flat surfaces, a recirculating flow field is set up between them. In this zone, the jet cannot pull in sufficient air from outside and a high concentration is formed (Fig. 4.2b).

In general, gas released in a room will be mixed with the air due to the actions of momentum jet flow, density differences and turbulent mixing with air supplied by ventilation. British Gas has performed a series of experiments on gas accumulation in rooms (Marshall 1983).

The first series was performed in unventilated rooms. The volume of the room ranged 8 - 55.6 m³. Gases of different densities ($\rho_0/\rho_a = 0.46$ (town gas), 0.6 (natural gas) and 1.5 (propane)) were released to the room. There were no openings in the walls except a small hole to let out the air displaced by the gas. Thus, the hole was situated near the ceiling for propane and near the floor for town gas and natural gas.

An important result of these experiments was that the time taken for an almost homogenous layer to form was short. Propane (representing dense gases) was found to form such a layer between the leak position and the floor (Fig. 4.3a). Town gas and natural gas (representing light gases) were found to form a similar layer between the leak position and the ceiling (Fig. 4.3b). As time went on, the thickness of the layer remained the same, but the concentration increased steadily (Fig. 4.4).
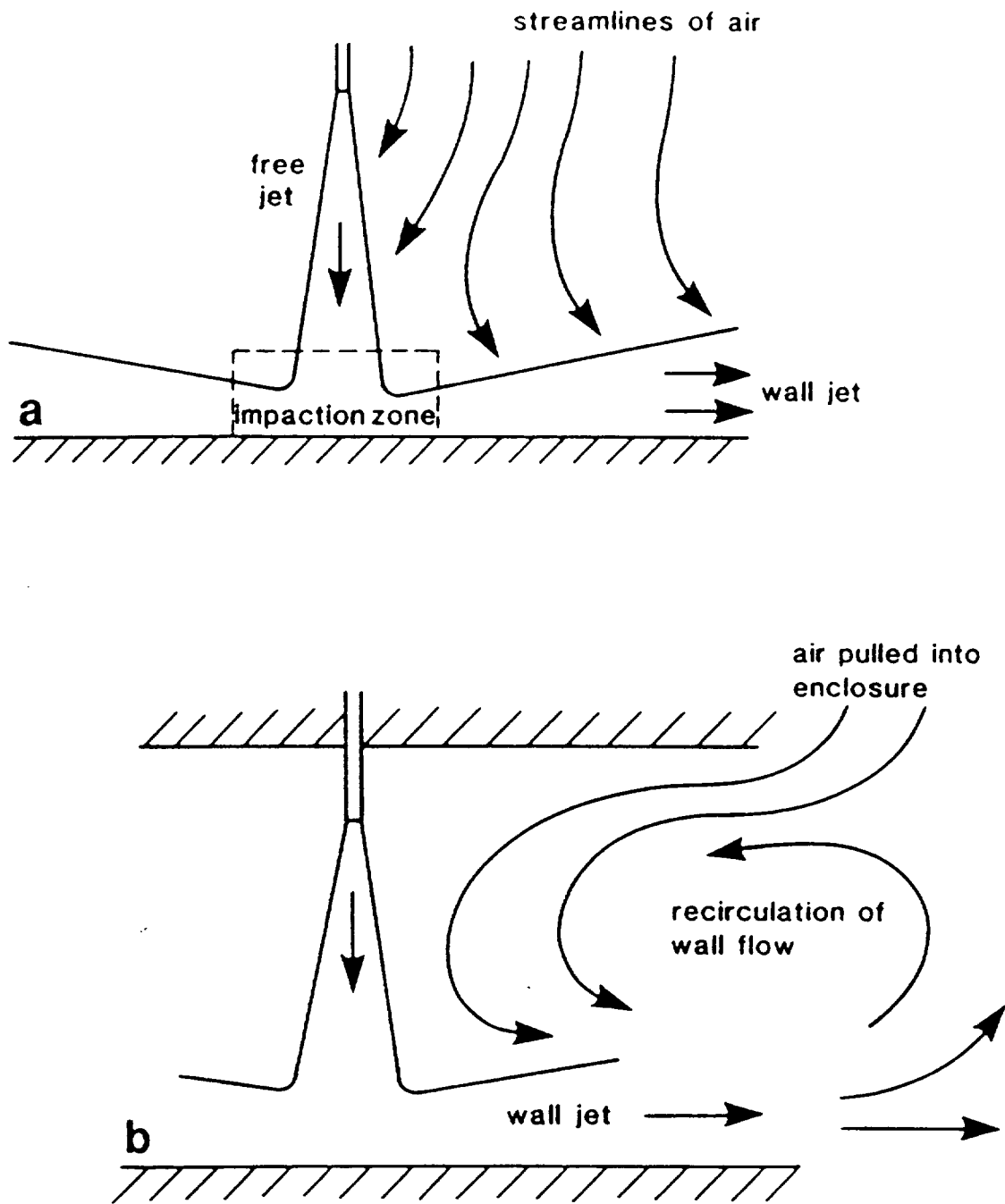
Figure 4.2. The effect of confinement in an impacting jet (Cleaver et al. 1994).
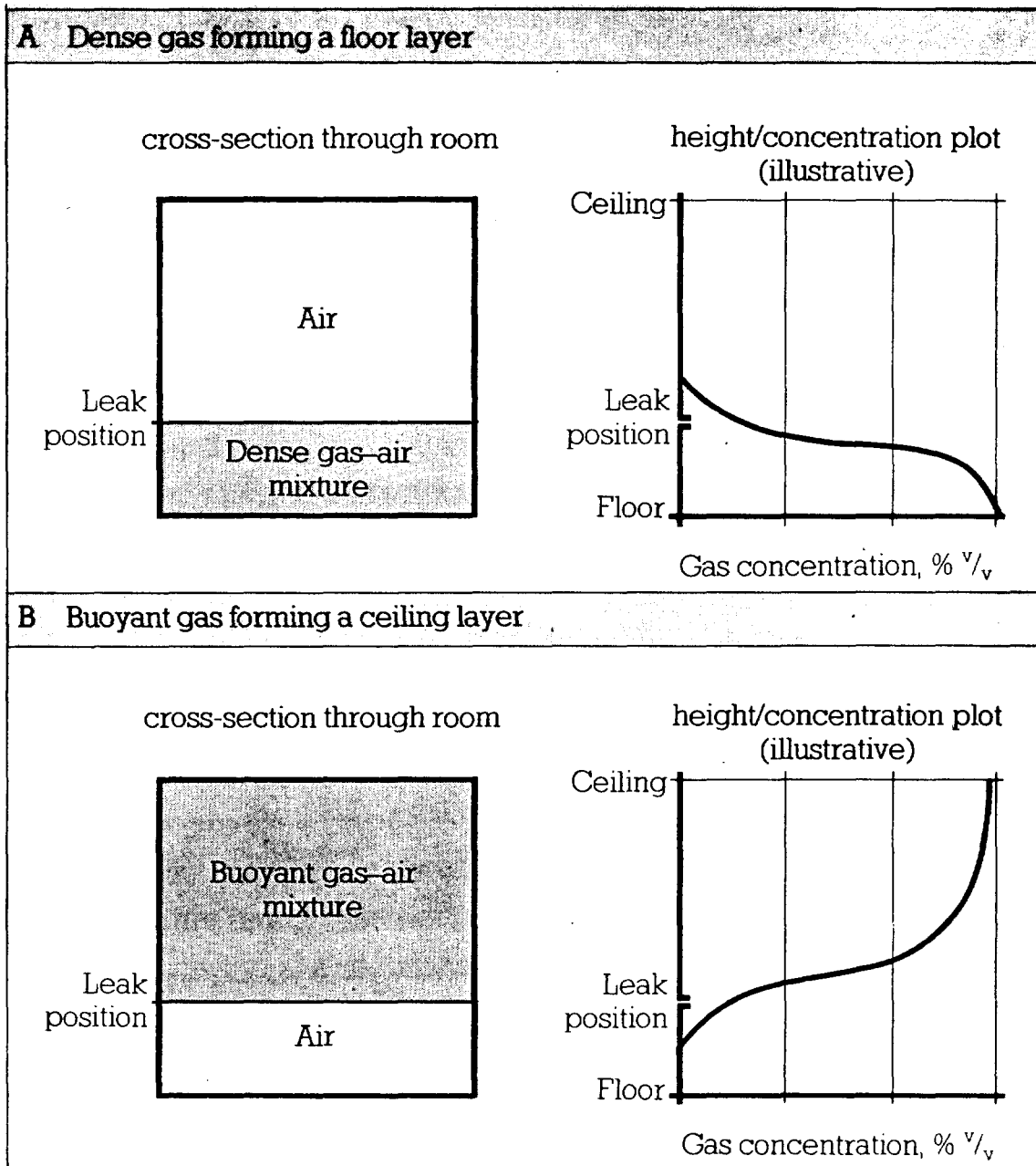
Figure 4.3. Typical concentration profiles in an unventilated room (Harris 1983).

When natural gas was released near the ceiling a shallow layer of high concentration was formed (Fig. 4.5a). An identical release near the floor filled the room with a mixture of a lower concentration (Fig. 4.5b). The concentration difference follows from the different volumes of air involved in the mixing process.
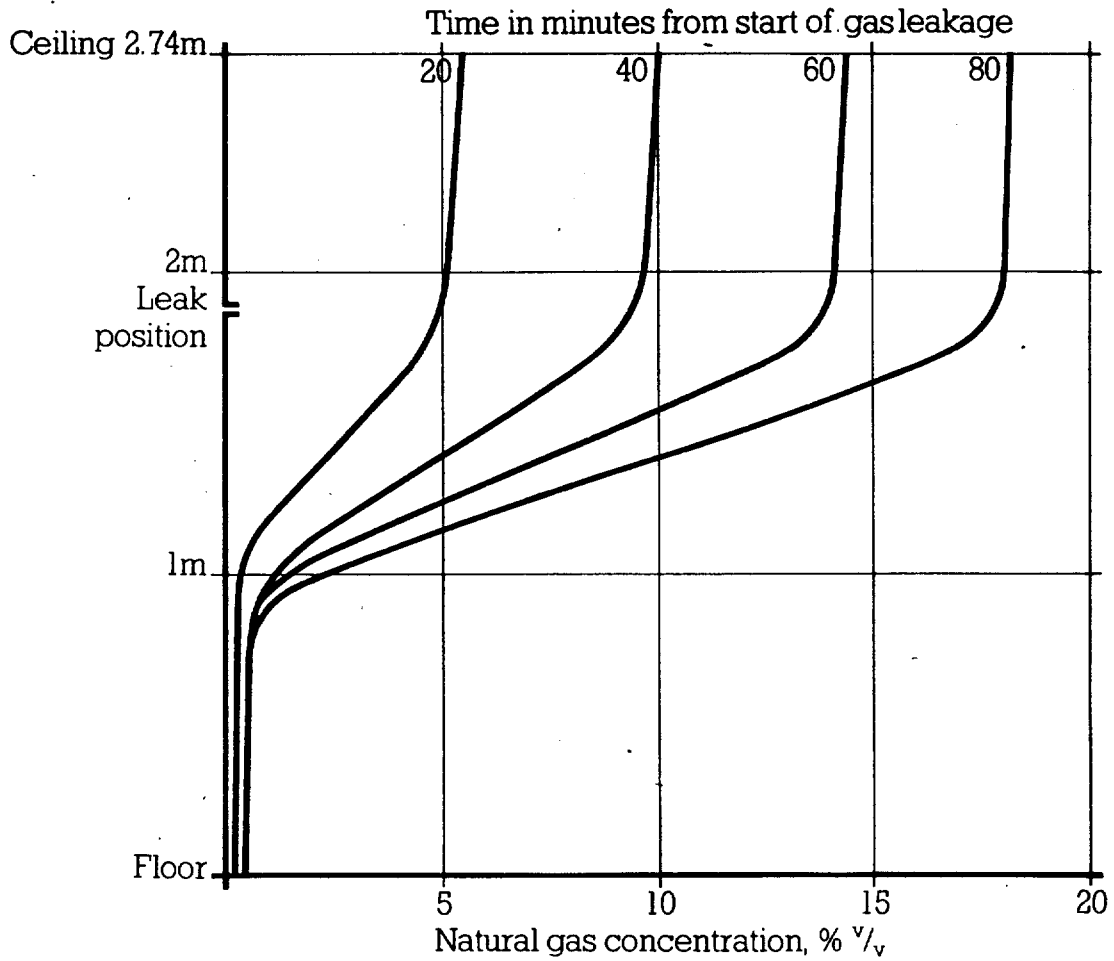
Figure 4.4. Development of a concentration profile with time in an unventilated room (Harris 1983).
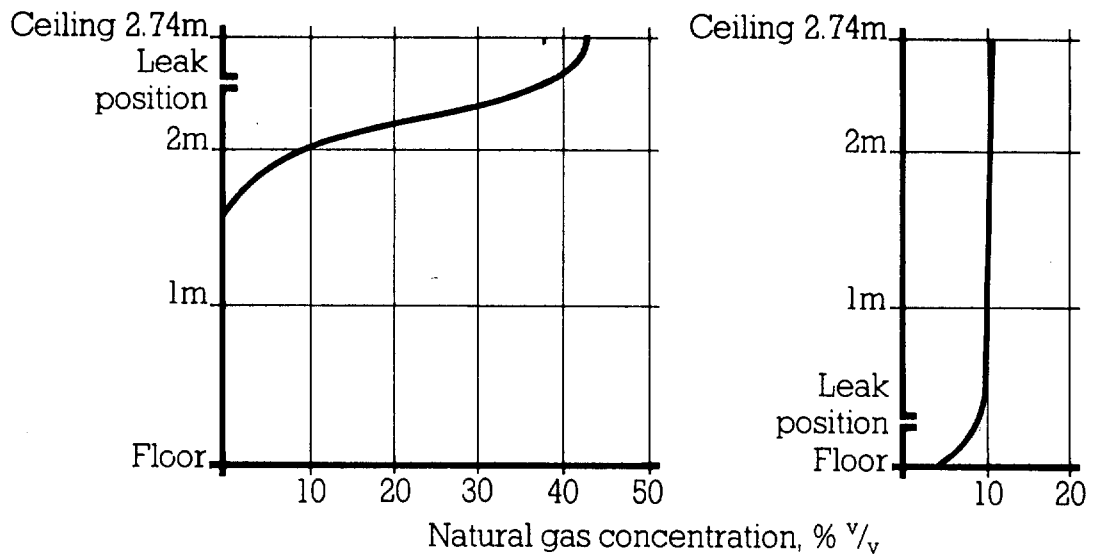
A   High leak position   B   Low leak position

Figure 4.5. Experimental concentration profiles in an unventilated room (Harris 1983).

29

The second series was performed in ventilated rooms. Most tests were performed in a cubical test chamber with a volume of 20.6 m³. Gas leakage rates ranged 0.28 to 9.8 m³/h and flow velocities 0.7 to 61 m/s. The room was equipped with mechanical ventilation and ventilation rates of between 0.5 and 6 volume changes per hour were used. Tests of similar nature were also made in naturally ventilated buildings (Marshall 1983).

Three different patterns of ventilation were used:

1. Upward ventilation (air enters near the floor and exits near the ceiling). This represents the usual pattern of mechanical ventilation and also of natural ventilation when temperature indoors is higher than that outdoors.
2. Downward ventilation (air enters near the ceiling and exits near the floor). This represents natural ventilation when temperature indoors is lower than that outdoors.
3. Cross-flow ventilation (air enters from openings on one side and exits through openings on the other side). This represents the wind-driven natural ventilation when temperature indoors is the same as outdoors.

In this report, only the first ventilation pattern is considered. After a certain time, steady state concentration profiles were established. Figure 4.6 shows the concentration profiles formed by a release at three different heights. The dashed line represents the theoretical steady state concentration C_s [%] which has been derived assuming perfect mixing of the gas and the air flowing through the room.

$$C_s = C_0 \frac{Q_g}{Q_a + Q_g}$$ (6)

where
C_0 is the initial concentration of the gas, usually 100 %
Q_a is the air flow rate through the room [m³/h]
Q_g is the gas release rate [m³/h].

It is seen from Fig. 4.6 that leak position does not affect much the value of the measured steady state concentration. Besides, the measured concentrations are quite close to the theoretical one.

If follows from Eq. (6) that the steady state concentration C_s can be decreased by increasing air flow rate Q_a or, equivalently the number of air changes an hour. This was also seen in experiments in which the gas release rate was kept constant, but the ventilation rate was increased from 1 to 6 changes an hour (Fig. 4.7).
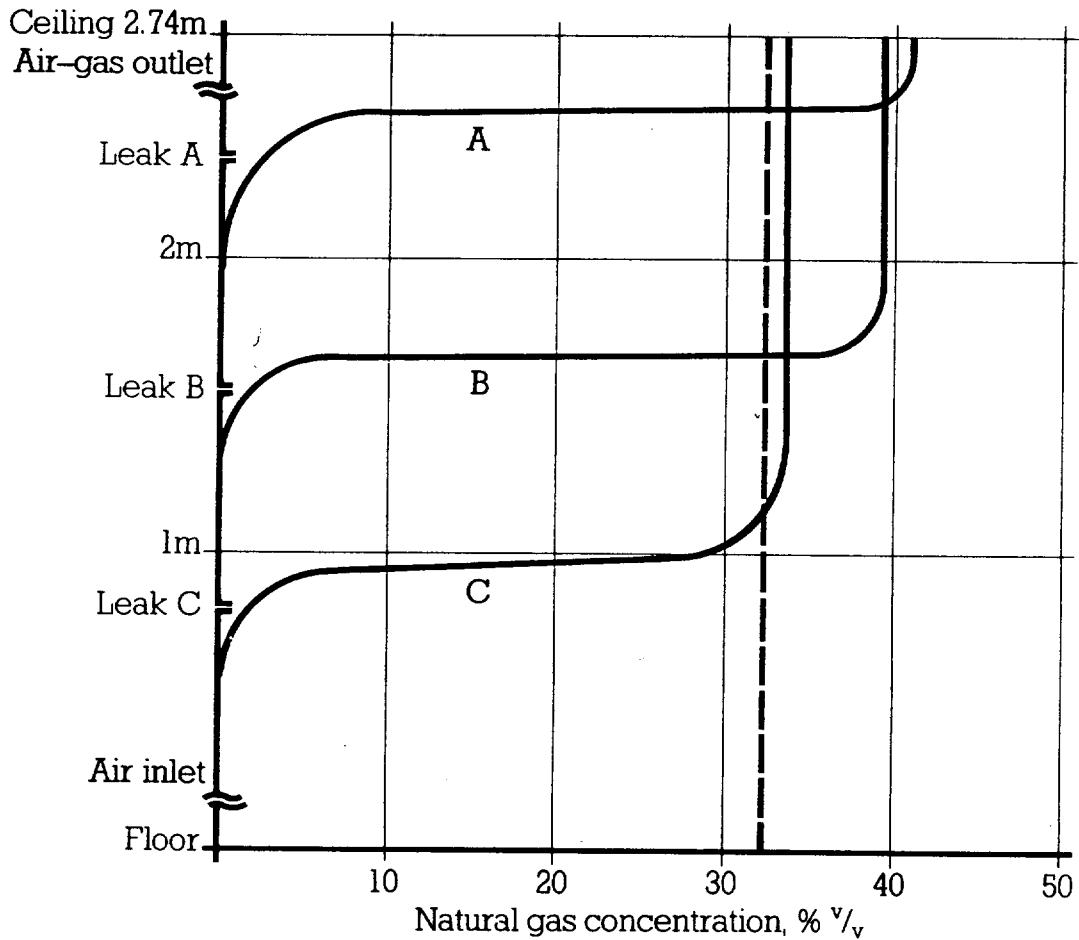
Figure 4.6. The effect of leak position on steady state concentration (Harris 1983).

Assuming perfect mixing, a simple equation can be derived for the time dependence of the gas concentration in a ventilated room (for the derivation see Harris 1983).

$$C(t) = C_0 \frac{Q_g}{Q_a + Q_g} \left[1 - \exp\left[-\frac{Q_a + Q_g}{V^*} t \right] \right]$$ (7)

where
V^* is the volume into which the gas is mixed [m³].

The first part of Eq. (7) is obviously the theoretical steady state concentration C_s of Eq. (6). The second part describes the build-up of the concentration to the steady-state value. For a light gas such as natural gas, the mixing volume V^* should be set equal to the part of the room between the leak level and the ceiling. Harris (1983) notes that for dense gases it may be more appropriate to set V^* equal to the total volume of the room. In this case, the buoyancy forces and inertia forces act in opposite directions, resulting into a thick mixing layer.

31
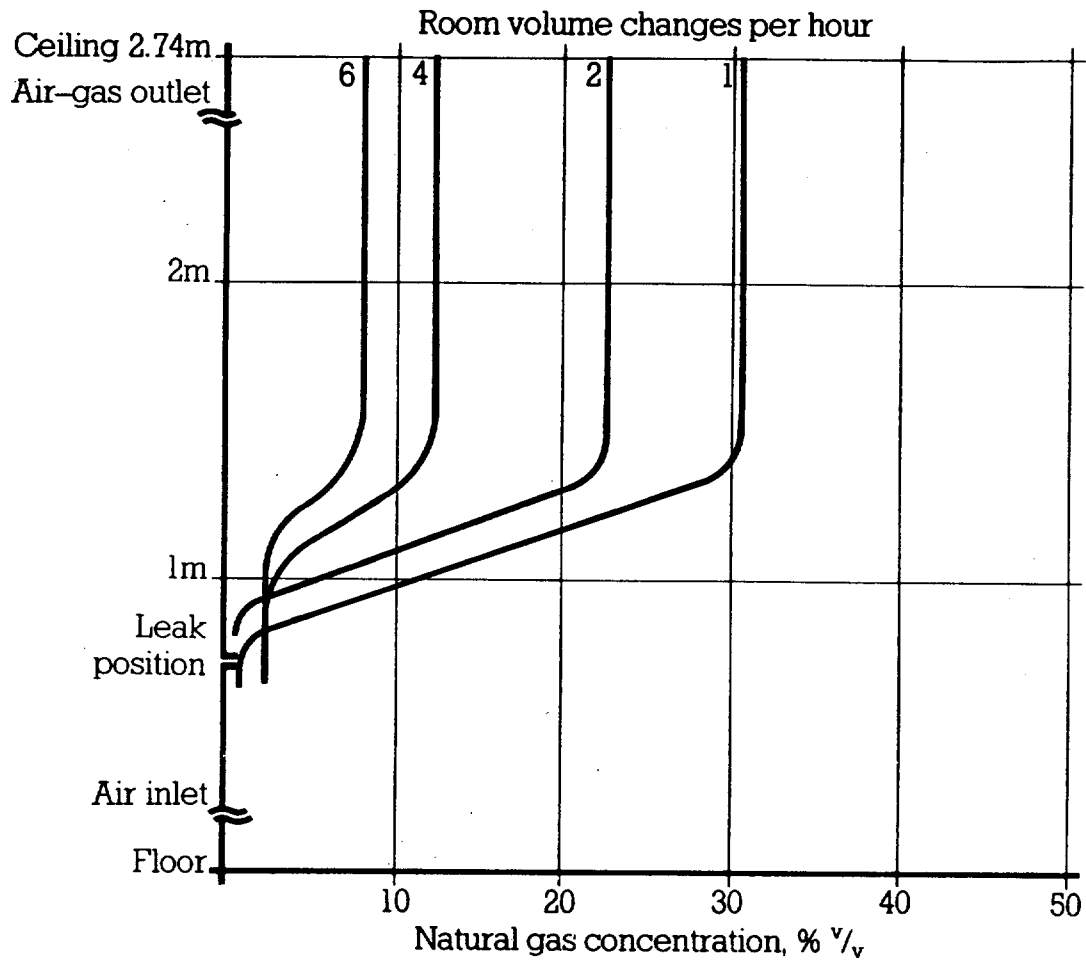
Figure 4.7. The effect of ventilation rate on steady state concentration (Harris 1983).

In rooms with natural ventilation, the formation of a gas layer may affect the ventilation rate if the density of mixture differs from that of air. Marshall and Stewart-Darling (1986) present a method by which the effect of a light mixture layer can be calculated. A light mixture increases the ventilation rate and thus reduces the concentration.

On the other hand, a layer of dense mixture reduces the ventilation rate increasing the concentration. Dense gases and vapours may also flow by gravity into drains and pits below the floor level. Even with a small release rate, the concentration in a poorly ventilated drain or pit may become flammable. An efficient ventilation in the room may not be enough to prevent this.

Mecklenburgh (1986) suggests a method by which the evaporation rate from a pool of flammable liquid can be calculated. The evaporation rate is calculated from different formulas depending on whether the flow over the pool is laminar or turbulent. The criterion for laminar flow is

$$Re_p = \frac{uL}{\nu} < 16\,600 \tag{8}$$

where

Re$_p$ is the Reynolds number of the pool
u   is the velocity of air flow [m/s]
L   is the length of the pool parallel to the air flow [m]
ν is the kinematic viscosity of air, $\nu = 1.4 \cdot 10^{-5}$ m^2/s.

The evaporation rate Q_v [m^3/s] for laminar flow is

$$Q_v = \frac{P_s}{P_a} W \left[\frac{uD_m L}{\pi} \right]^{\frac{1}{2}} \tag{9}$$

where

P$_s$ is the saturated vapour pressure of the liquid [kPa]
P$_a$ is the atmospheric pressure, P$_a$ = 101.3 kPa
W   is the width of the pool perpendicular to the air flow [m]
D$_m$ is the diffusion coefficient of the vapour in air [m^2/s].

If the condition for laminar flow Eq. (8) is not satisfied the formula for turbulent flow must be used:

$$Q_v = 0.9 \frac{P_s}{P_a} D_m^{1/2} (uL)^{4/5} W \tag{10}$$

According to Mecklenburgh (1986) the concentration in the room can be can calculated inserting $Q_g = Q_v$ in the steady state formula Eq. (6) (actually he uses an upper limit of this which is valid when $Q_g << Q_a$). This is valid when the air flow in the room is turbulent ie.

$$Re_r = \frac{uD_r}{\nu} > 2\,300 \tag{11}$$

where

Re$_r$ is the Reynolds number of the room
D$_r$ is the hydraulic diameter of the room [m].

The hydraulic diameter of the room D$_r$ is defined

$$D_r = \frac{2 W_r H_r}{W_r + H_r} \tag{12}$$

where

W$_r$ is the width of the room perpendicular to air flow [m]
H$_r$ is the height of the room perpendicular to air flow [m].

Actually, Eqs. (9) and (10) are valid only initially when there is no vapour the air flowing over the pool. When the circulation starts bringing vapour back the term P_s must be replaced by $P_s - P_p$, where P_p (kPa) is the partial pressure of the vapour "upwind" of the pool.

In real situations, there may be several factors which can change pool evaporation rate and the amount of flammable mixture created eg.
- the liquid in the pool cools due to evaporation
- if the liquid is warm and the pool is large it may create significant natural convection in the room
- the vapour may form a layer of dense mixture above the floor.

5 THE GENERATION OF PRESSURE IN GAS EXPLOSIONS

5.1 EXPLOSIONS IN EMPTY ROOMS

When a gas cloud consisting of stoichiometric mixture burns outdoors the volume increases during the combustion (flash fire) by the expansion factor E. For most gases in Table 3.1, this factor is close to 8. When a similar mixture fills a pressure vessel the absolute pressure in the vessel increases during the combustion (confined explosion) by a factor that is somewhat larger than E. Neglecting heat losses to the walls, the (calculated) pressure ratio P_f/P_i is about 9 (Fig. 5.1). In an adiabatic process, the pressure ratio would be $P_f/P_i = E$. The difference is caused by the compressive heating of unburned mixture and combustion products.
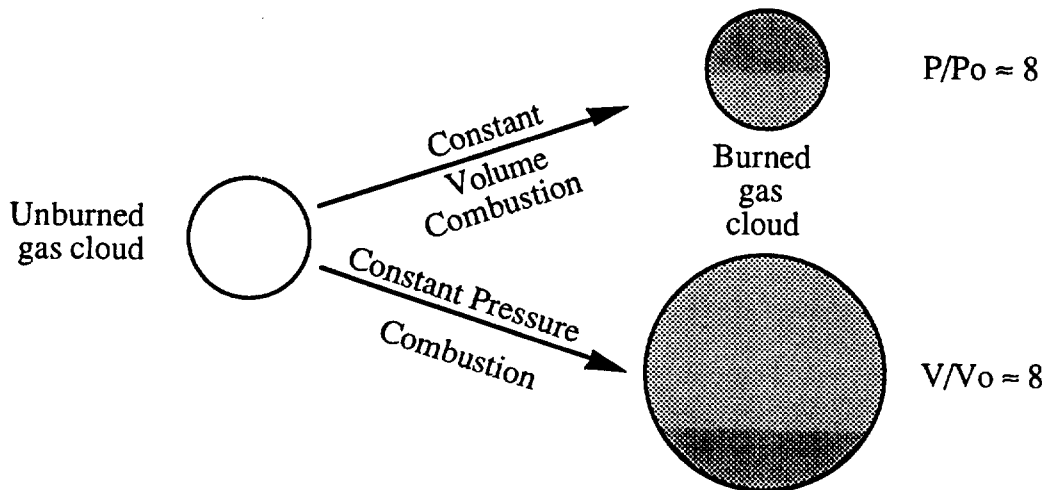
Figure 5.1. Constant volume and constant pressure combustion (Bjerketvedt et al. 1993).

Figure 5.2 shows the overpressures in a cubical vessel of volume 1 m³ calculated for stoichiometric mixtures of three gases. Heat losses to the walls are included. The rise time of the pressure depends on the burning velocity S_0, and hence on flame speed. Ethylene has the highest and methane the lowest burning velocity (Table 3.2). Thus ethylene has the shortest and methane the longest rise time.

Closed vessels have been used to measure explosion characteristics of flammable gas-air mixtures. Models for the time dependence of explosion overpressure in closed spherical vessels result in expressions for the rate of pressure rise in the form (Harris 1983)

$$\frac{dP}{dt} = K_1 \frac{S_0}{r_f} \tag{13}$$

where
K_1 is a constant [bar]
r_f is the radius of the flame front [m].
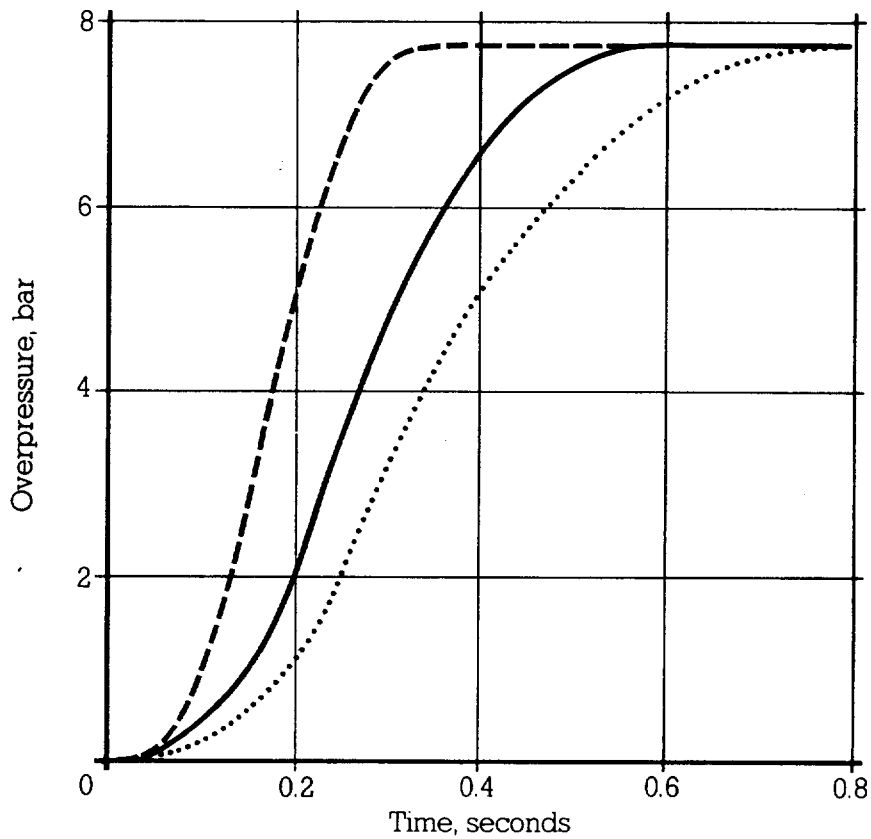
Figure 5.2. Pressure-time curves for confined explosions in a cubical vessel of volume 1 m³. Dashed line = ethylene, solid line = propane, dotted line = methane (Harris 1983).

Assuming that the maximum rate of pressure rise occurs at maximum flame area, r_f can be replaced by the radius of the sphere, or equivalently cube root of its volume V [m³]

$$(\frac{dP}{dt})_{max} = \frac{K_g}{V^{1/3}}$$

(14)

Eq. (14) is usually written in the form (called the **cube root law** or cubic law)

$$(\frac{dP}{dt})_{max} V^{1/3} = K_g$$

(15)

The cube root law with experimental values of the constant K_g [bar · m/s] has been used to predict the explosion overpressure in vented explosions (Bartknecht 1981). However, the method does not consider geometrical factors. The cube root law is applicable to nearly cubical rooms ($L_{max}/L_{min} \approx 1$), but it will fail for rooms differing from cubical form ($L_{max}/L_{min} > 1$) because the flame front reaches the walls earlier than in a spherical geometry. (L_{max} [m] is the longest and L_{min} the shortest dimension of the room.) The cube root law will fail also for non-central ignition (Harris 1983).

36

A more serious flaw in the use of the cube root law with an experimental value of K_g is that it does not include turbulence effects. An experiment performed in a small test vessel gives little information of the turbulence that can develop in large rooms due to instabilities and obstacles. Thus the constant K_g cannot be considered a basic quantity of a given gas. On the other hand, the burning velocity S_0 is such a quantity and it has been shown to represent well the effect of gas reactivity on the pressure in vented explosions (British Gas 1990).

The cube root law is used extensively to measure explosion properties of flammable dusts. This is mainly due to the fact that a flammable dust-air mixture can only be maintained in a turbulent flow. Thus, laminar burning velocity cannot be measured for such mixtures without special arrangements. The constant of the cube root law for a dust-air mixture is called K_{St} and the respective values for different dusts can be looked up in reference works.

The pressure generated in closed explosion vessels has little relevance to vented explosions in rooms. Windows, doors and walls fail already at pressures that are about 1 % of the explosion overpressure in closed vessels. The maximum overpressure P_{red} [kPa] is thus determined primarily by the sizes and opening pressures of the vents.

It has been known for decades that to relieve the explosion overpressure effectively, the vents must have a sufficient total area A_v [m^2] and as low an opening pressure P_v [kPa] as possible. In houses, the windows perform the task of explosion vents. In industrial buildings, explosion relief panels or doors are often used to achieve a low opening pressure and to avoid the damage caused by flying glass fragments.

The vents should open fast enough to relieve the pressure ie. they should have low inertia. For explosion relief panels flying away, the mass per unit area w [kg/m^2] is a suitable quantity describing the inertia. Relief doors should have as low a moment of inertia I [kgm^2] as possible.

The vent opening pressure P_v has a lower limit due to the requirement that the explosion relief panels or doors must not be opened by high winds. However, it cannot be usually assumed that the maximum pressure of a vented explosion P_{red} will be approximately the opening pressure of the vents P_v. The maximum pressure P_{red} will be higher, but it must be limited to prevent the damage of the walls and other load-bearing structures.

Thus, tests aimed at dimensioning the explosion vents correctly have been performed for decades, already. In these tests different fuel gases were used and the parameters varied were usually A_v, P_v and w. The test chambers were room-sized or smaller and the time dependence of the internal pressure was measured. Correlations of the measured peak pressures P_{red} were presented in terms of the parameters V, A_v, P_v, w and S_0. Usually these correlations (called venting guidelines) are used to select the vent parameters A_v, P_v and w, from the parameters S_0, P_{red} and V determined by the fuel and building, respectively.

Lunn (1985) presents a review of gas explosion tests performed and of correlations derived between 1955 and 1980. He also compares the capabilities of the different venting guidelines to predict the peak pressures P_{red} measured in other test series than those they have been derived from. The conclusion is that some formulas predict the experimental pressures better than others and the use of these is recommended. There are, however, test series where the pressures are significantly higher than those predicted by any of the formulas.

The devastating vapour cloud explosions in Flixborough, UK in 1974 and Beek, the Netherlands in 1975 emphasized the need to understand how a blast wave is generated in a vapour cloud explosion, and to be able to predict the parameters of the blast wave. A literature study shows that vapour cloud explosions have occurred for decades mainly in the hydrocarbon processing and chemical industries, but their losses have increased, reflecting the trend towards larger and larger processing units (Mahoney 1991).

Experimental research leading to the unravelling of the mystery of the blast generation in vapour cloud explosions was performed by TNO in the Netherlands and other research organizations in the early 1980's. The conclusion was that vapour cloud explosions were not "unconfined" but partially confined, and the additional factor needed to create a blast wave was repeated turbulence generating obstacles or jet ignition (AIChE 1994).

Another factor triggering research into gas explosions was the discovery of large gas and oil fields in the North Sea and the subsequent exploitation of the fields. Extensive research programs were started in Norway in 1978 by Christian Michelsens Institutt (now Christian Michelsen Research) and Det norske Veritas. In UK, the research has been performed at British Gas Midlands Research Station and Shell Thornton Research Centre.

The main difference between explosions at offshore platforms and vapour cloud explosions was that the release occurs in a room or other containment, leading to a vented explosion. Most of these rooms, however, are congested with pipes, vessels and other turbulence-causing obstacles. This provides the connection to vapour cloud explosion research (van Wingerden 1995).

The gas explosion research aimed at effective methods and tools by which the explosion overpressure could be reliably predicted. One should also be able to compare different design alternatives to select the one leading to the lowest pressure. One set of methods were the existing venting guidelines whose validity for large empty rooms had to be verified.

The research of British Gas produced a significant contribution to the understanding of vented gas explosions in empty rooms. Cooper et al. (1986) showed that the pressure as function of time can be described in terms of four distinct pressure peaks which can (but do not have to) occur (the four peak model). Each peak is produced by different physical processes at successive stages during a vented explosion (Fig. 5.3).

38
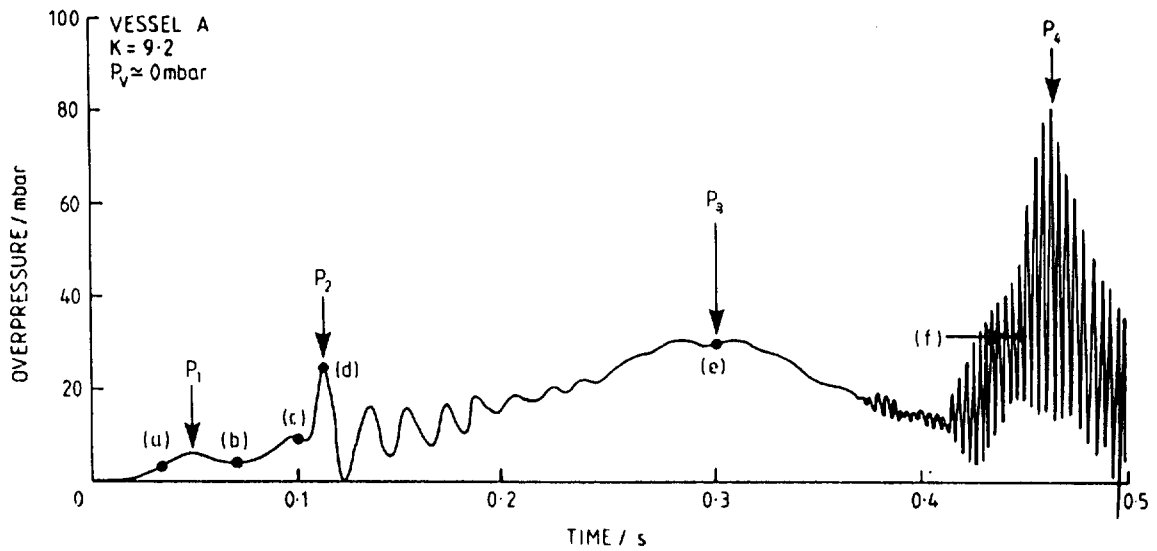
Figure 5.3. Time dependence of a vented explosion in a near-cubic vessel with an explosion relief opening at low pressure. The four peaks have been identified (Cooper et al. 1986).

The four peaks are (British Gas 1990, Gardner & Hulme 1995):

P_1 which is associated with the pressure drop following the removal of the explosion relief vent and subsequent venting of unburned gas.

P_2 which is associated either with the pressure drop following venting of burned gas, or corresponds to the pressure pulse caused by a possible external explosion due to ignition of previously vented unburned gas by the flame emerging from the vent.

P_3 a long duration but generally small amplitude peak associated with the maximum rate of combustion within the room (this typically occurs when the flame front reaches the walls).

P_4 which is an oscillatory pressure peak attributed to excitation of acoustic resonances in the gaseous combustion products within the room. The resulting high combustion rate may cause a significant net overpressure to be developed in the room.

The creation of the first peak P_1 can be described as follows: Before the vent opens, the pressure increase is caused by the production of hot combustion products generated by the flame front travelling at the flame speed S_f. The rate of volume generation dV/dt (V is the volume of the gas mixture at the initial pressure) is the difference of hot combustion products appearing and unburned mixture disappearing (Bradley & Mitcheson 1978a):

$$\frac{dV}{dt} = 4\pi r_f^2 S_f E - 4\pi r_f^2 S_f = 4\pi r_f^2 S_f (E-1) \tag{16}$$

The pressure in the room is equalized by compression waves travelling at sound velocity and reflecting from the walls of the room. Thus, at any moment the internal

39

pressure P [kPa] will be the same throughout the room. At the initial stage, the internal pressure follows approximately the formula (Harris 1983)

$$P - P_a = \frac{4\pi r_f^3}{3V} P_a \qquad (17)$$

where
V   is the volume of the room [m^3].

When the vent is fully open the flow of gases can be calculated from the formula (Harris 1983):

$$\frac{dV}{dt} = C_d A_v (\frac{2\Delta P}{\rho})^{\frac{1}{2}} \qquad (18)$$

where
C_d is the discharge coefficient of the vent, usually $C_d = 0.61$
ΔP is the pressure difference across the vent [kPa]
ρ is the density of the gases flowing to the vent [kg/m^3].

If the opening pressure of the vent P_v is low the vent opens early. The radius of the flame front r_f and, consequently, the rate of volume generation Eq. (16) are still small. If also the size of the vent A_v [m^2] is large enough the outflow rate Eq. (18) will be larger than the rate of volume generation at that time. The volume of the gas in the room will then decrease as will the pressure. In this way, the first pressure peak P_1 is generated (Fig. 5.4). If the vent is open initially (as in some experiments) there will be no peak P_1.

If the vent opens early the flame front radius r_f keeps increasing during a significant time after the first peak. The rate of volume generation Eq. (16) becomes soon larger than the outflow rate Eq. (18) and, consequently, the internal pressure starts to rise.

The pressure rises until the flame front reaches the vent. Now hot combustion products start to flow out of the vent. Their density is the density of unburned mixture divided by the expansion factor E. Consequently, the outflow rate Eq. (18) is suddenly increased by the factor $E^{1/2} \approx 2.8$ when the flame reaches the vent. The outflow rate becomes again larger than the rate of volume generation Eq. (16), resulting in the second pressure peak (Fig. 5.4).

This is the traditional explanation for the second pressure peak presented eg. by Harris (1983). However, the second peak may also be caused by a different mechanism. The unburned mixture released through the vent forms a turbulent momentum jet. Note that the momentum jet is not yet fully developed and, consequently, has a vortex ring at its head. When the flame front emerges from the vent it proceeds to propagate in a highly turbulent flow. The flame increases in area significantly and becomes spherical after reaching the jet head (Fig 5.5).
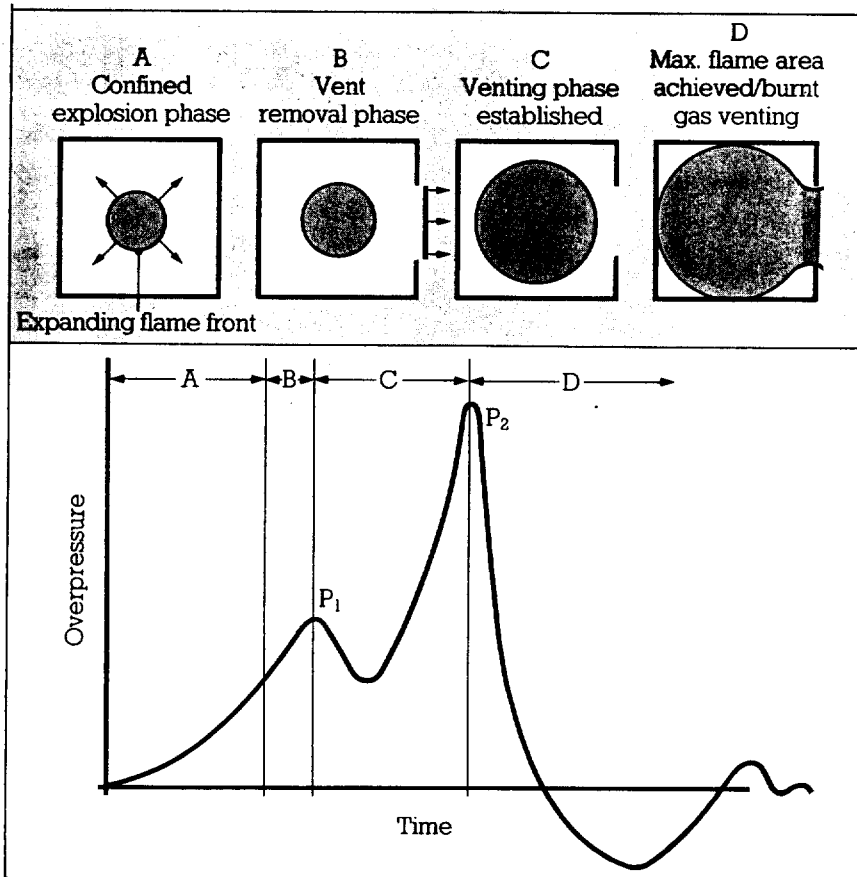
Figure 5.4. Origin of the first and second pressure peaks (Harris 1983).
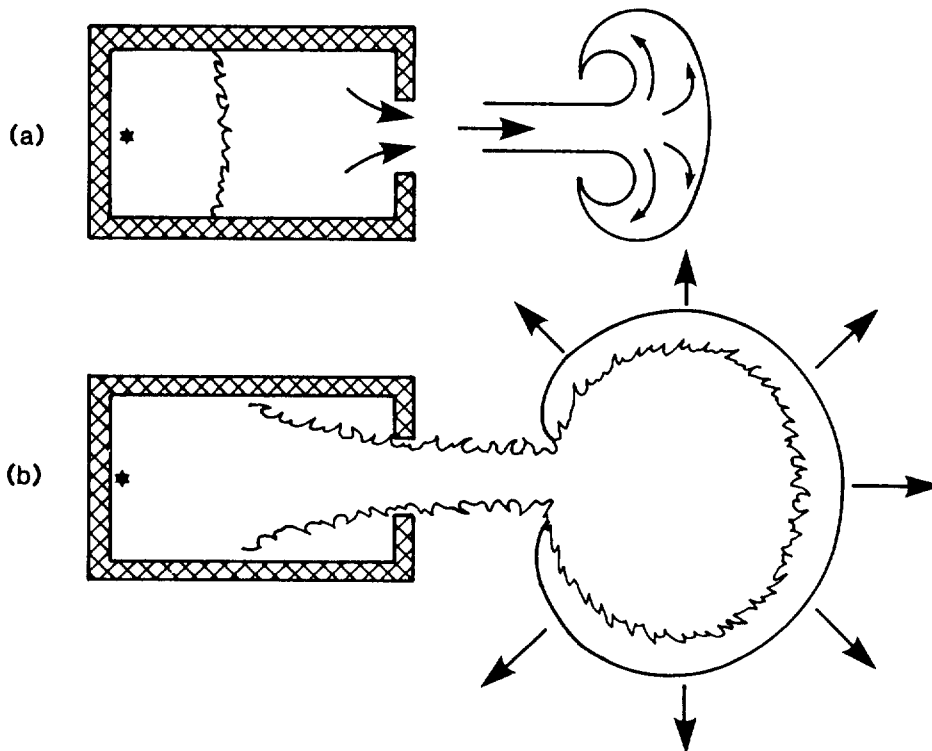
Figure 5.5. Jet of unburned mixture and external explosion (British Gas 1992).

41

The external explosion is particularly important when assessing the effects of a vented explosion to surrounding objects. It can produce a strong blast wave, and the explosion centre will be at a distance from the vent and closer to the surrounding objects than expected. The external explosion also creates a back pressure at the vent. The pressure difference across the vent ΔP is reduced or even reversed temporarily. The result is a higher internal pressure during the external explosion.

The strength of the external explosion is dependent on the amount of the unburned mixture released through the vent. Thus, a large amount is released when the ignition point is far from the vent and the vent opens at a low pressure P_v. When the ignition point is close to the vent the flame emerges from the vent early, when there is still little unburned mixture outside. Consequently, there will be no external explosion.

When the vent opening pressure P_v is high the vent opens relatively late and the flame emerges soon after the opening of the vent. Also in this case there will be little unburned mixture outside and no external explosion. Because the venting of hot combustion products starts early the pressure peaks P_1 and P_2 will merge into a single peak (Fig. 5.6).
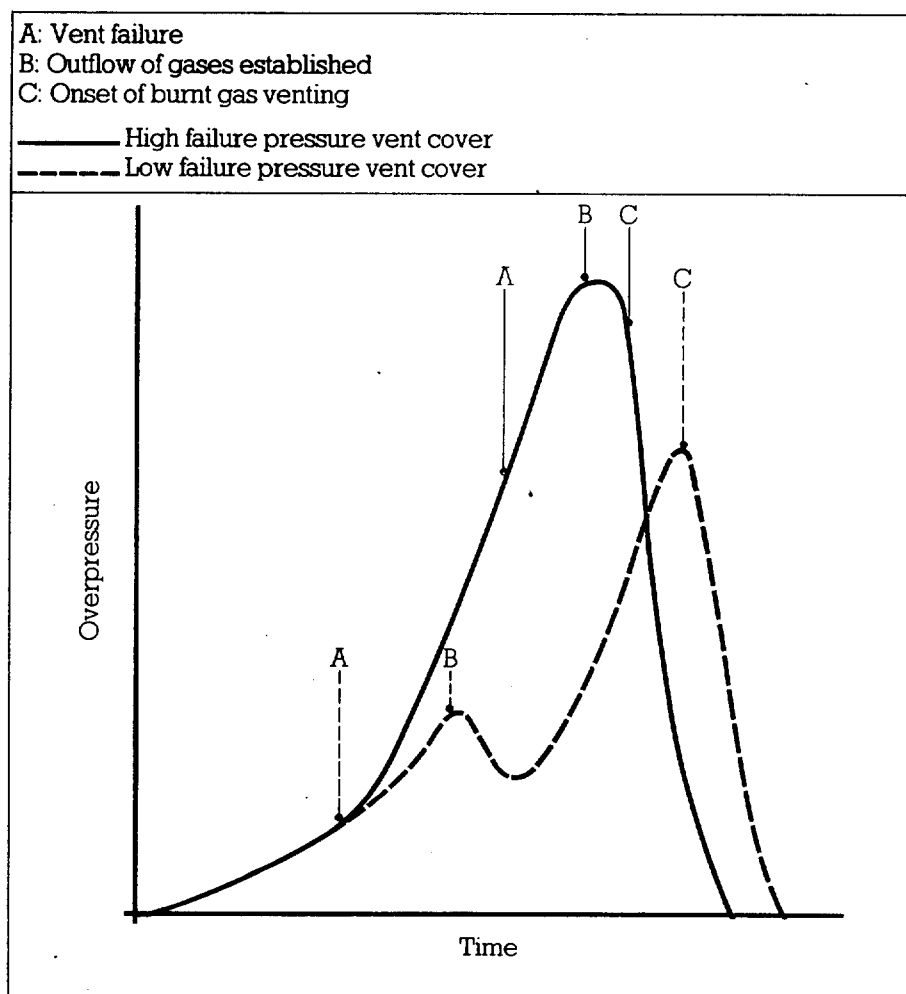
Figure 5.6. The effect of vent opening pressure on the pressure peaks P_1 and P_2 (Harris 1983).

The second pressure peak may be followed by low amplitude pressure oscillations at the frequency of standing acoustic wave (organ pipe type oscillations) (Fig. 5.3). The rate of volume generation increases sufficiently for the internal pressure to increase, while the oscillations themselves are gradually damped out as the flame front expands. These may induce instabilities at the part of flame front farthest away from the vent (Fig. 3.6a). Instabilities may also be generated in the turbulent boundary layer between the flow towards the vent and the unburned mixture (Fig. 3.6b) (Cooper et al. 1986).

The third pressure peak P_3 is caused by the reduction of the flame front area towards the end of the explosion when it reaches the walls. The area of the flame front has been increasing constantly until this moment. The flame front continues to propagate in the isolated pockets of unburned mixture while its area is decreasing. The pressure starts to fall due to the decrease of the rate of volume generation Eq. (16). The third peak is of long duration and usually not the dominant one.

The pressure in the room continues to fall until a high frequency oscillatory pressure peak P_4 occurs. This is caused by the coupling of the pressure waves generated in the combustion of the remaining pockets of unburned mixture to the standing acoustic wave in the room. Because the room is now almost filled with hot combustion products the frequency of the oscillation is higher (sound velocity is proportional to $T^{1/2}$) than the one after the second pressure peak (Fig. 5.3).

The pressure oscillations induce a cellular structure in the flame front, giving rise to very high combustion rates (and rates of volume generation). This creates a significant net overpressure in the room (Cooper et al. 1986).

Most vented explosion tests have been performed in rooms filled with a stoichiometric mixture. This has been considered the worst case because the explosion overpressure in a confined explosion is highest for stoichiometric mixture and 100 % fill. In practical situations, the room will usually be only partially filled with a flammable mixture due to layering of the light or dense gas.

Pappas (1984) presents a recommendation for two model situations that cover most cases of partially filled rooms with a single explosion relief vent and no obstacles. It is assumed that the room is cubical or nearly cubical ($L_{max}/L_{min} \leq 5$) and the ignition is effected far from the vent (Kees van Wingerden, Christian Michelsen Research, private communication). The first situation is a mixture layer close to the explosion vent (Fig. 5.7a). This has been investigated experimentally by Buckland (1980) in a 27 m^3 room for methane layers of different heights. The maximum pressures P_{red} measured in a test series is shown in Fig. 5.7a with the experimental correlation proposed by Buckland (1980).

$$\frac{P_l}{P_{red}} = (\frac{V_l}{V})^{\frac{1}{2}}$$

(19)

where
P_l is the maximum pressure for a flammable layer [kPa]
V_l is the volume of the flammable layer [m^3].
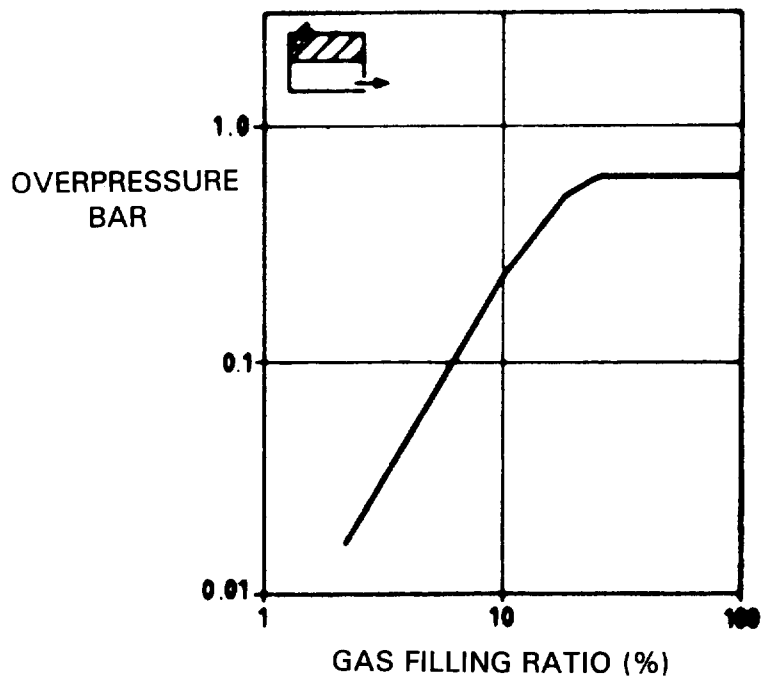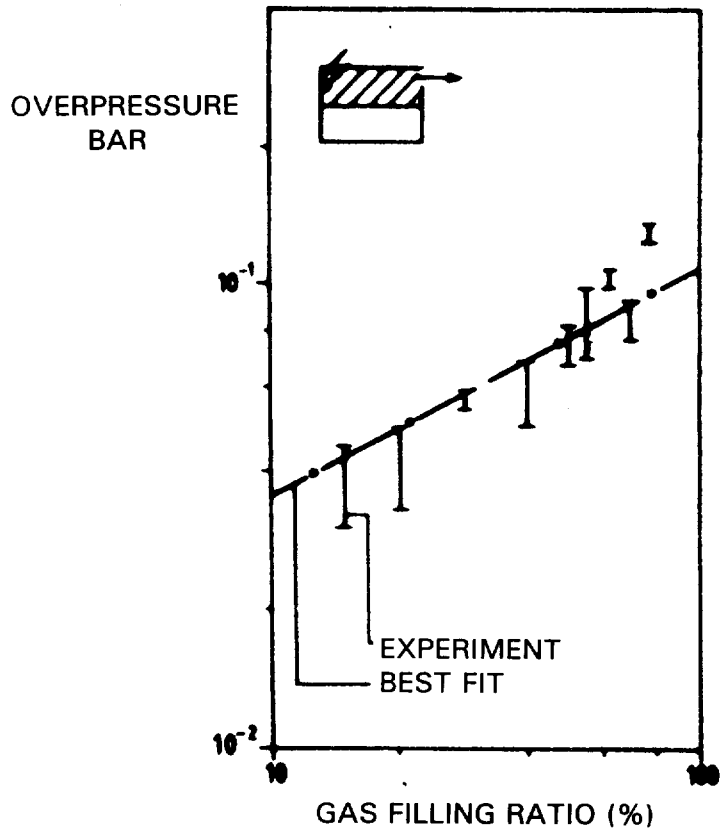
Figure 5.7. Maximum explosion overpressure in partially filled rooms as a function of fill ratio. a) Mixture layer close to the vent. Experimental points and curve fit by Buckland (1980). b) Mixture layer far from the vent (Pappas 1984).

44

In other words, the maximum pressure in the first situation is proportional of the square root of the fill ratio V_l/V. The second situation is a mixture layer located far away from the vent. The situation has been modelled by an explosion model developed by Det norske Veritas with the result shown in Fig. 5.7b. It is seen from Fig. 5.7b that the maximum pressure is the same as for 100 % fill provided the fill ratio V_l/V is larger than about 30 %.

The curve of Fig. 5.7b is the result of calculations with a early simple explosion model. When the second situation is considered in the light of the four peak model, the following observations can be made:

- when the flammable layer fills 30 % or more of the volume it will fill the room with hot combustion products
- when the flammable layer is ignited it pushes initially air out of the vent
- the first pressure peak P_1 is not expected to depend on the fill ratio since it is caused by the opening of the vent and the resulting outflow of air or unburned mixture
- when the second pressure peak P_2 is caused by an external explosion it is expected to increase with increasing fill ratio since more unburned mixture is pushed out
- when P_2 is caused by the venting of hot combustion products it is not expected to depend on the fill ratio
- the third P_3 and fourth P_4 pressure peaks are not expected to depend on the fill ratio since they occur towards the end of the explosion when most of the room is filled with hot combustion products.

5.2   THE EFFECT OF OBSTACLES

Two effects can be identified by the which the presence of obstacles could lead to an increase in flame speed. Firstly, the flame front is distorted as it flows around the obstacles leading to an increase in the flame area (**flame folding,** Fig. 5.8). Secondly, turbulence is generated in the unburned mixture as it flows over and around any obstacle (Fig. 5.9).

When the flame front reaches the turbulent area (wake) behind the obstacles the flame front is accelerated. The precise effect causing this depends on the intensity and scale of turbulence produced (determined by the size of the turbulent eddies, in turn determined by the size of the obstacles, Fig. 3.5) (Harris and Wickens 1989). The combined effect of flame folding and turbulence can cause a drastic increase of flame area and, consequently, flame speed (Fig. 5.10).
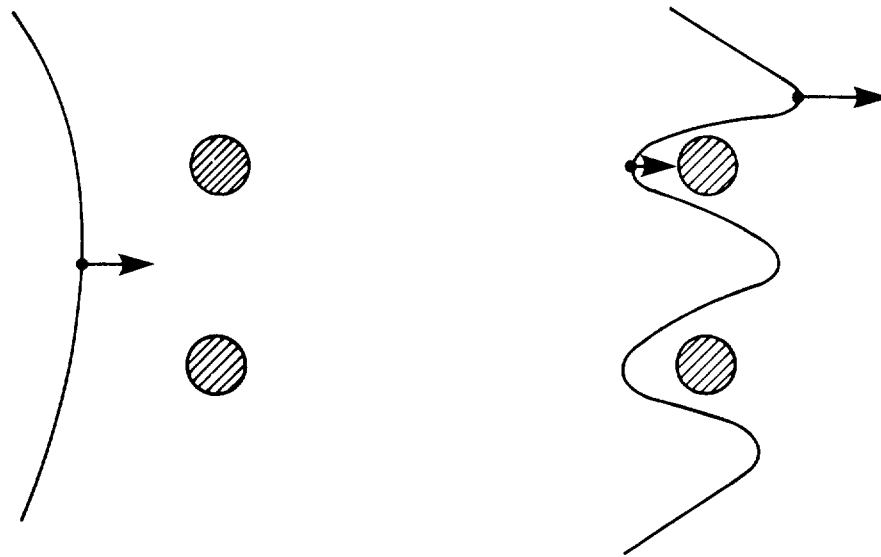
Figure 5.8. Flame folding caused by obstacles (British Gas 1992).
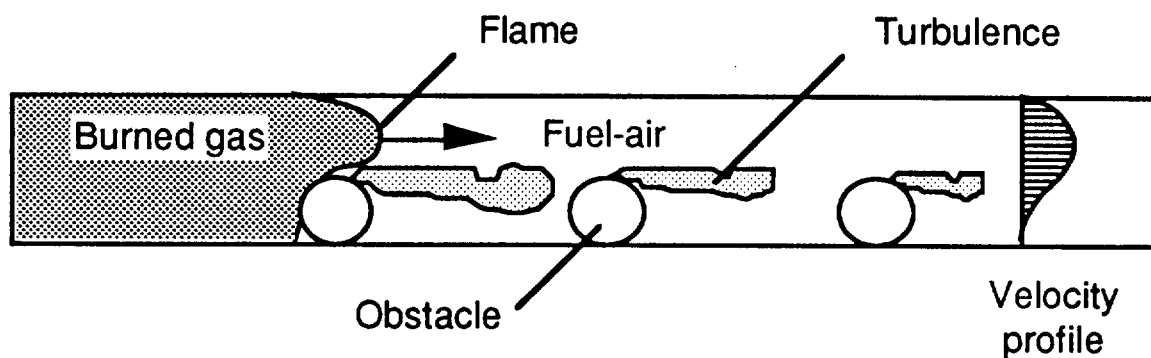
Figure 5.9. Turbulence generation in the wake of obstacles (Bjerketvedt et al. 1993).

The experimental research into the effect of obstacles on explosion overpressure started with idealized geometries. This approach was necessary to see the basic effects of obstacles on flame propagation. The experimental research at Christian Michelsens Institutt in Norway started with the following geometries (Hjertager 1991):

1. tube with sharp edged rings (Fig. 5.11),
2. a wedge-shaped vessel (two parallel planes) with sharp and round obstacles (Fig. 5.12)
3. a corner consisting of three perpendicular planes with different numbers of round obstacles (Fig. 5.13).
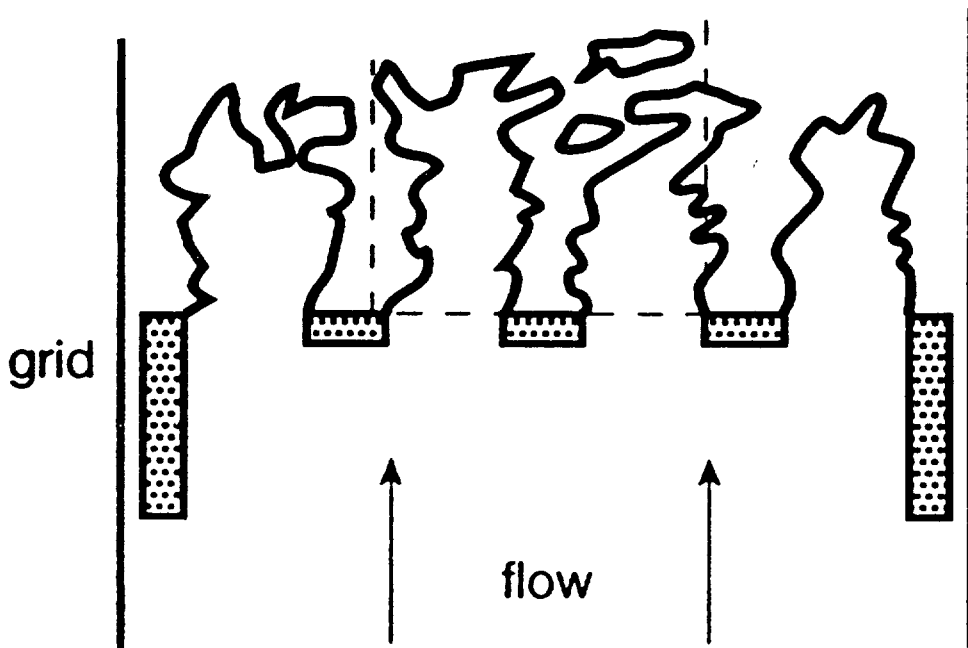
Figure 5.10. The form of flame front behind a row of obstacles (Mercx 1995).
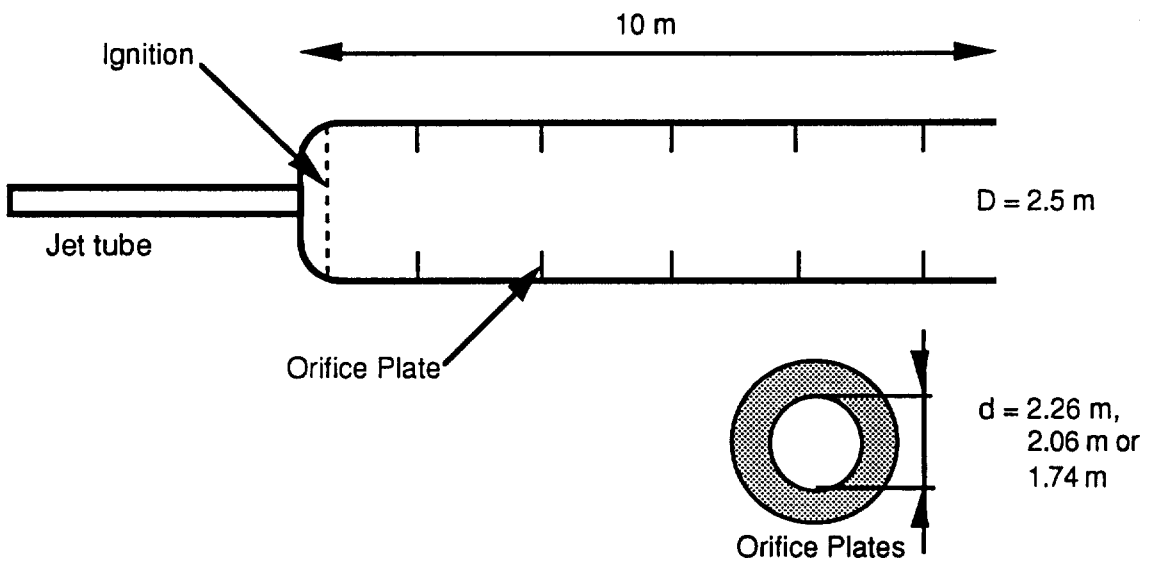
Figure 5.11. An explosion tube with orifice rings (Bjerketvedt et al. 1993).
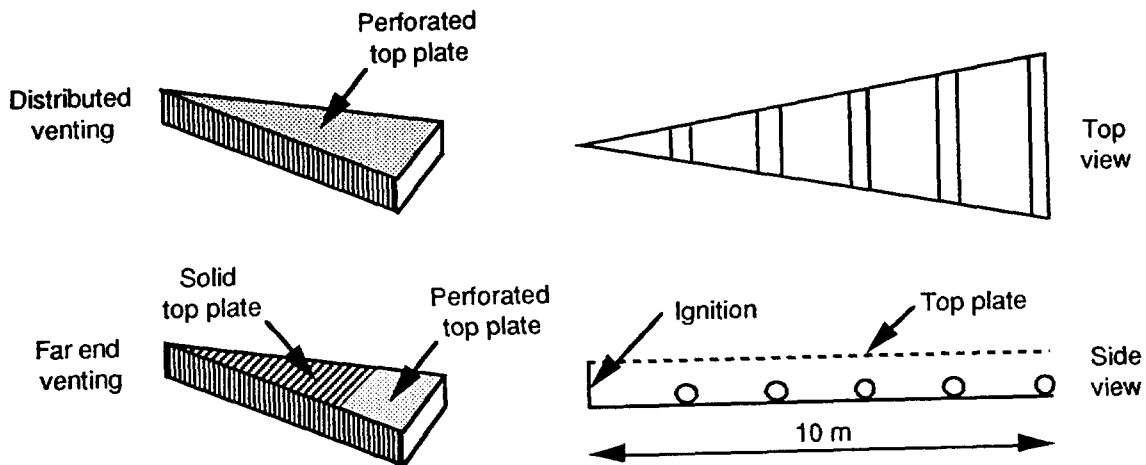
Figure 5.12. An wedge-shaped explosion vessel (Bjerketvedt et al. 1993).
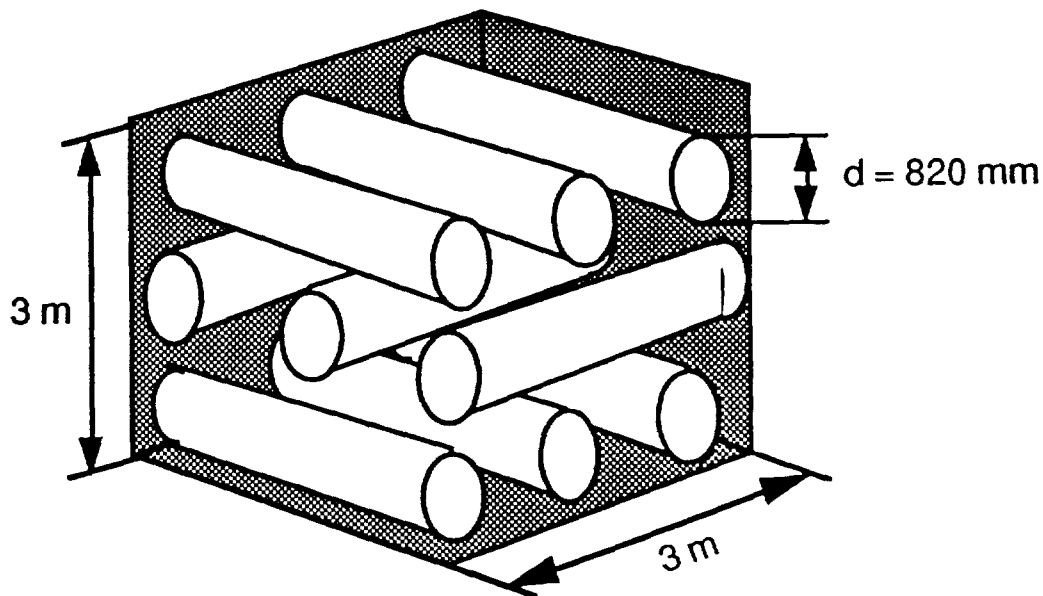
Figure 5.13. A corner with pipes (Bjerketvedt et al. 1993).

These represent the three basic modes of propagation of the flame front (Fig. 3.3):

1. a tube: axial propagation where the flame area remains constant
2. two parallel planes: cylindrical propagation where the flame area increases proportional to the distance covered
3. a corner: spherical propagation (1/8 of a sphere) where the flame area increases proportional to the square of the distance covered.

If the flame front is assumed to travel at constant speed S_f the pressure generated, when the gas is expanding against the atmosphere, can be calculated numerically (Fig. 5.14). It is seen that for any flame speed the highest pressure is generated in an axial geometry and the lowest in a spherical geometry.

48
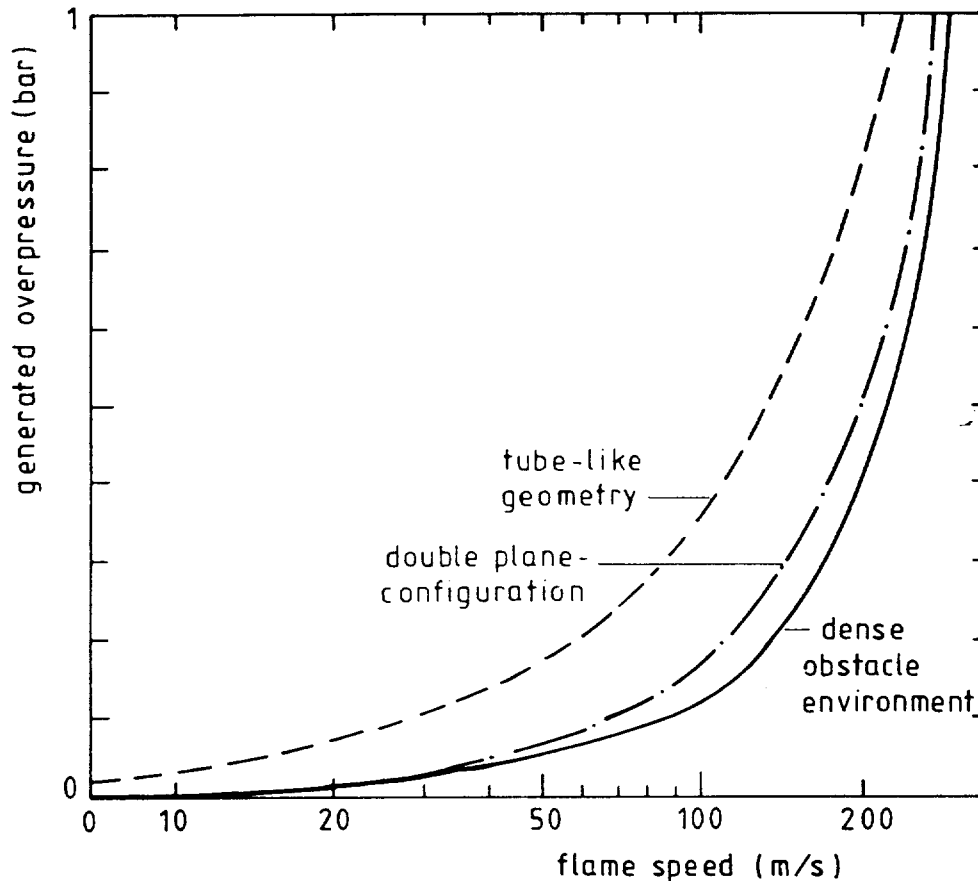
Figure 5.14. Overpressure as a function of flame speed in three geometries (AIChE 1994).

The amount of obstacles to the flow is usually expressed by two quantities. The **blockage ratio** is defined as the ratio of the total area of the obstacles to the total cross section of the vessel or room. In experiments in idealized geometries, the blockage ratio was the same for each row of obstacles. In real congested rooms, the blockage ratio will vary considerably when moving through the room (Fig. 5.15).

The **volume blockage ratio** is defined as the ratio of the total volume of obstacles to the volume of the room. This quantity is a constant describing a given room.

Hjertager (1991) makes the following points of the Christian Michelsens Institutt experiments:

- peak overpressures in propane-air explosions may be two to three times larger than in methane-air explosions
- sharp-edged obstacles generate double the pressure produced by round obstacles
- a grid of small obstacles (in a plane) cause higher explosion overpressure than a single obstacle with the same blockage ratio
- a non-homogenous mixture can explode with equally great violence as a homogenous stoichiometric mixture
- the explosion overpressures in the tube were two to three times higher than those in the radial geometries (ie. wedge-shaped and corner) for the same obstacle number and blockage ratio.
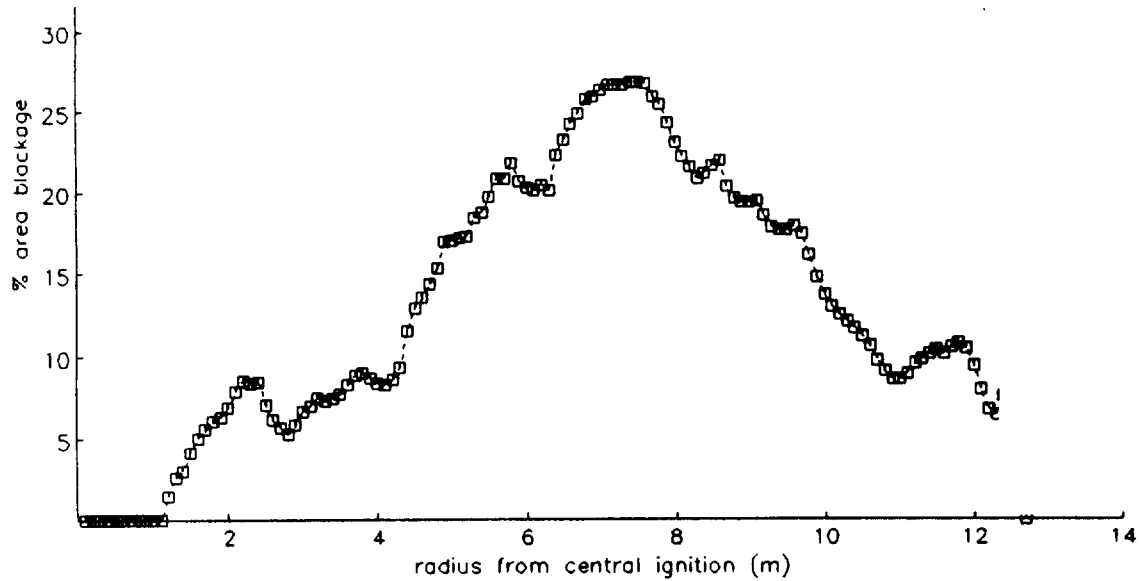
Figure 5.15. The blockage ratio in a room of an offshore platform (British Gas 1990).

Similar experiments have been made by TNO in the Netherlands since the early 1980's. Most of the work has been done in a parallel planes configuration where the obstacle grids are concentric circles around the ignition point. The idea is that the flame front will be cylindrical and meet one obstacle grid at a time (Fig. 5.16).
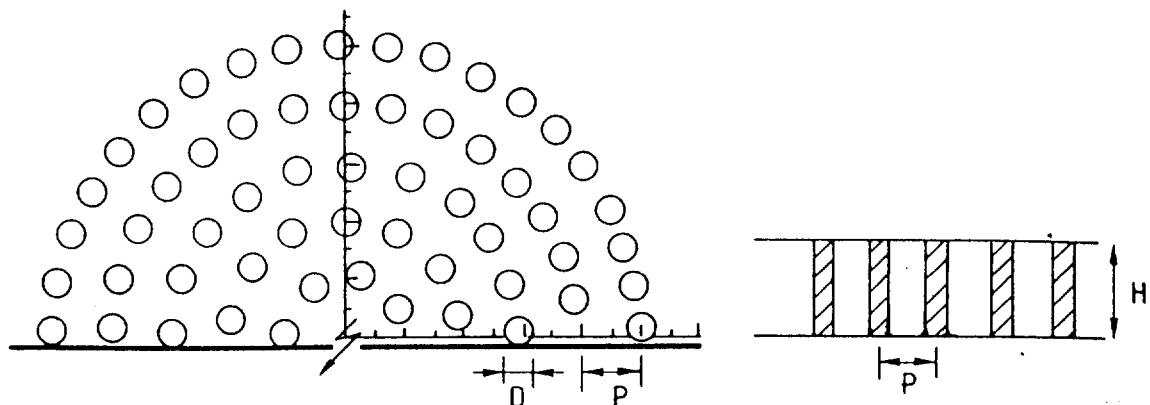
Figure 5.16. The explosion rig used by TNO. The obstacles are vertical pipes set up on concentric circles between two parallel planes (Mercx 1992).

The experiments have been performed in different scales to find out the scaling laws of the peak pressure. An obvious result was that the flame speed increased at each obstacle grid, but decreased after the flame had exited the experimental rig. The flame speeds and the resulting overpressures were significantly larger at large scale (Mercx 1992).

The effect of repeated obstacles on flame speed is caused by the positive feedback loop shown in Fig. 5.17. Combustion of the unburned mixture is followed by expansion of the combustion products and increase of pressure. Assuming that the geometry is such that the combustion products are trapped behind the frame front, a flow of unburned mixture is created, sometimes called **flame induced wind** (British Gas 1992).

50

The flow interacts with obstacles generating a turbulent flow field. When the flame front propagates into the turbulent flow field the burning rate is increased significantly. This increased burning rate will further increase the flow velocity and turbulence at new obstructions ahead of the flame. When a propagating flame front encounters repeated obstacles the positive feedback loop is circled several times. This mechanism of **flame acceleration** due to repeated obstacles (Fig. 5.17) may result in very high overpressures (over 1 bar) within relatively short distances of flame propagation (less than 1 m) (van Wingerden 1995).
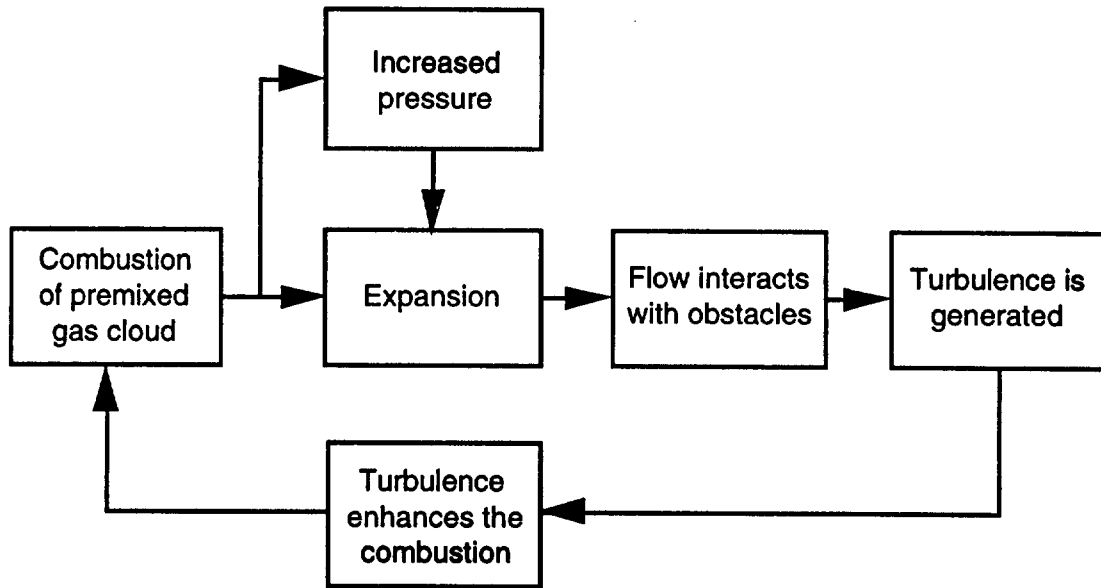
Figure 5.17. Positive feedback loop causing flame acceleration due to turbulence (van Wingerden 1995).

The first field experiments by British Gas on flame acceleration by obstacles were carried out in a 45 m long open side rig, through which the flame front propagated. Grid obstacles consisting of parallel pipes represented pipework arrays. The blockage ratio of each grid was 40 %. When four grid arrays were placed at 3 m intervals the maximum flame speeds attained were up to 10 times higher than in tests without obstacles.

Tests were also carried out where grid arrays were placed at 1.5 m intervals over the first 22.5 m length of the grid. The flame accelerated at each grid, reaching a maximum flame speed at the end of the obstructed region. Immediately after the flame emerged from the obstructed region in the unobstructed part of the rig, the flame rapidly decelerated (Fig. 5.18) (Harris & Wickens 1989).

Van Wingerden (1995) summarizes the effect of the different parameters of the obstacle configuration on flame speed:

- The most important parameter is the blockage ratio (Fig. 5.19). The higher the blockage ratio, the stronger the flame acceleration is. The reasons for this are the higher flow velocities causing stronger turbulence in the wake of obstacles and the larger volumes of unburned mixture behind the flame tip.

- The distance between two subsequent obstacles or rows of obstacles, often referred to as **pitch** (Fig 5.19). If the pitch is too large a continuous flame acceleration is not possible. If the pitch is too small the pocket of unburned mixture between the obstacles is too small to contribute to flame acceleration. Thus there is a range of values of the pitch corresponding to the largest flame acceleration.

- If the obstacles in a channel are placed in staggered configuration the generated explosion overpressures will be higher than in a non-staggered situation with the same blockage ratio (Fig. 5.19). The unburned pockets during flame propagation will be larger in the staggered configuration resulting in higher energy release rates. The way in which the obstacles are arranged will also hamper the outflow more, which will also increase the explosion overpressure.

- The shape of the obstacles has a dramatic effect on flame propagation. Experiments performed in cylindrical geometry show that sharp-edged obstacles can give terminal flame speeds that are twice those for cylindrical obstacles. The main reason for this is the larger turbulence generated in the wake of sharp-edged obstacles. A considerable reduction of the turbulence can be achieved by smoothing the edges of the obstacles.

- The laminar flame speed can be used as a scaling parameter for gas reactivity. Figure 5.20 shows the flame speeds measured for different fuels in the same rig divided by the laminar flame speed of the respective fuels. The flame radius increasing, the experimental ratios follow the same curve for all the fuels.
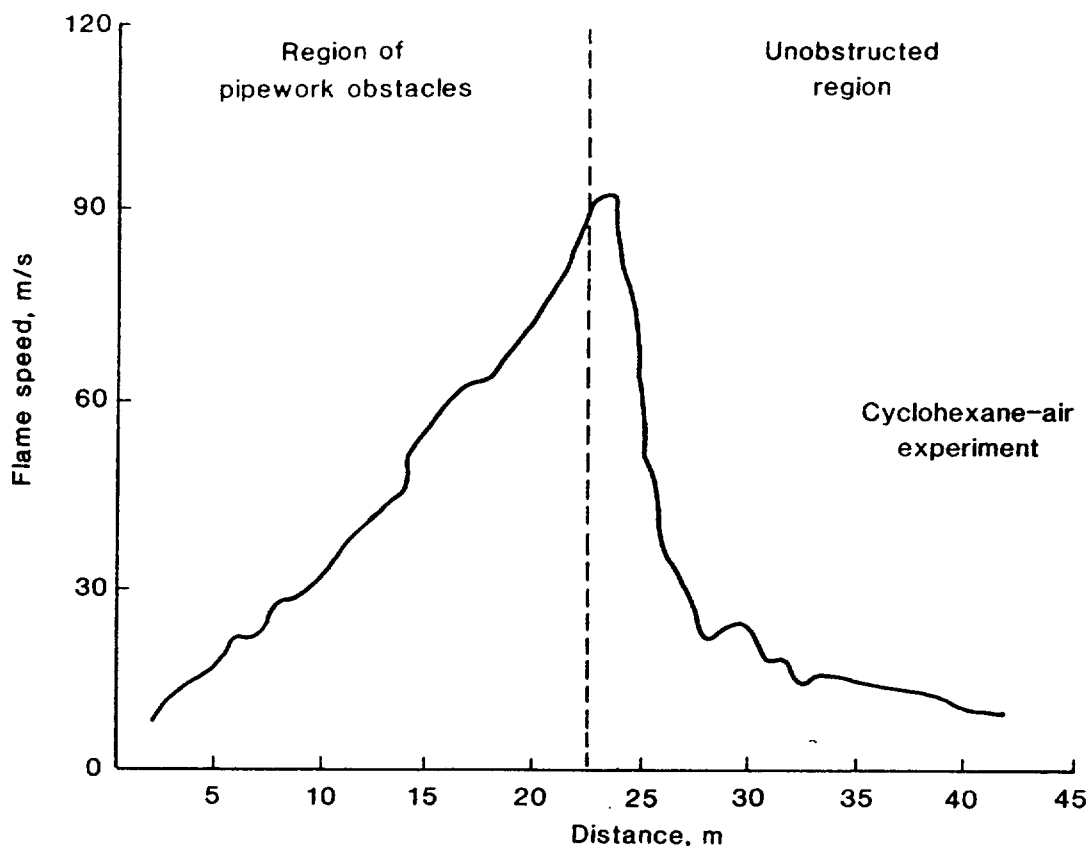
Figure 5.18. Flame acceleration in region of repeated obstacles and deceleration on emerging into unobstructed region (Harris & Wickens 1989).
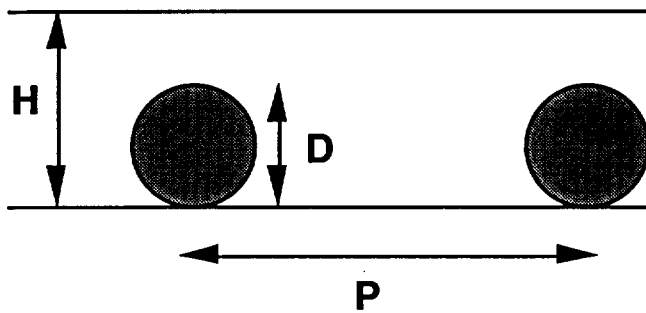
Figure 5.19. Obstacle parameters influencing flame propagation (van Wingerden 1995).
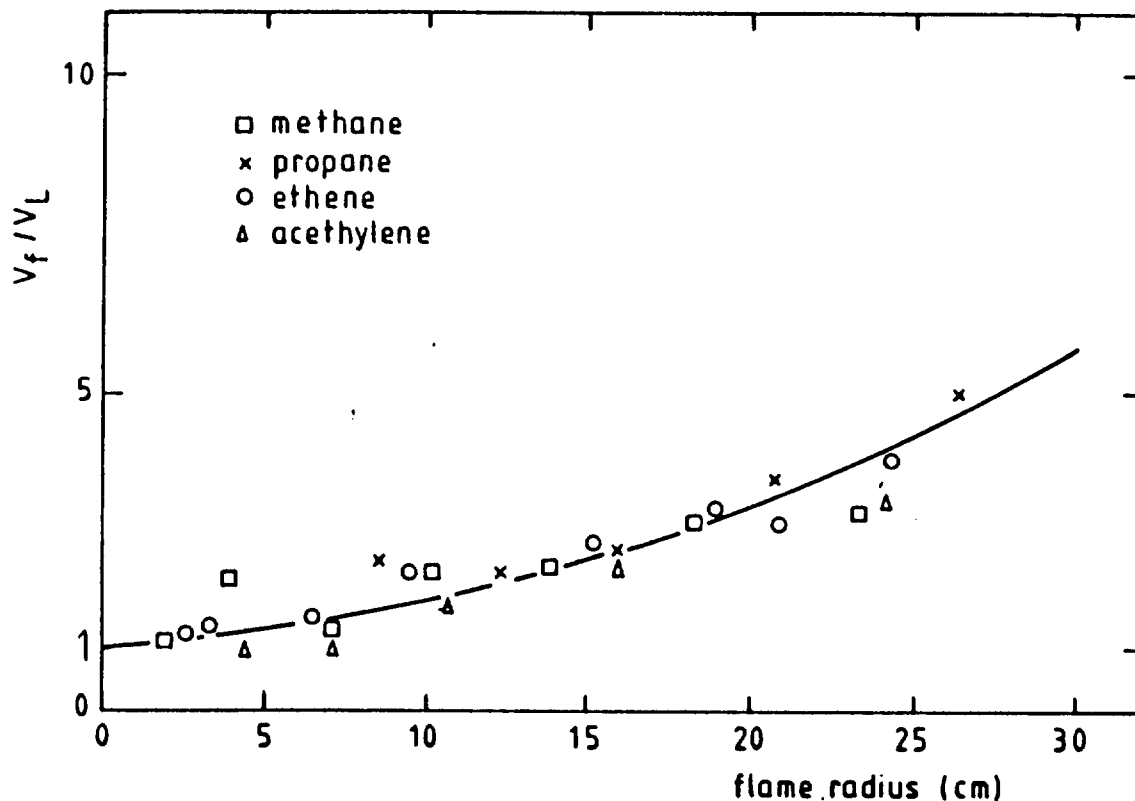
Figure 5.20. The ratios of experimental flame speeds to the laminar flame speed of different fuels (van Wingerden 1995).

Flame acceleration by repeated obstacles can to some extent be avoided by venting the hot combustion products at an early stage of the explosion. This can be achieved by using several suitably placed vents. Thanks to the vents, the hot combustion products will not be trapped behind the unburned gas. The flow velocity of unburned mixture and the resulting turbulence will be reduced. Early venting of hot combustion products is a very effective way of minimising the flame acceleration by repeated obstacles.

Early venting of hot combustion products is shown schematically in Fig. 5.21 which should be compared with Fig. 5.9. Normally all the explosion vents will open at the same pressure. This means that both unburned mixture and hot combustion products are vented simultaneously. However, if the flow of unburned mixture leads it past repeated obstacles, flame acceleration will most likely occur (Bjerketvedt et al. 1993).

The efficiency of early venting has been demonstrated in several test series. The wedge-shaped explosion vessel in Fig. 5.12 was used to study the effect of various types of vent arrangements in combination with repeated obstacles. A perforated top plate (distributed venting in Fig 5.12) was used to accomplish early venting. The porosity (the ratio of total area of holes to the area of the top plate) in different tests was 10, 20 and 50 %. In Fig. 5.22 the term "top confinement" means 100 % - porosity.

54
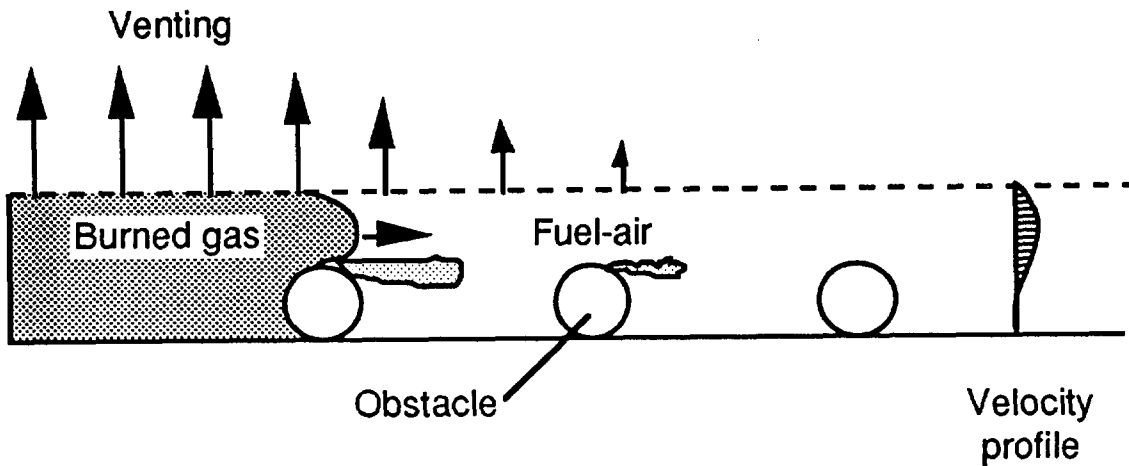
Figure 5.21. Early venting of hot combustion products will reduce turbulence generated by obstacles (Bjerketvedt et al. 1993).

Other tests were made with late venting. For 100 % top confinement the top plate was solid and the only vent opening was at the end of the vessel (with respect to ignition point). In the other late venting tests, the holes in the top plate were located at the far end of the vessel (far end venting in Fig. 5.12).

The explosion overpressures measured in these tests are shown in Figure 5.22. It is seen that without any vents in the top plate (100 % top confinement) the maximum explosion overpressure P_{red} was 2.8 bar. The maximum overpressure was reduced somewhat with a perforated top plate at the far end, but remained larger than 1 bar even with 50 % porosity (50 % top confinement).
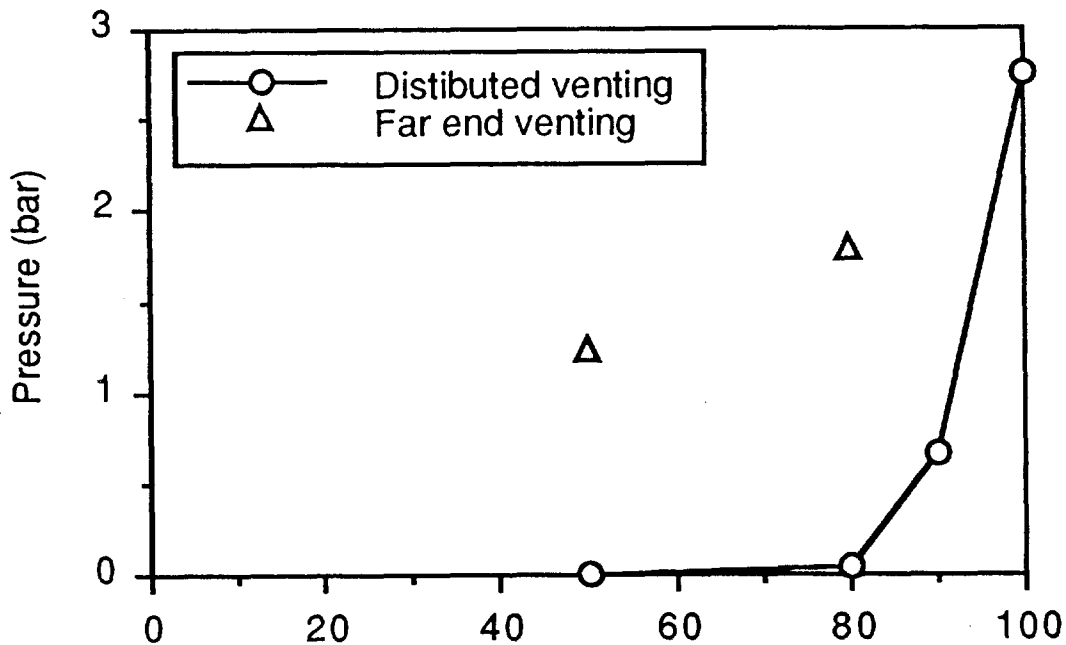
Figure 5.22. Explosion overpressure for propane-air mixtures as function of average top confinement [%] (Bjerketvedt et al. 1993).

On the contrary, a major reduction in explosion overpressure is achieved with early venting. Already distributed vents with 10 % porosity (90 % top confinement) were able to reduce the explosion overpressure by 75 % (from 2.8 to 0.6 bar). When the porosity was 20 % (80 % top confinement) the explosion overpressure was only 0.05 bar (98 % reduction) (Bjerketvedt et al. 1993).

Similar results were found by the using the rig in Fig. 5.16. Figure 5.23 shows the flame speeds measured for 7.5 % ethylene-air mixture and different porosities from evenly distributed vents. Already for the porosity 5 %, the flame speed was reduced by 65 %. The corresponding reduction in explosion overpressure was considerable larger. This can be estimated with the help of Fig. 5.14 and the result is about 85 % reduction. For a porosity of 25 % the flame acceleration was small and comparable to that measured without a top plate.
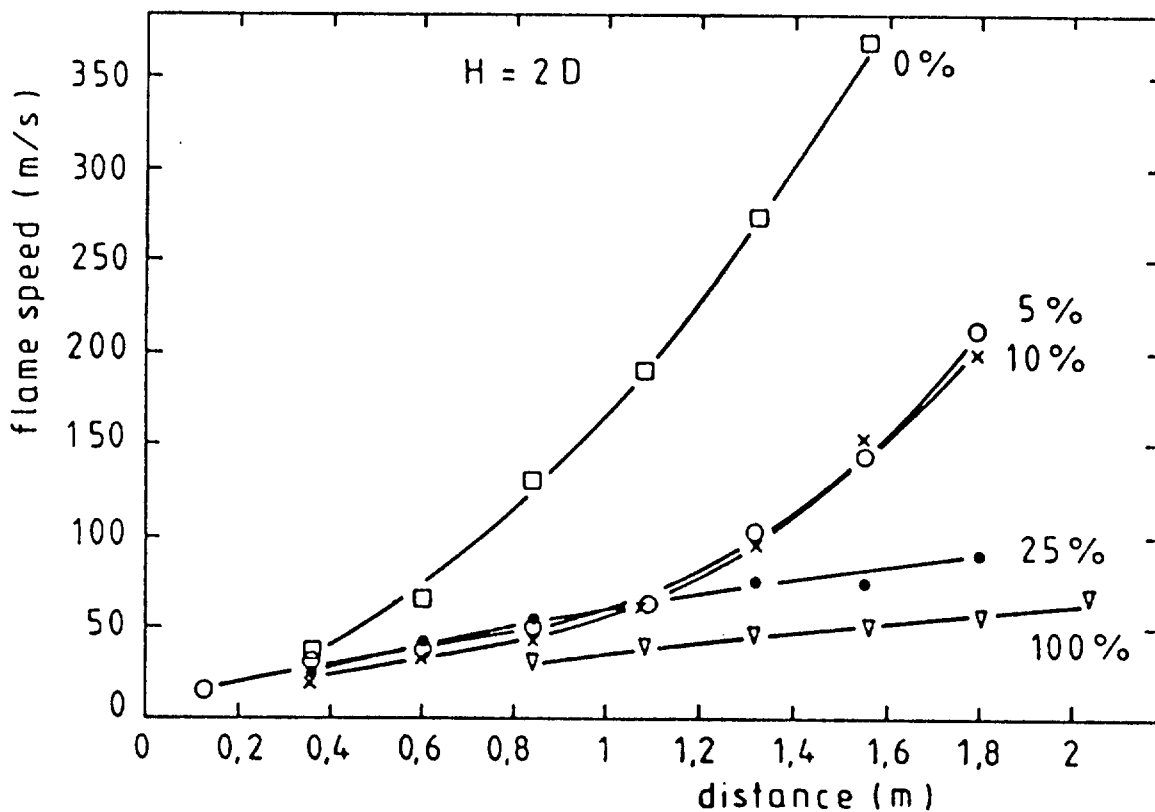
Figure 5.23. Flame speed versus distance for a 7.5 % ethylene-air mixture and different porosities (van Wingerden 1989).

In an earlier series of tests, horizontal pipes were used as repeated obstacles between two parallel planes. When the ignition point was moved from the centre of the rig to the edge, larger final flame speeds were measured (Fig. 5.24). This is a direct result of the fact that the flame had to pass more obstacles than for central ignition. It is true that the effect of hot combustion products venting at the back edge reduced the flow velocities and turbulence ahead the flame front (Fig 3.4). However, this effect was overcome by the larger number of obstacles (van Wingerden & Zeeuven 1986).
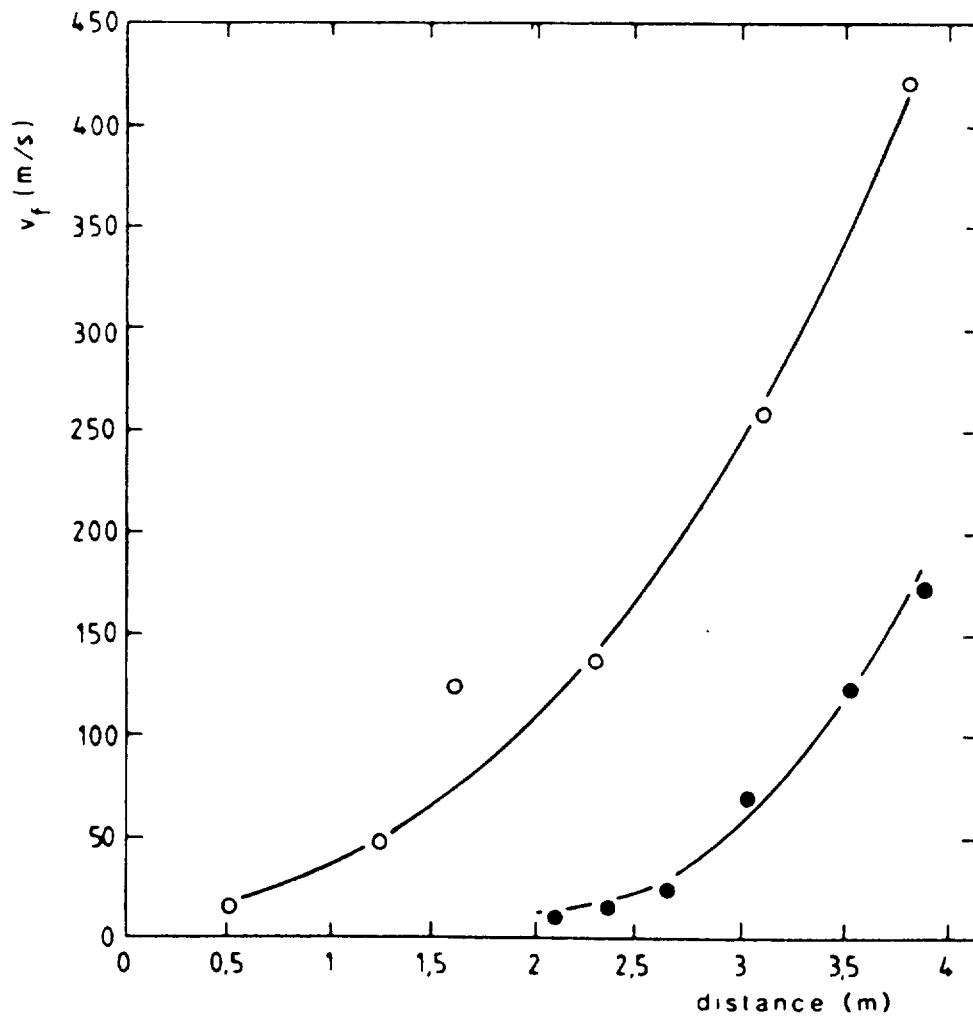
Figure 5.24. Flame speed versus distance for centrally (●) and edge-ignited (○) explosions in a double-plate configuration with obstacles (van Wingerden & Zeeuven 1986).

6 PREDICTION OF PRESSURES IN VENTED GAS EXPLOSIONS

Although the venting guidelines have been extensively used to design explosion vents for large rooms (several hundreds or several thousands of m³'s), they are based on tests in room-sized (up to 35 m³) or smaller chambers. The gas-air mixture has been initially quiescent and there have been no obstacles in the chamber. Thus it is not at all clear whether the guidelines are applicable to rooms of industrial scale.

British Gas (1990) performed a critical evaluation of venting guidelines. The aim was to find out whether they can be used for typical rooms (modules) of offshore platforms having volumes of 200 - 300 m³. Also the existence of obstacles in the room were kept in mind during the evaluation.

The results of original explosion tests had to be reassessed in the light of the four peak model. Usually only one pressure peak had been reported. Even when separate pressure peaks had been identified, there was a certain degree of ambiguity and confusion between authors. Usually only the first peak P_1 had been identified correctly. "The second peak" could be any one of P_2, P_3 and P_4.

Usually the venting guidelines are used to select the vent parameters A_v, P_v and w, from the parameters S_0, P_{red} and V determined by the fuel and building, respectively. Because the maximum explosion overpressure P_{red} is inversely proportional to A_v, the latter parameter is usually replaced by the dimensionless **vent coefficient** K. The vent coefficient K is defined in some guidelines as (Harris 1983)

$$K = \frac{A_s}{A_v} \tag{20}$$

where
A_s is the area of cross section of the room in the plane of vent [m²].

When K is defined by Eq. (20), it has the smallest possible value of 1. However, for non-cubical rooms this definition leads to vents of different sizes, depending upon which wall they are placed. This problem is usually solved by replacing the area A_s with the geometric mean of the areas of the walls

$$K = \frac{V^{2/3}}{A_v} \tag{21}$$

where
V is the volume of the room [m³].

The definition of vent coefficient Eq. (21) can be used for rooms with L_{max}/L_{min} no larger than 3. Studies by British Gas have shown that, in practice, reasonable agreement with experiment and the venting guidelines is obtained using Eq. (21). Some explanation for this result is that larger walls are closer to the ignition point (room

centre), leading to earlier onset of hot combustion products venting (Harris 1983).

Harris (1983) recommends the use of Eq. (20) when the vent is to be installed in the wall with largest area. When the vent is installed in a wall with a smaller area Eq. (21) should be used.

British Gas (1990) presents what was known in 1990 about the effects of explosion parameters such as vessel volume V, vessel shape L_{max}/L_{min}, vent coefficient K, reactivity of the mixture and turbulence on the magnitudes of the four pressure peaks. The analysis of published data, together with (confidential) studies by British Gas, indicate that the pressure peaks do not depend in the same way on these parameters.

It is to be stressed that British Gas (1990) considers only methane-air mixtures which are known to be little reactive and have little inclination to cellular instabilities. Thus, all the conclusions may not be valid for more reactive gas-air mixtures (eg. ethylene-air) and those capable of developing cellular instabilities (eg. rich propane-air).

6.1 THE FIRST PRESSURE PEAK P_1

All the available data demonstrates that P_1 is inversely proportional to the cube root of the room volume ie. $P_1 \propto 1/V^{1/3}$. This term is also included in some venting guidelines.

All the published data on vented explosions indicates that P_1 is directly proportional to the vent coefficient K ie. $P_1 \propto K$.

Because this peak is caused by the opening of the relief vent (which occurs at an early stage in the explosion process), vessel geometry has only a small influence on P_1. All the common venting guidelines are stated to be applicable to rooms with $L_{max}/L_{min} < 3$. In practice, this could probably be extended to $L_{max}/L_{min} \leq 6$ without any significant error.

Most of the empirical guidelines assume that P_1 is directly proportional to the burning velocity ($P_1 \propto S_0$) and this tends to be supported by published data.

Because P_1 is caused by the opening of the relief vent, it is anticipated that turbulence will not have significant effect on this peak pressure. Nevertheless turbulence, particularly pre-existing one caused by ventilation, will have some effect.

To predict P_1, two venting guidelines are recommended by British Gas (1990). The method is selected on the basis of relief vent opening pressure P_v.

The **Cubbage and Simmonds formula** is based on explosion tests in chambers of 0.2, 1.5, 2.8 and 14 m^3 volume using mainly town gas-air mixtures ($S_0 = 1.2$ m/s), although some experiments were carried on with other gases and vapours ($S_0 = 0.3 - 1.3$ m/s) (Cubbage and Simmonds 1955, 1957). The explosion relief panels were restrained either by gravity or a minimal amount of friction. Consequently, the formula

is strictly applicable only to situations in which P_v does not exceed about 2 kPa. P_1 is given in kPa by the formula

$$P_1 = \frac{S_0 (0.43 Kw + 2.8)}{V^{1/3}}$$ (22)

where
S_0 is the laminar burning velocity [m/s]
K   is the vent coefficient, $K = V^{2/3}/A_v$
w   is the mass per unit area of the vent cover [kg/m^2]
V   is the volume of the room [m^3].

Eq. (22) has been used successfully to predict P_1 in volumes up to 200 m^3, under non-turbulent conditions. The formula can be applied with confidence to empty rooms of volumes up to 200 - 300 m^3 having $L_{max}/L_{min} < 3$, provided that the rooms have relatively smooth internal surfaces. In addition, Eq. (22) should be applied only to those situations in which the mixture is initially quiescent. The vent coefficient K should be less than 5 and mass per unit area of the vent cover w should not exceed 24 kg/m^2.

The **Cubbage and Marshall formula** is based on experiments in chambers of volumes up to 30 m^3, using a variety of fuel gases to maximize the range of S_0. This venting guideline is applicable to situations in which the explosion relief vent is positively fixed and must be broken by the internal pressure to create an open vent. Consequently, the formula is applicable to situations where P_v is larger than about 2 kPa. P_1 is given in kPa by the formula

$$P_1 = P_v + \frac{2.3 S_0^2 Kw}{V^{1/3}}$$ (23)

Under these conditions of application, the formula Eq. (23) has been used successfully to predict explosion overpressures in rooms of volumes up to 200 m^3. The formula will provide good estimates for P_1 or A_v for non-turbulent explosions of mixtures having $S_0 < 0.5$ m/s.

The fact that Eq. (23) is proportional to S_0^2, and not to S_0, leads to some overestimation of P_1 for mixtures with $S_0 > 0.5$ m/s. On the basis of experiments with such mixtures, British Gas (1990) recommends that the coefficient in Eq. (23) should be reduced to 0.7

$$P_1 = P_v + \frac{0.7 S_0^2 Kw}{V^{1/3}}$$ (24)

The **modified Cubbage and Marshall formula** Eq. (24) is found to agree with experimental data for S_0 in the range 0.5 - 1 m/s. Besides, the modification does not significantly affect the accuracy of prediction for mixtures with $S_0 < 0.5$ m/s since for these mixtures the first term P_v tends to be dominant.

Eq. (23) or Eq. (24) can be applied with confidence to empty rooms of volumes up to 200 - 300 m³ having $L_{max}/L_{min} < 3$, provided that the rooms have relatively smooth internal surfaces. In addition, Eqs. (23) or (24) should be applied only to those situations in which the mixture is initially quiescent. The vent coefficient K should be less than 6 and mass per unit area of the vent cover w should be in the range 2.4 to 24 kg/m². The product Kw should not exceed 73 kg/m².

6.2   THE SECOND PRESSURE PEAK P_2

The only venting formula for P_2 is due to Cubbage and Simmonds and does not include a volume term. Studies by British Gas indicated that P_2 is approximately proportional to the cube root of the room volume ie. $P_2 \propto V^{1/3}$. This approximate correlation was validated only up to volumes of 27 m³.

The one available venting formula indicates that P_2 is linearly proportional to K ie. $P_2 \propto K$. Analysis of published data and more recent studies carried out by British Gas tend to confirm this relationship.

In effect, P_2 depends on the volume of unburned mixture expelled from the room through the relief vent before the flame emerges. Consequently, although room geometry will have an influence, P_2 will depend more on the relative locations of the relief vent and source of ignition together with P_v.

The empirical formula by Cubbage and Simmonds indicates that $P_2 \propto S_0$. An analysis of literature data and more recent studies by British Gas tend to support this relationship. British Gas (1990) did not find much published data on the influence of turbulence on P_2, but considered it reasonable to assume that the turbulence will lead to an increase in P_2.

However, the turbulence of an external explosion will be increased if unburned mixture is vented into a partially confined area. This fact had already been recognized in some published guidelines which provide guidance on the spacing of relief vent from external obstructions, such as walls, to minimize this effect. For similar reasons, even a short vent discharge duct will increase significantly P_2.

The **Cubbage and Simmonds formula** for P_2 is based on the same explosion tests (Cubbage and Simmonds 1955, 1957) as their formula for P_1, Eq. (22). P_2 is given in kPa by the formula

$$P_2 = 5.8 S_0 K \tag{25}$$

Eq. (25) has successfully been used to predict P_2 in volumes up to 200 m³, under non-turbulent conditions. However, it is known that Eq. (25) overpredicts P_2 at small volumes for mixtures with S_0 less that about 0.5 m/s. At larger volumes, this may not be so. British Gas (1990) includes volume dependence to get a closer agreement with experimental data (the **modified Cubbage and Simmonds formula** for P_2).

$$P_2 = 5.8 S_0 K V^{1/3} \tag{26}$$

Eq. (26) can be applied to rooms of volumes up to about 300 m^3 having $L_{max}/L_{min} <$ 3 to provide an indication of P_2. The vent coefficient K should be less than 5 and mass per unit area of the vent cover w should not exceed 24 kg/m^2. However, P_2 will depend more on the relative locations of the relief vent and source of ignition than on V (British Gas 1990). The volume term is probably valid for central ignition, only (Kees van Wingerden, Christian Michelsen Research, private communication).

Bimson et al. (1993) have performed explosion tests in a rectangular (10 m x 8.75 m x 6.25 m) 550 m^3 chamber with a single 27 m^2 vent. The chamber was filled with fuel rich mixture of methane-air or propane-air and ignited remote from the vent. In the first five tests there were no obstacles in the chamber. The internal peak pressures P_{red} ranged 4.7 - 5.3 kPa (methane) and 9.4 - 12.8 kPa (propane). Inserting K defined by Eq..(21) and S_0 in Eq. (25) one finds $P_2 = 6.4$ kPa (methane) and 7.4 kPa (propane), which are quite satisfactory predictions. The modified formula Eq. (26), however, overpredicts P_{red} significantly: $P_2 = 52$ kPa (methane) and 60 kPa (propane).

6.3   THE THIRD PRESSURE PEAK P_3

P_3 is associated with the maximum rate of generation of combustion products and usually occurs when the flame area is a maximum. Assuming that explosion chambers are geometrically similar and have the same K, P_3 should be independent of V, provided the flame speed remains a constant. However, studies by British Gas in a number of cubical chambers ranging in volume from 0.05 m^3 to 27 m^3 demonstrated that P_3 increases with V. Data from experiments by Zalosh (1980) support this.

Probably this is due to an increase in flame speed as a result of perturbations on the flame front as the flame propagates over the larger distances characteristic of the larger chambers. However, there is no simple method by which the observed increase in P_3 can be related to V.

Experimental data obtained by British Gas for natural gas-air explosions in chambers up to 27 m^3 indicate that $P_3 \propto K^2$. The simple venting guideline by Runes (1972) includes the same relationship. The tests by Zalosh (1980) in chambers of volumes 0.18 - 11.1 m^3 lead to a relationship $P_3 \propto K^n$ where n = 1.5 - 1.7.

Vessel geometry has a marked influence on P_3. All the available data indicates that P_3 will be larger in a cubical room than a room of the same volume but $L_{max}/L_{min} > 1$.

There are no published formulas which relate P_3 to S_0. However, analysis of published data suggests a relationship of the form $P_3 \propto S_0$. The simple, semi-empirical venting guideline of Runes (1972) also indicates such a relationship.

As P_3 is associated with the maximum rate of volume generation, it is to be expected that turbulence will have a considerable effect on P_3. This is confirmed both by British

Gas studies and published data. However, there is no guidance as to how the published data can be incorporated into a simple empirical relationship and hence extrapolated to other situations.

Normally, P_3 will not be the dominant one in a vented explosion, and will be considerable smaller than P_1. It only becomes of significant magnitude
- with small explosion vents (K > 10) and/or
- in non-cubical, duct-like rooms (L_{max}/L_{min} > 6) or
- under turbulent conditions.

6.4   THE FOURTH PRESSURE PEAK P_4

The fourth pressure peak P_4 is defined as the net overpressure developed by the high combustion rate. The pressure oscillations at the frequency of the standing acoustic wave have higher peak values, but they are too fast to cause any loads on the walls and other load-bearing structures (Fig. 6.1).
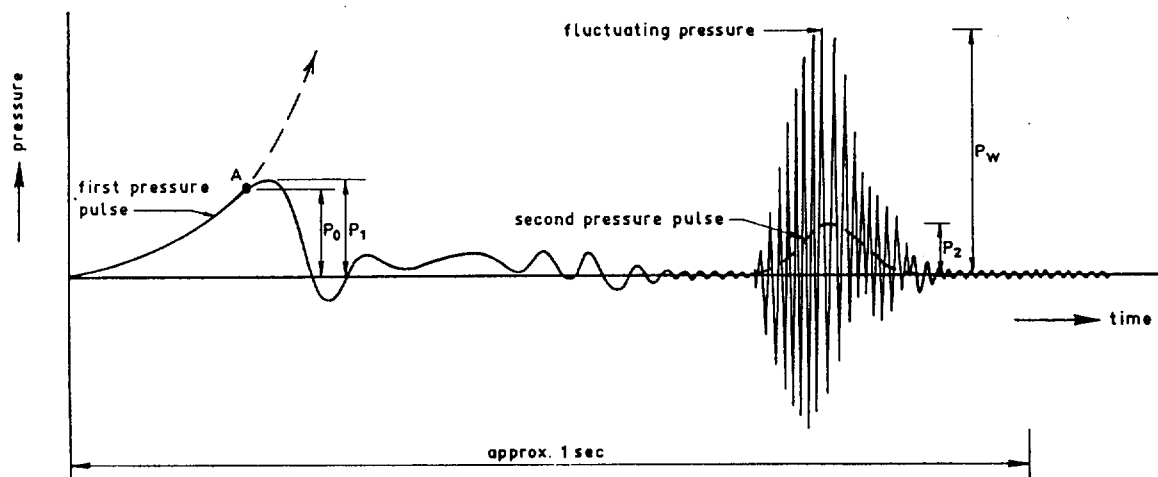
Figure 6.1. An experimental pressure-time curve (Dragosavić 1973). Notation differences: $P_0 = P_v$, second pressure pulse = fourth pressure peak, $P_2 = P_4$.

Published data, together with studies carried by British Gas, indicate that P_4 is independent of chamber volume for V < 50 m³. However, the British Gas studies have demonstrated that this oscillatory peak will occur more readily in larger volumes - presumably because the excitation energy associated with the fundamental acoustic mode of a chamber is less in a larger volume.

Based on an extensive series of experiments by British Gas, P_4 [kPa] for 3.5 < K < 10 can be described as (British Gas 1990)

$$P_4 = 30K - 70 \tag{27}$$

This relationship also describes adequately the published data.   Eq. (27) applies strictly to cubical vessels. Both the British Gas studies and published information show that P_4 decreases considerably as the vessel geometry becomes more rectangular, the

other factors remaining constant.

Data available in the literature indicates that P_4 increases with fuel reactivity and this is confirmed by British Gas studies. The magnitude of all four peaks P_1 to P_4 vary with fuel concentration. P_1 to P_3 have a maximum at the concentration corresponding to the maximum S_0 (British Gas 1990). However, P_4 is greater for mixtures exhibiting a cellular instability of the flame front.

The cellular instability of the flame front occurs when the mixture becomes locally more reactive (ie. fuel concentration changes so that S_0 is increased) due to selective diffusion of reactants. As a result it occurs more easily for rich mixtures of fuels with a diffusivity lower than that of oxygen and in lean mixtures of fuels with a higher diffusivity than oxygen (Kees van Wingerden, Christian Michelsen Research, private communication).

In contrast to the three first peaks P_1 to P_3, the presence of turbulence in the unburned mixture leads to a reduction of P_4. Where the turbulence is caused by obstacles in the room, P_4 may not be produced. The obstacles can prevent the formation of the standing acoustic wave necessary for the generation of P_4.

6.5 BARTKNECHT'S METHOD

Bartknecht's method for predicting P_{red} or A_v is based on the cube root law with experimental values of the constant K_g. Bartknecht (1981) showed that, for a given vent opening pressure P_v, in order to maintain the same explosion overpressure P_{red} in vessels of different volumes V, the **vent ratio** $f = A_v/V$ must also follow the cube root law ie. $fV^{1/3}$ is a constant. This quantity is the inverse of the vent coefficient $K = V^{2/3}/A_v$ which, thus, must be a constant.

Bartknecht (1981) verified this relationship in a series of experiments in a range of explosion vessels having $L_{max}/L_{min} < 5$ and volumes up to about 30 m^3. The opening pressure of the plastic foil bursting disc relief was 10 - 50 kPa. Mixtures of methane, propane, coke gas and hydrogen with air were used. Based on these tests, nomograms are presented which allow A_v to be calculated from known P_v, V, P_{red} and K_g. Although the nomograms refer to vessel volumes up to 1000 m^3, they have only been verified up to about 30 m^3.

Bartknecht's method should provide adequate predictions of P_1 or A_v when applied to empty vessels having $L_{max}/L_{min} < 5$ and volumes not exceeding about 100 m^3. The vessels should also have relatively smooth internal surfaces. The method should be applied with some caution to larger vessels, particularly in situations where significant levels of turbulence may be developed (British Gas 1990).

Bartknecht (1993) has re-evaluated several hundred gas explosion tests carried out over the last 20 years. The nomographs are replaced by a formula which holds for cubic or nearly cubic vessels $(L_{max}/L_{min} < 2)$ filled with non-turbulent stoichiometric gas-air mixtures. The necessary vent size A_v $[m^2]$ can be calculated from the experimental

constant K_g characterizing the mixture, the maximum acceptable internal pressure P_{red} [bar], the static opening pressure of the vent P_v [bar] and the vessel volume V [m³] from the formula

$$A_v = \left[\frac{0.1265 \log K_g - 0.0567}{P_{red}^{0.5817}} + \frac{0.1754 (P_v - 0.1)}{P_{red}^{0.5722}} \right] V^{2/3} \qquad (28)$$

The additional limitations of validity of Eq. (28) are:
- 50 m·bar/s $\leq$ K_g $\leq$ 500 m·bar/s
- 0.1 bar $\leq$ P_{red} $\leq$ 2 bar
- 10 kPa $\leq$ P_v $\leq$ 50 kPa
- 0.1 $\leq$ V $\leq$ 1000 m³.

The relatively high values of P_v in Bartknecht's method preclude the application of the method to normal buildings.

6.6 VENTING GUIDELINES NOT RECOMMENDED BY BRITISH GAS

The **vent ratio method** uses the vent ratio defined as the relief vent size A_v divided by the room volume V: $f = A_v/V$. Usually, in order for the maximum explosion overpressure P_{red} to remain constant for a particular fuel, f is assumed to remain constant for all values of V. In practice however, the vent sizes A_v calculated from small-scale test data are excessive for large rooms. This method is not recommended by British Gas (1990) and has actually been superseded by others (using the vent coefficient K) in the more recent guidelines.

Runes' method is based on the assumption that the maximum pressure developed in vented explosion occurs when the rate of volume generation Eq. (16) and the outflow rate Eq. (18) are equal. The volume generation rate Eq. (16) is taken to have its maximum value which is assumed to occur at maximum flame area ie. just before the flame is quenched by contact with the walls. On this basis, Runes (1972) presents an equation relating vent size A_v and maximum explosion overpressure P_{red}

$$A_v = \frac{C_R L_1 L_2}{\sqrt{P_{red}}} \qquad (29)$$

where
C_R is a constant depending on the fuel and turbulence [kPa$^{1/2}$]
L_1 and L_2 are the two largest dimensions of the room [m].

In effect, the ratio $L_1 L_2/A_v$ is the vent coefficient K. Thus, Runes' venting formula Eq. (29) can be simplified to

$$P_{red} = C_R^2 K^2 \tag{30}$$

The derivation by Runes (1972) actually leads to an equation for the prediction of P_3. The method predicts significantly larger vent sizes A_v than are necessary in non-turbulent explosions, even for large V and/or non-cubical rooms. In turbulent explosions, the method would provide reasonable estimates for P_{red}, if an appropriate value for the parameter C_R could be defined. However, there is no acceptable way to determine C_R for turbulent explosions, other than a full-scale experiment. For these reasons, British Gas (1990) does not recommend the Runes' method.

NFPA 68. The document distinguishes between the venting of explosions in low and high strength enclosures, recommending different methods of calculation for each type. A variation of Runes' method is recommended for low strength enclosures, capable of withstanding overpressures of no more than 10 kPa. For high strength enclosures, capable of withstanding overpressures of more than 10 kPa, the Bartknecht nomograms are recommended.

The usefulness of NFPA 68 is reduced considerably by the choice of the Runes equation as the recommended method for calculating the venting requirements of low strength enclosures. This has serious shortcomings and does not provide good estimates of A_v or P_{red} in most situations. Application of the document is limited in effect to the use of the Bartknecht nomograms (British Gas 1990).

Decker's method (Decker 1971) is based on a similar calculation procedure to that of Runes. The method is based on the assumption that the venting rate is proportional to the rate of pressure rise at the moment the relief vent opens ie. at the pressure P_v. Decker's method effectively predicts P_1. However, as the method predicts an A_v which is large enough to limit P_1 to P_v, the calculation leads to vent sizes A_v that are well in excess of those actually required. For these reasons, British Gas (1990) does not recommend the Decker's method.

The **Rasbash formulas** are based on experiments in small chambers using propane-air mixtures and explosion relief panels with P_v up to about 4 kPa. The original empirical formula was generalized for gases other than propane and the resulting formula for P_{red} [kPa] is (Rasbash 1969)

$$P_{red} = 1.5P_v + 7.77S_0K \tag{31}$$

The first term describes the effect of P_v and the second term expresses that of A_v. The second term is based on a collation of available information on experiments using propane and other gases with similar combustion properties. Later, Rasbash modified Eq. (31) to include the parameters w and V (Rasbash et al. 1976). The additional term is just the Cubbage and Simmonds formula for P_1 Eq. (22).

$$P_{red} = 1.5 P_v + \frac{S_0(0.43 Kw + 2.8)}{V^{1/3}} + 7.77 S_0 K \tag{32}$$

The Rasbash formulas, in fact, describe P_{red} as the sum of P_1 and P_2. However, according to the four peak model, the pressure peaks are produced in successive stages of the explosion and the individual peaks are not additive. Except for the term of the Cubbage and Simmonds formula in Eq. (32), the Rasbash formulas do not include a volume term. Extrapolation of the formulas from the small-scale tests on which they are based to larger volumes V is therefore difficult.

While the Rasbash formulas have a fairly widespread usage, British Gas (1990) does not recommend them for the reasons outlined above.

The **Bradley and Mitcheson method** is based on a theoretical model of vented explosion (Bradley & Mitcheson 1978a). The model uses the dimensionless parameters $\bar{A}$ and $\bar{S}_0$ defined as

$$\bar{A} = \frac{C_d A_v}{A_s} \tag{33}$$

where
C_d is the discharge coefficient of the vent, $C_d = 0.6$
A_s is the area of cross section of the room in the plane of vent [m^2].

$$\bar{S}_0 = \frac{S_0(E-1)}{c_0} \tag{34}$$

where
c_0 is the velocity of sound in the unburned mixture [m/s].

The model was applied a large amount of small-scale test data. The aim was to derive a "safe recommendation" for the vent size A_v so that it should provide an upper limit to all test results. This lead into two curves, one for initially uncovered vents and the other for covered vents opening at P_v (Bradley & Mitcheson 1978b).

The curve for uncovered vents is not relevant to this report. The curve for covered vents was based on the criterion that the maximum explosion overpressure P_{red} should not exceed P_v.

$$\frac{\bar{A}}{\bar{S}_0} \geq \left[\frac{2.4}{P_v} \right]^{1.43} \quad \text{for } P_{red} > 101 \text{ kPa} \tag{35}$$

and

$$\frac{\overline{A}}{S_0} \geq \left[\frac{12.3}{P_v} \right]^{\frac{1}{2}} \quad \text{for} \quad P_{red} < 101 \text{ kPa} \tag{36}$$

The curve determined by Eqs. (35) and (36) is drawn in Fig. 6.2 with the experimental and theoretical data used by Bradley and Mitcheson (1978b).
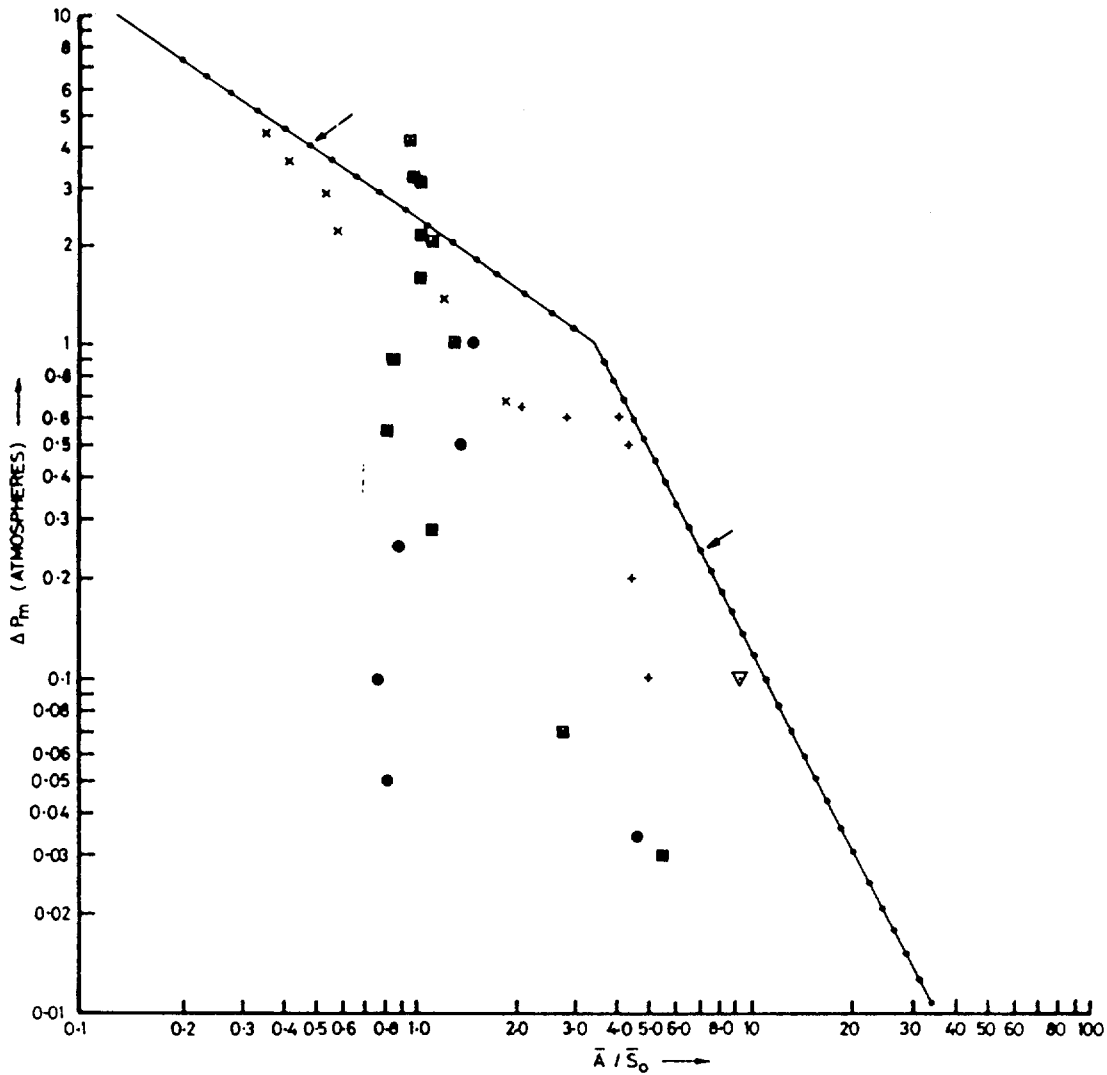
Figure 6.2. The "safe recommendation" for A_v by Bradley & Mitcheson (1978b).

The Bradley and Mitcheson method is based on an analysis of relative small-scale experimental data obtained under zero or low turbulence conditions. For covered relief vents, Eq. (36) predicts larger A_v than are necessary for non-turbulent explosions in rooms up to a few cubic metres in volume. However, for larger rooms ($V > 50$ m^3), particularly when significant turbulence can be generated, the recommendations for A_v are inadequate. For these reasons, British Gas (1990) does not recommend the Bradley and Mitcheson method.

Zeeuwen and van Wingerden (1985) have verified the Bradley and Mitcheson method with data from explosion incidents and large-scale experiments. The maximum pressures in explosion incidents were estimated by analysing the damages. For explosions in more or less empty rooms (dwellings, schools and boiler rooms), Eqs. (35) and (36) give a good prediction of the maximum pressure P_{red} (Fig. 6.3).
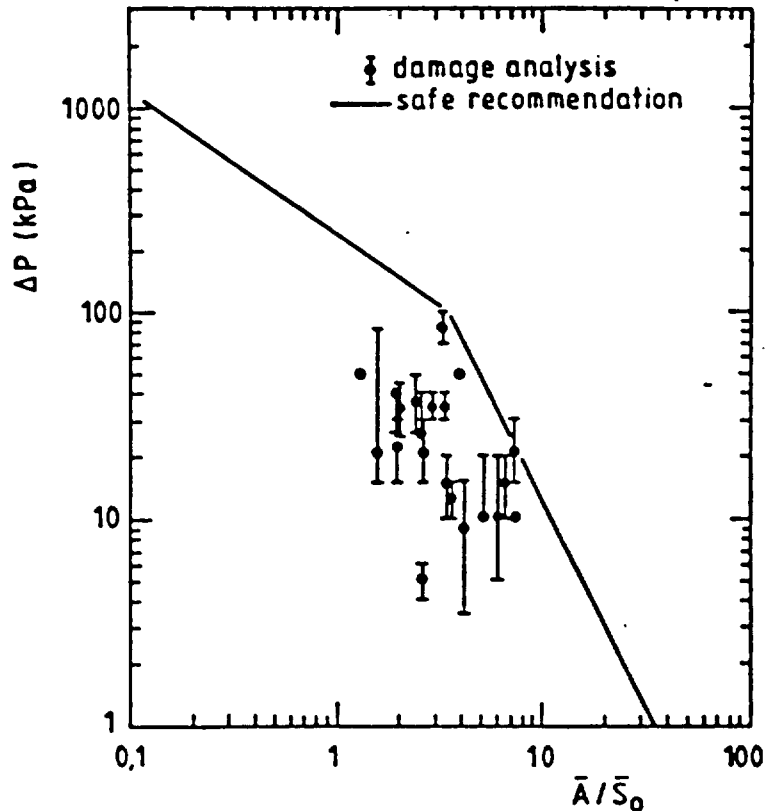
Figure 6.3. Verification of the Bradley and Mitcheson method with data from explosions in dwellings, schools and boiler-rooms (Zeeuwen & van Wingerden 1985).

For explosions in industrial installations (Fig 6.4), the Bradley and Mitcheson method may underestimate P_{red} because it neglects flame acceleration by obstacles. Eqs. (35) and (36) also underestimate the oscillatory peak P_4 measured in some large-scale explosion tests in empty chambers. When neither of these effects is present Eqs. (35) and (36) can be applied with confidence to estimate P_{red} (Kees van Wingerden, Christian Michelsen Research, private communication).
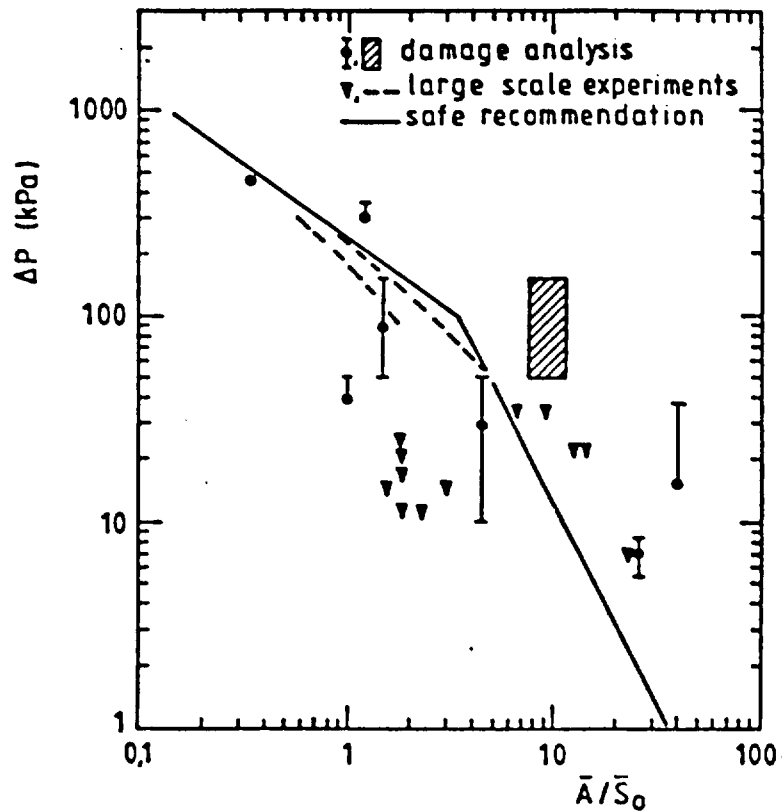
Figure 6.4. Verification of the Bradley and Mitcheson method with data from explosions in industrial installations and large-scale explosion tests (Zeeuwen & van Wingerden 1985).

6.7 LONG ROOMS AND DUCTS

As stated previously, P_1 will be normally unaffected by the room geometry if L_{max}/L_{min} ≤ 6. However, in long rooms and ducts P_1 is unlikely to be the largest pressure peak, more likely this will by P_2 or P_3. The most comprehensive venting guideline for such rooms is by Rasbash and Rogowski (1960, 1963). For values of the vent coefficient K between 2 and 32 and values of the length to diameter ratio L/D of the duct between 6 and 30, and with a single vent positioned at the end remote from the ignition source P_{red} [kPa] is

$$P_{red} = 5.6K \ ... \ 12.6K \tag{37}$$

For a vent with K = 1 and L/D in the range 6 - 48, P_{red} varied as

$$P_{red} = 0.49 \frac{L}{D} \tag{38}$$

where
L   is the length of the duct [m]
D   is the (hydraulic) diameter of the duct [m].

Much lower pressures P_{red} were observed when the mixture was ignited close to the vent.

Studies by British Gas in ducts with L/D up to 18 confirm these results in that P_{red} was found to conform to the relationship

$$P_{red} \propto \frac{l}{D} K V^{1/3} \tag{39}$$

where

l   is the distance between the vent and ignition source [m].

The volume term in Eq. (39) confirms that P_{red} corresponds to P_2 or P_3 rather than P_1 (British Gas 1990).

Tite et al. (1991) have carried out tests in ducts with square cross section having widths 0.61 and 0.92 m and L/D in the range 3 to 15. The results obtained were used to derive empirical expressions for P_{red} in ducts containing initially quiescent natural gas-air mixtures. The expressions can be used to specify appropriate explosion relief requirements for such ducts.

6.8   EXTERNAL EXPLOSIONS

The following discussion on external explosion is based mainly on the review article by van Wingerden (1993). The first published study on blast waves due to vented explosions was by Solberg et al. (1979). The experiments were performed with propane in a rectangular (2.5 m x 3.5 m x 4 m) 35 m³ chamber. The mixture was ignited in the centre of the chamber.

The result showed that, in spite of very high pressure peaks inside, only a weak blast wave was generated. The blast wave consisted of a single sharp pressure peak which, according to the authors, corresponded to the opening of the vent. Later during the explosion, much higher pressures were measures in the chamber but no corresponding effect was detected outside.

Palmer & Tonkin (1980) investigated the blast wave from a vented natural gas explosion in a 28 m³ chamber. Different vent sizes and vent covers were used. The mixture was ignited at the wall remote from the vent. Explosion overpressures were measured both inside the chamber and at several points outside the chamber. The results showed that the maximum pressures at 18 m from the vent were half the maximum pressures at 9 m. This result is in agreement with the acoustic decay of the blast wave with distance ($P_{ext} \propto 1/r$).

Fig. 6.5 shows the relationship between the maximum pressure P_{ext} at 9 m from the vent and the maximum pressure in the chamber P_{red}. The experimental points indicate a linear relationship between these peak pressures.
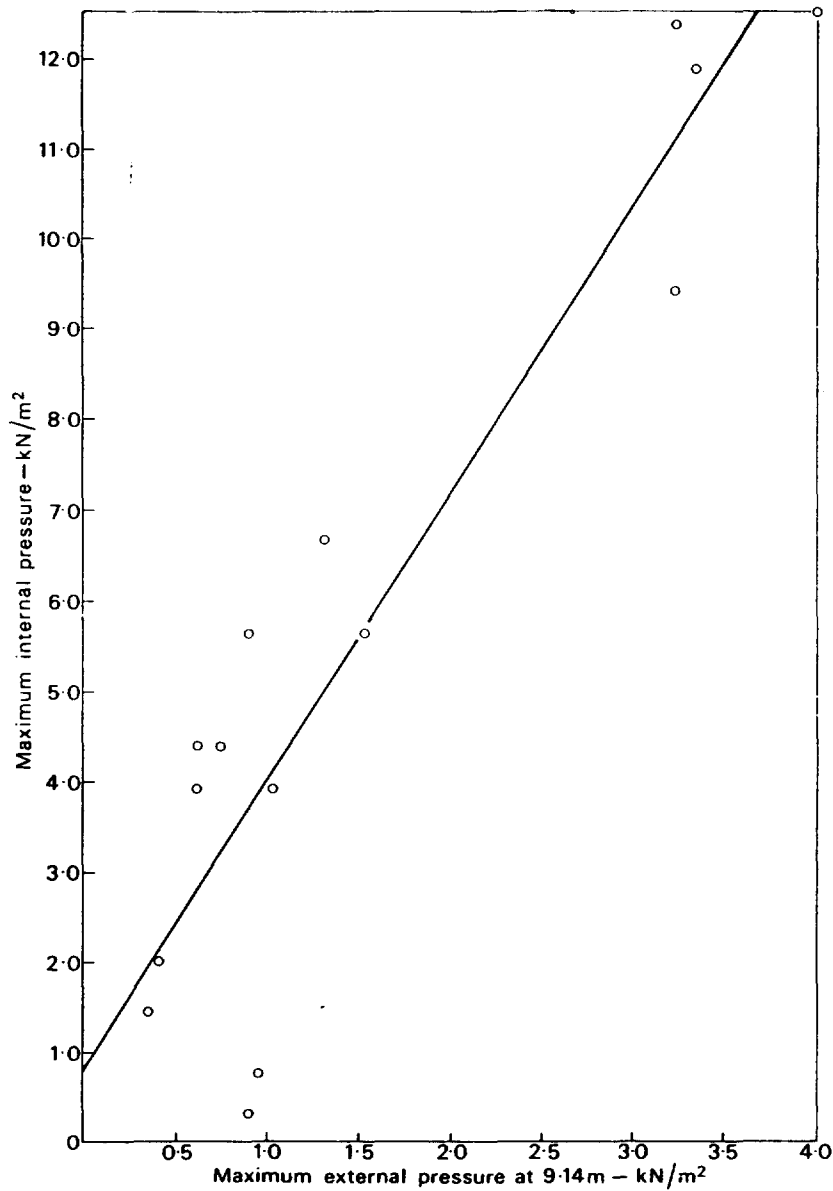
Figure 6.5. Relationship between the internal maximum pressure and external maximum pressure measured at 9 m from the vent (Palmer & Tonkin 1980).

Fig. 6.6 shows the inverse of the maximum pressure outside $(1/P_{ext})$ as a function of the distance from the vent r. The curve shows that the blast centre appears to be located at about 3 m from the vent. Although not appreciated by the authors, this is in agreement with the concept of external explosion (van Wingerden 1993).

72
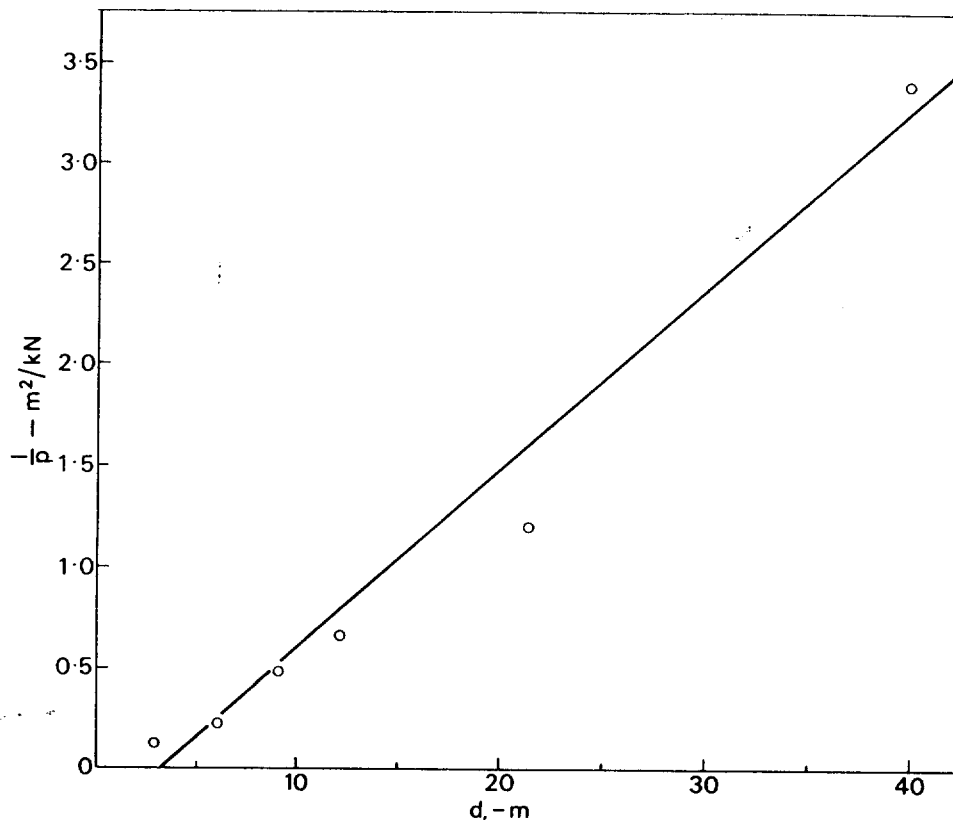
Figure 6.6. Relation between the inverse of maximum external pressure and the distance from the vent (Palmer & Tonkin 1980).

Harrison and Eyre (1987) studied vented natural gas and propane explosions in a 30 m^3 chamber. Based on a careful comparison between the pressure-time histories measured in the chamber and outside, the authors were able to show that the blast wave was caused by the external explosion. The external explosions were particularly strong when the mixture was ignited near the rear wall of the chamber.

Figure 6.7 shows the peak pressures for three tests measured at different distances outside the vent. Only the vent size A_v was varied (K = A_s/A_v = 1.88, 3.85 and 8.9; labelled in Fig. 6.7 as 1/2, 1/4 and 1/8). The measured pressures at distances larger than 10 m were highest for the intermediate vent size (K = 1.88). Though the maximum peak pressure was highest for the smallest vent size (K = 8.9), the size of the flammable cloud was small due to high flow velocity and the resulting efficient dilution.

It is seen that the peak pressure has a maximum value at a considerable distance away from the vent. For the weaker explosions (K = 1.88, 1/2 in Fig. 6.7) the decay was acoustic ($P_{ext} \propto 1/r$), whereas for the stronger explosions (K = 3.85 and 8.9; 1/4 and 1/8 in Fig. 6.7) the peak pressures decayed faster ($P_{ext} \propto 1/r^{1.3}$).

73
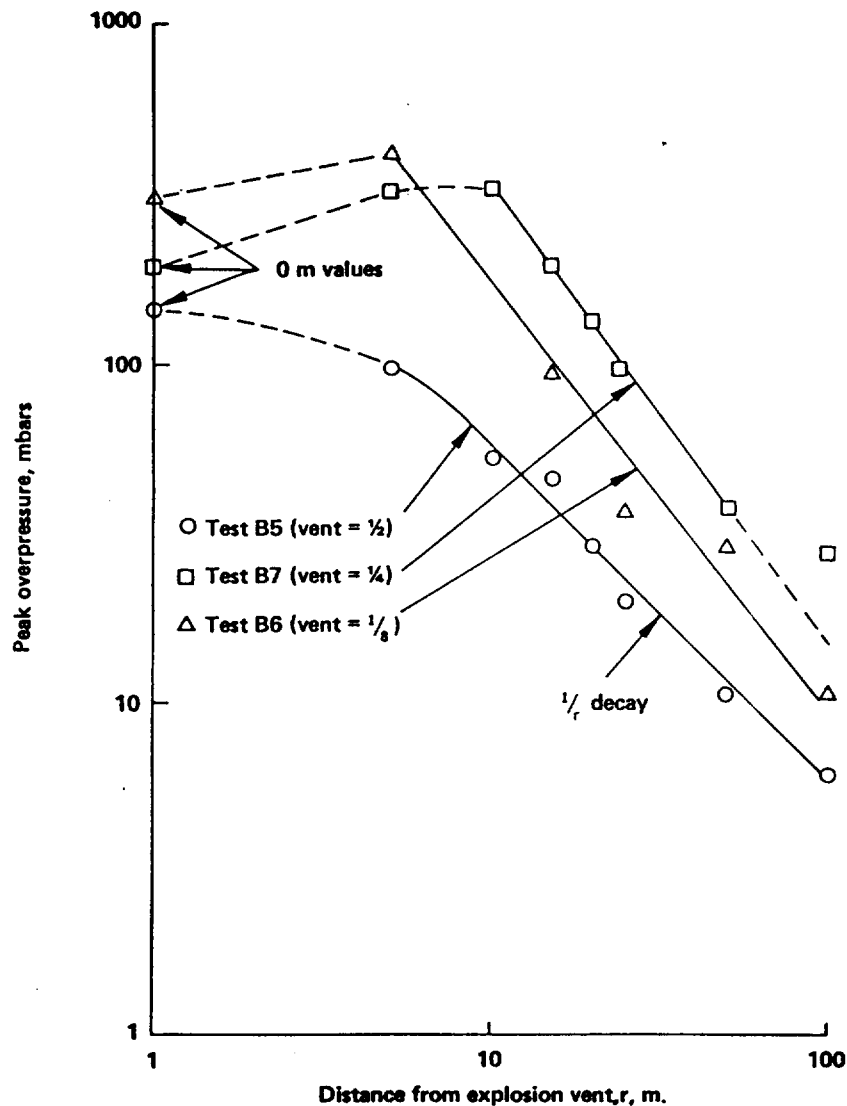
Figure 6.7. Peak pressures measured outside the chamber for three vent sizes (Harrison & Eyre 1987).

The external explosion has been investigated also in vented dust explosions (see van Wingerden 1993 for a review of the early experiments). On the basis of experimental data of tests performed before 1993, van Wingerden (1993) draws the following conclusions:

- The strongest distant blast wave effects are caused by explosions of unburned mixture pushed out of the room/vessel and subsequently ignited by flames emerging from the vent.
- The maximum pressure due to the external explosion outside the room/vessel is dependent on the vent size A_v, the volume V of the room/vessel and the maximum internal pressure P_{red}.
- The blast decay beyond the location of maximum pressure is acoustic or stronger than acoustic.
- The generated blast waves show directionality.

- The external explosion is less important for rooms with small vent sizes A_v and for vessels in which very strong explosions occur.
- The blast waves due to external explosions are accompanied by a significant negative pressure pulse.

A simple method to estimate the peak pressure of the blast wave from a vented dust explosion has been proposed by Wirkner-Bott et al. (1992). The method is based on tests performed with corn-starch (some cases with wheat-dust or propane) in vessels of volumes ranging 0.3 - 250 m³. The dust concentration was chosen to lead to maximum explosion overpressure in a closed vessel. The vent coefficient K ranged 2.2 - 12.5 and vent opening pressure P_v was 10 - 50 kPa. The dust-air mixture was ignited in the centre or the back of the vessel (in a few cases near the vent).

In a large number of tests with identically chosen explosion parameters, two different types of explosion events were observed (Wirkner-Bott et al. 1992):

1.   **External explosion.** Coherent flame propagation leading to a more or less spherical flame. A significant blast wave is generated.

2.   **Cloud burn-out.** Flame propagation is initiated at several locations in an incoherent way. An overpressure generated at a point of the cloud coincides at a pressure transducer with an underpressure generated at another point. The resulting pressure signal is rather complex without significant pressure peaks.

Wirkner-Bott et al. (1992) propose an empirical correlation for the maximum flame length L_f [m]

$$L_f = 8\,V^{0.3}$$
(40)

The distance of the blast centre from the vent R_b [m] is

$$R_b = 0.25 L_f = 2\,V^{0.3}$$
(41)

The maximum pressure of the external explosion P_{em} [kPa] is generated at the blast centre and it can be related to the vent size A_v [m²], vessel volume V [m³] and maximum internal pressure P_{red} [kPa] by the empirical equation

$$P_{em} = 0.2 A_v^{0.1} V^{0.18} P_{red}$$
(42)

With increasing distances r, the peak pressure of the external explosion P_{ext} [kPa] decreases approximately according to the formula

$$P_{ext} = \left[\frac{R_b}{r}\right]^{1.5} P_{em} \quad \text{for } r \geq R_b$$
(43)

The empirical equations proposed by Wirkner-Bott et al. (1992) have been amended by Crowhurst et al. (1995). The latter authors performed tests with maize starch or coal dust in a chamber of volume 20 or 40 m³. The vent coefficient K was either 5 or 7.5,

and the vent opening pressure P_v was 5, 10 or 20 kPa. Two values of the dispersion pressure of the dust into the chamber were used. Dust concentrations and ignition delays were chosen in such a way that the resulting internal pressures P_{red} were in accordance of the VDI guidelines for the sizing of explosion relief vents. The ignition source was either in the centre or in the rear of the chamber.

As in the tests described by Wirkner-Bott et al. (1992), two different types of explosion events were observed. The types are described as follows (Crowhurst et al. 1995):

1.   The largest external explosions were generated when A_v was large and/or P_v was low, and the ignition source was remote from the vent. In these explosions, large clouds of unburned mixture were vented and subsequently ignited by the emerging flame.

2.   The explosions were characterized by a strong flame jet with little preceding unburned material. These explosions were observed particularly for small A_v and high initial turbulence in the chamber. These conditions tended to promote rapid burning in the chamber.

The explosion overpressures measured outside for both types of explosion events are shown in Fig. 6.8. To make comparison easier, both the pressure P_{ext} and the distance r have been scaled. The scaled variables in Fig. 6.8 are P_{ext}/P_{em} and r/R_b. It is seen that the pressure of Type 1 explosion follow closely the acoustic curve $P \propto 1/r$ whereas that for Type 2 decays much more slowly.
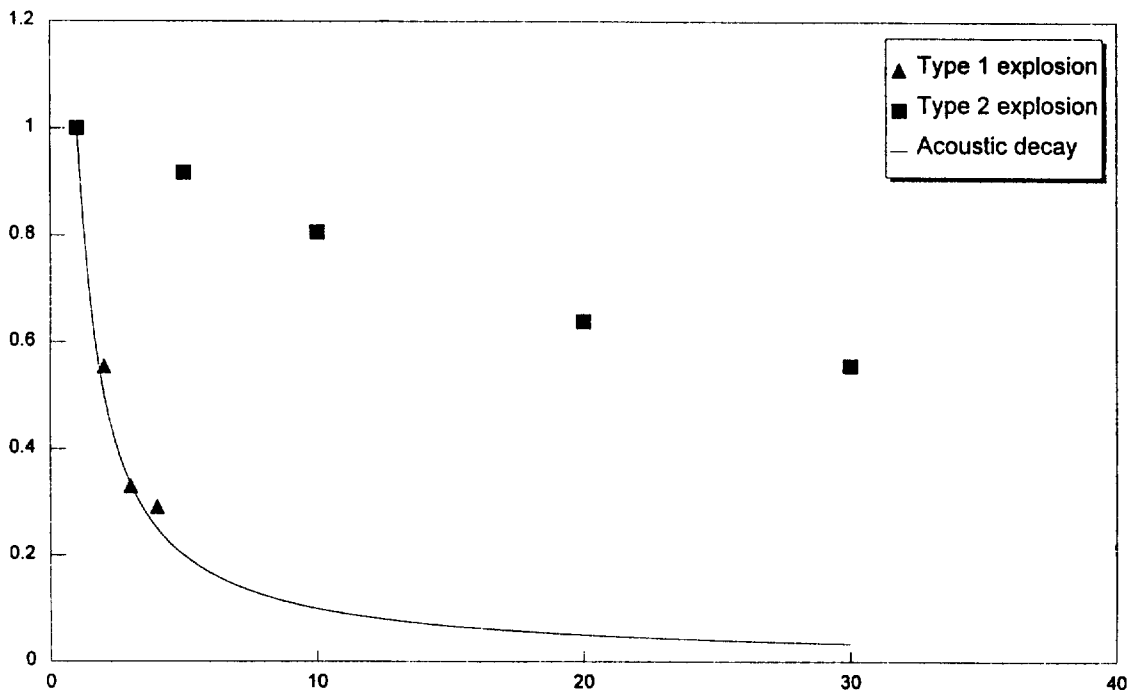
Figure 6.8. Scaled maximum external pressure vs. scaled distance for the two types of external explosion (Crowhurst et al. 1995).

76

The difference in decay of P_{em} with distance was explained as follows:

- In Type 1 explosions, the dust cloud had little forward momentum at the time of ignition. Thus, it formed a large fire ball which moved away with relatively low velocity.
- In Type 2 explosions, the dust cloud itself was either moving rapidly away from the vent or was ignited by a strong jet. Thus, as the pressure wave was generated the cloud was moving rapidly away from the vent, and the decay was therefore less than acoustic.

The flame lengths measured were compared with predictions of Eq. (40). The 20 m³ chamber was equipped with one relief vent. The average flame length was 26 m and the maximum one over 30 m. The measured flame lengths were larger than the predicted one: $L_f = 22$ m. The 40 m³ chamber was equipped with two equal relief vents. The spacing between the vents was varied. When the vents were close together the average flame length was 25 m and the maximum one over 30 m. These are close to the predicted one: $L_f = 27$ m. When the separation distance between the two vents was increased the flame lengths decreased below the predicted one.

Crowhurst et al. (1995) conclude that Eq. (40) underestimates the observed maximum flame lengths. The difference may arise because in the earlier experiments venting was in most cases vertically upwards. In the experiments by Crowhurst et al. (1995) venting was always horizontal. Besides, the proximity to ground may have acted to increase L_f. The authors propose to amend Eq. (40) in the following way:

$$L_f = 10\,V^{1/3} \qquad\qquad (44)$$

For several relief vents with large separation distances, Eq. (44) tends to overestimate L_f. However, the lateral flame spread should not be ignored when considering vent separation as a means to reduce flame length.

Eq. (41) must be modified to match Eq. (44):

$$R_b = 0.2L_f = 2\,V^{1/3} \qquad\qquad (45)$$

Figure 6.9 is a plot of P_{em} versus P_{red} for all the experiments undertaken by Crowhurst et al. (1995). The following conclusions can be drawn from Fig. 6.9:

- P_{em} was always less than P_{red}.
- Stronger external explosions were observed when ignition was remote from the relief vent ie. at the rear of the chamber.
- For central ignition, the ratio P_{em}/P_{red} decreased with increasing P_{red}.
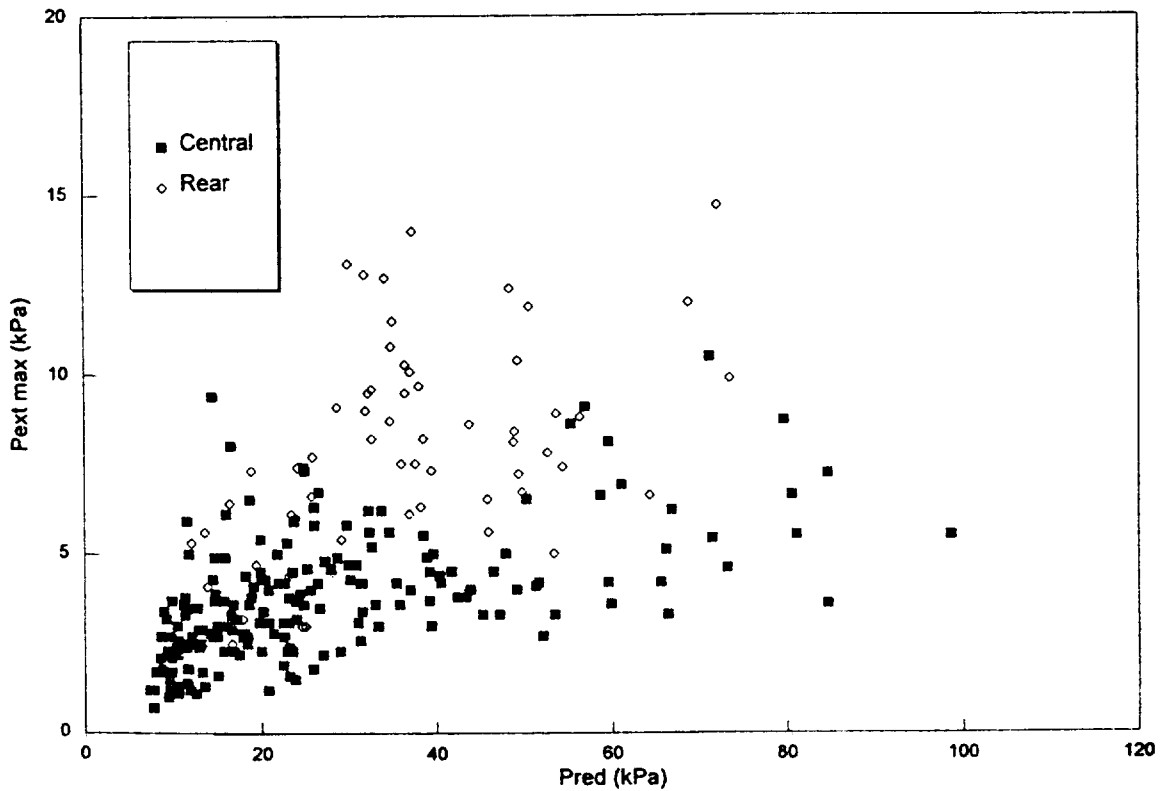
Figure 6.9. The external peak pressures P_{em} versus the internal peak pressures P_{red} measured in the dust explosion tests by Crowhurst et al. (1995).

Eq. (42) was verified by inserting the values of P_{red} measured in the tests and comparing the calculated values of P_{em} with the experimental ones. This comparison is shown in Fig. 6.10. Crowhurst et al. (1995) conclude that Eq. (42) gives un upper limit to the experimental values of P_{red}. However, the decay of P_{ext} with distance was acoustic or weaker and, thus, not described by Eq. (43).

An upper value for both Type 1 and Type 2 explosions can be had by assuming acoustic decay with distance. Thus, Eq. (43) is modified to

$$P_{ext} = \frac{R_b}{r} P_{em} \quad \text{for } r \geq R_b \tag{46}$$

No such simple models have been derived for the external explosion of vented gas explosions. van Wingerden (1993) reviews the data of vented dust and gas explosion tests. In Fig. 6.11 the measured flame lengths are compared with the predictions of Eq. (40). It is seen that Eq. (40) provides an upper limit to flame lengths measured in gas explosions. Actually, the value of the coefficient of Eq. (40) would be 3.5 for the tests by Bartknecht (1981) in vessels of volume 2, 2.5 and 10 m^3, and 6 for the tests by van Wingerden (1989) in a chamber of volume 38.5 m^3.
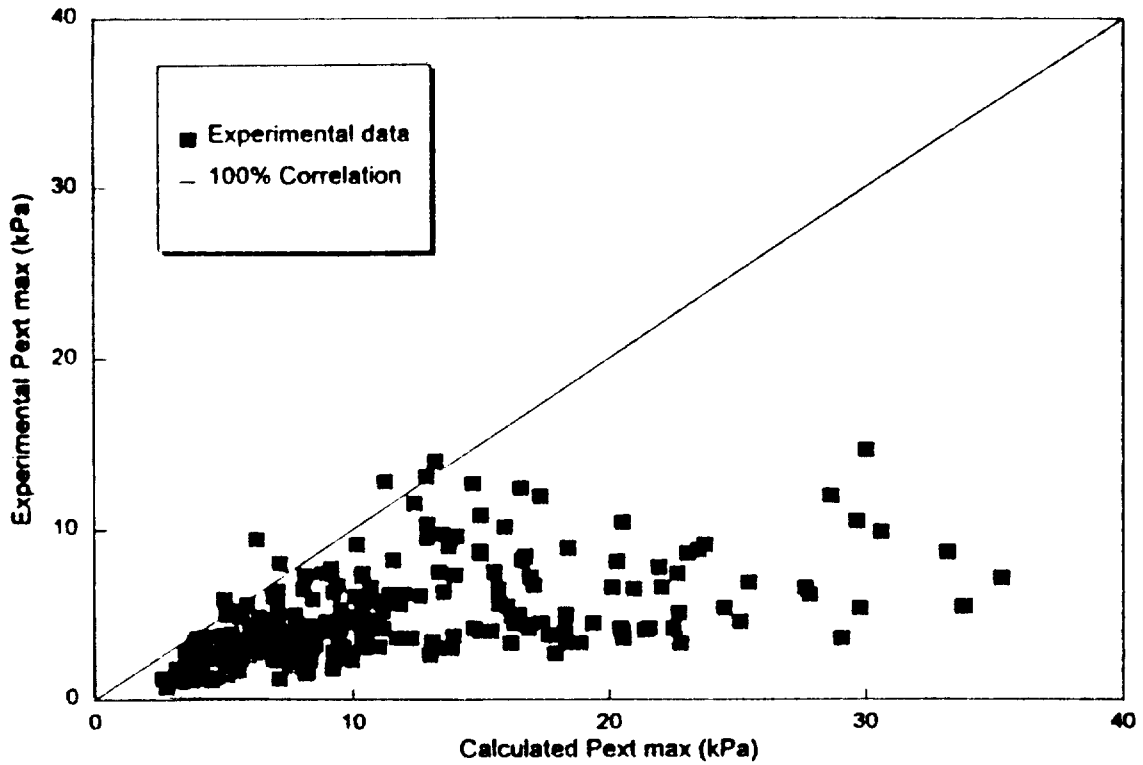
Figure 6.10. Values P_{em} calculated with Eq. (42) (using experimental values of P_{red}) compared to measured values of P_{em} (Crowhurst et al. 1995).
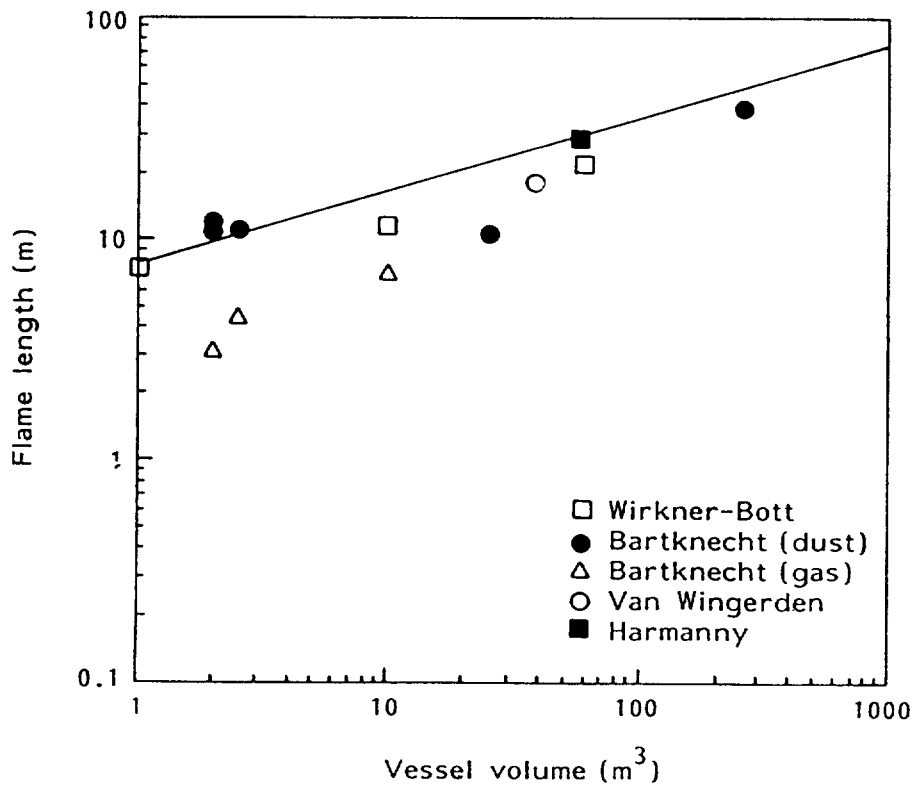
Figure 6.11. Comparisons of measured flame length in dust (Wirkner-Bott, Bartknecht (dust) and Harmanny) and gas (Bartknecht (gas) and van Wingerden) explosions (van Wingerden 1993).

It is not known whether Eq. (42) can be used for gas explosions to predict the maximum external pressure P_{em} after P_{red} has been estimated with a suitable venting guideline. However, the gas explosion tests by Harrison and Eyre (1987) and Bimson et al. (1993) may give some indication. Harrison and Eyre performed 18 tests in a 30 m^3 (5.92 m x 2.38 m x 2.16 m) chamber filled with a mixture of either natural gas or propane with air. Except for two of the tests, the concentrations were nominally 1.1 times the stoichiometric one and corresponded to the highest S_0.

In the front wall there was a square vent with area A_v 2.74, 1.33 or 0.58 m^2. The vent was covered with thin polyethylene sheeting. In two tests, the mixture was ignited in the front. In other tests, the ignition source was either in the centre (6 tests) or at the rear wall (10 tests) of the chamber. There were two pressure transducers in the chamber: one at the front and one at the rear. Outside the chamber, five pressure transducers were located at intervals of 5 m starting immediately outside the chamber and several were located in the far field.

The internal pressure curve shows a variety of characteristics including single, multiple and oscillatory peaks (Fig. 6.12). One consistent feature of the pressure traces, however, is an early small amplitude peak (1 - 2 kPa) which Harrison and Eyre (1987) attribute to release of vent cover.

Front ignition produced only very small pressures except for the oscillatory peaks that occurred towards the end of explosion. Oscillatory peaks also occurred with central ignition but there was little evidence of them with rear ignition. The curves from centrally ignited tests have two major peaks with superposed oscillations, whereas those from tests ignited in the rear have only one major peak (Fig. 6.12). For any given fuel and vent size, the pressures obtained with rear ignition were greater than those with central ignition.

The external pressure consisted typically of a single peak of short duration followed by a longer duration negative phase. The peak external pressure invariably occurred before the peak internal pressure but well after the vent cover released (Fig. 6.13). In some cases, the peak external pressure temporarily exceeded the peak internal pressure, resulting in a reversal of the pressure difference across the vent ΔP.

The external explosion can influence the internal pressure in, at least, three ways (Harrison & Eyre 1987):

1. The temporary reduction or reversal of the pressure difference across the vent impedes the vent flow and thus increases the quasi-static internal pressure.

2. The blast wave generated by the external explosion can also propagate through the vent into the chamber and so increase or decrease the internal pressure. The blast wave is reflected from the rear wall and can result in larger and narrower pressure peaks at the rear than at the front, because of the coincidence of the incident and reflected waves. The external pressure also introduces a negative phase into the internally measured pressure.

3. The external explosion may induce instabilities of the interface between the unburned and burned gases.

80
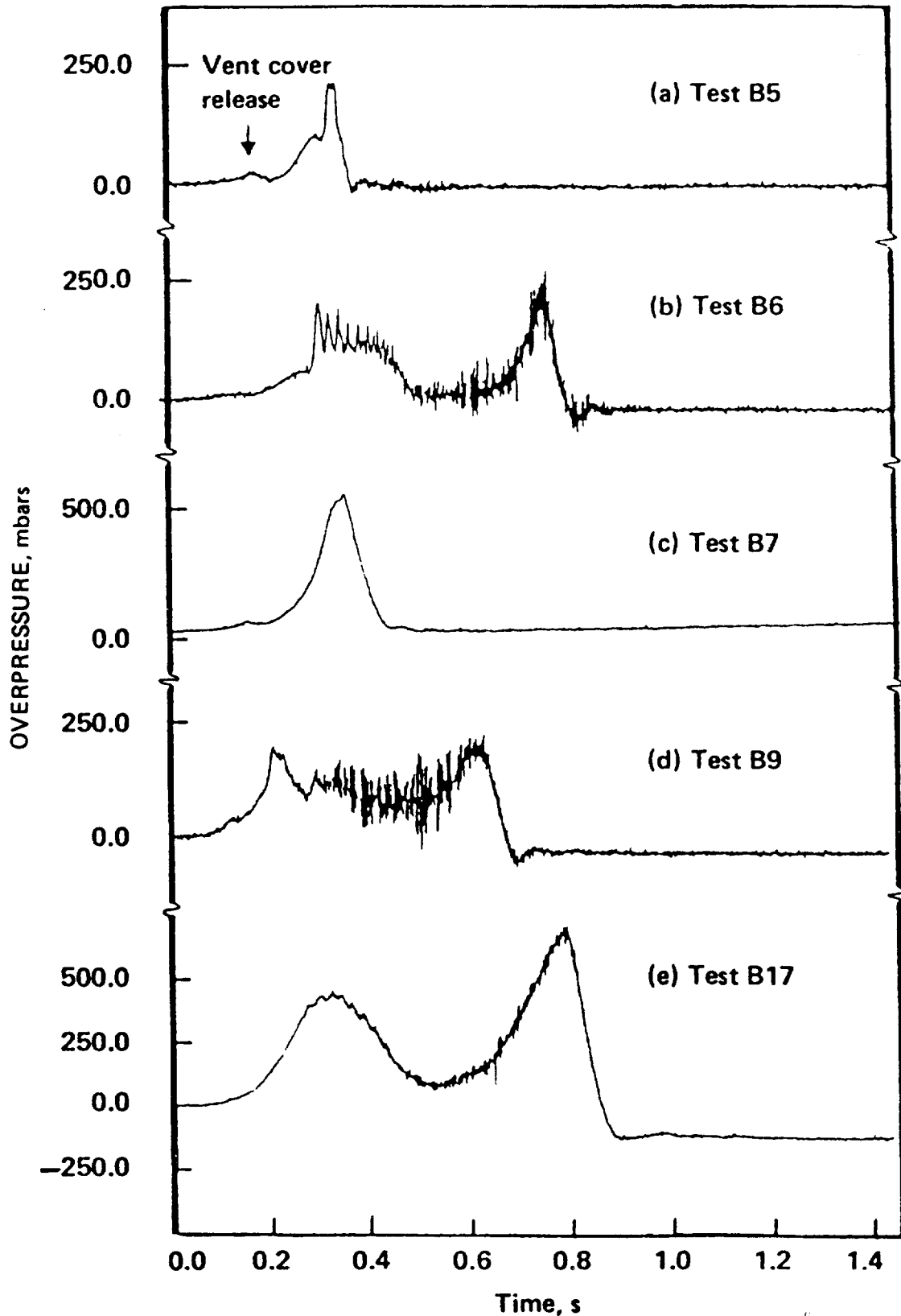
Figure 6.12. Examples of various internal pressures recorded at rear of the 30 m^3 chamber. Curves b, d and e refer to central ignition and curves a and c to rear ignition (Harrison & Eyre 1987).

Fig 6.13 shows how the external explosion may affect the internal pressure. Both in Fig. 6.13a (rear ignition) and Fig. 6.13b (central ignition) the first major peak of the internal pressure is caused by the reversal of the pressure difference across the vent. In Fig. 6.13b, the internal peak is followed by pressure oscillations caused by a Taylor instability of the flame front (see Fig. 3.6a). This type of instability is not possible for rear ignition and, thus, is not seen in Fig. 6.13a.
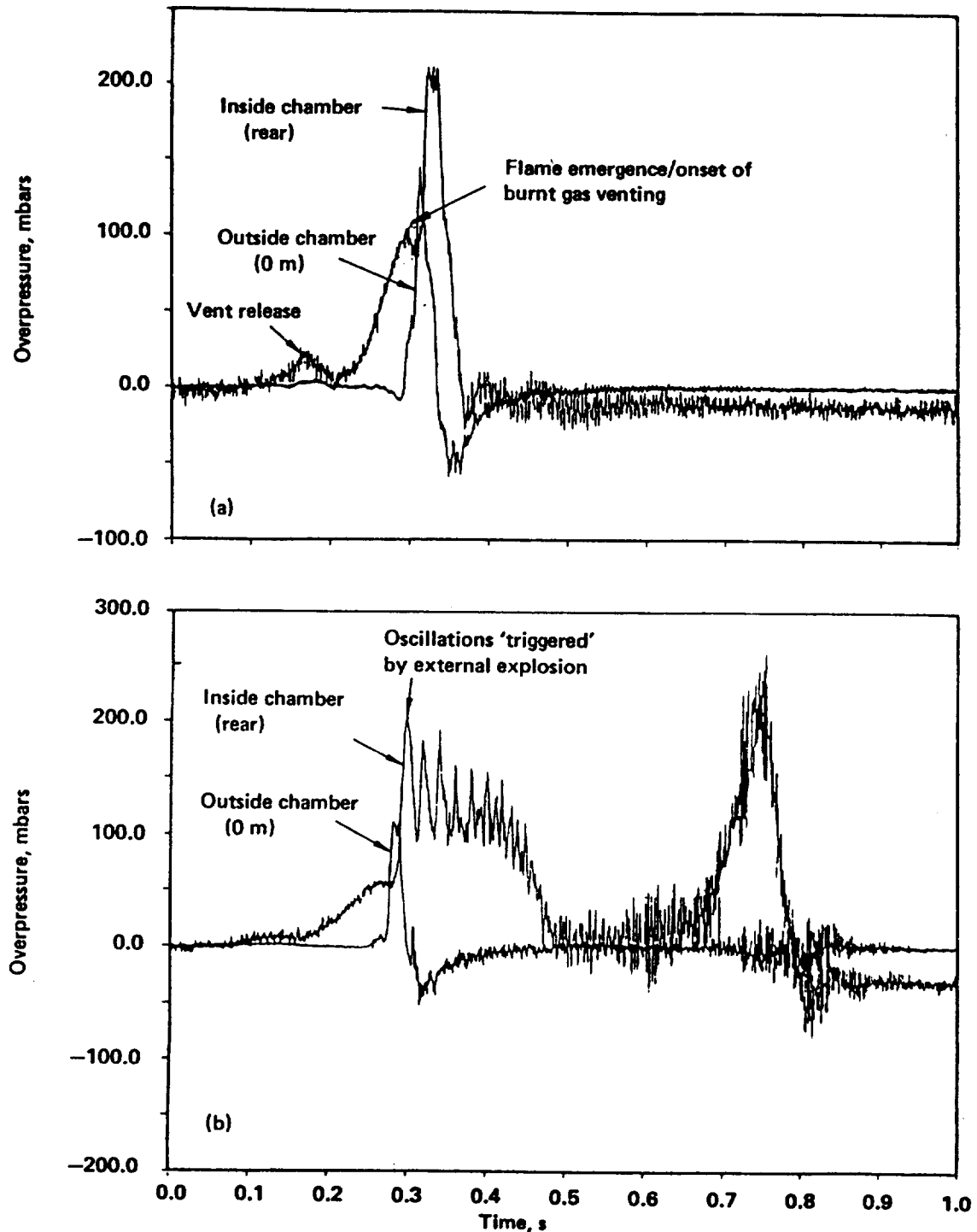
Figure 6.13. Comparison of pressure signals measures inside (at rear) and outside the explosion chamber in two tests with natural gas. a) Test B5, rear ignition, A_v = 1.33 m^2, b) Test B6, central ignition, A_v = 0.58 m^2 (Harrison & Eyre 1987).

The measured peak pressures at rear of chamber P_{red} and the maximum external peak pressures P_{em} are given in Table 6.1 with the relevant test parameters for 14 of the 18 tests (tests B2 and B8 with front ignition, test B13 with lean mixture and test B14 with no pressure data have been left out). The internal pressure is that of the first main peak (excluding the small peak due to vent opening). The later (single or oscillatory) peaks have been neglected (Harrison & Eyre 1987).

Table 6.1. Peak pressures inside and outside the 30 m^3 chamber.

test	A_v m^2	P_{red} kPa	P_{em} kPa	P_{em}/P_{red}
central ignition				
natural gas				
B4	2.74	5.2	2.6	0.50
B6	1.33	20.5	11.2	0.55
B15	0.58	40.3	14.5	0.36
propane				
B1	2.74	17.0	10.8	0.64
B9	1.33	19.5	10.4	0.53
B17	0.58	42.5	22.1	0.52
rear ignition				
natural gas				
B5	2.74	21.5	14.5	0.67
B7	1.33	54.2	32.4	0.60
B12	1.33	3.6	4.6	1.3
B16	0.58	106.7	34.5	0.32
propane				
B3	2.74	28.6	22.7	0.79
B10	1.33	89.2	68.2	0.77
B11	1.33	110	44.5	0.41
B18	0.58	134	41.8	0.31

Figure 6.14 shows a comparison of the value of the first major peak of the internal explosion P_{red} with the value of P_2 predicted by Eq. (26). The vent coefficient K is defined by Eq. (21). The prediction is very good for tests with central ignition. However to get the peak pressures measured in tests with rear ignition, the predicted P_2 must be multiplied by a factor of 2.5 - 5 (the average value of seven tests is 3.16).

Figure 6.15 shows the external peak pressures P_{em} versus the internal peak pressures P_{red} measured in the explosion tests by Harrison & Eyre (1987). Similar conclusions can be drawn from Fig. 6.15 as from Fig. 6.9:

- P_{em} was always less than P_{red}.
- P_{em} was about half of P_{red}.
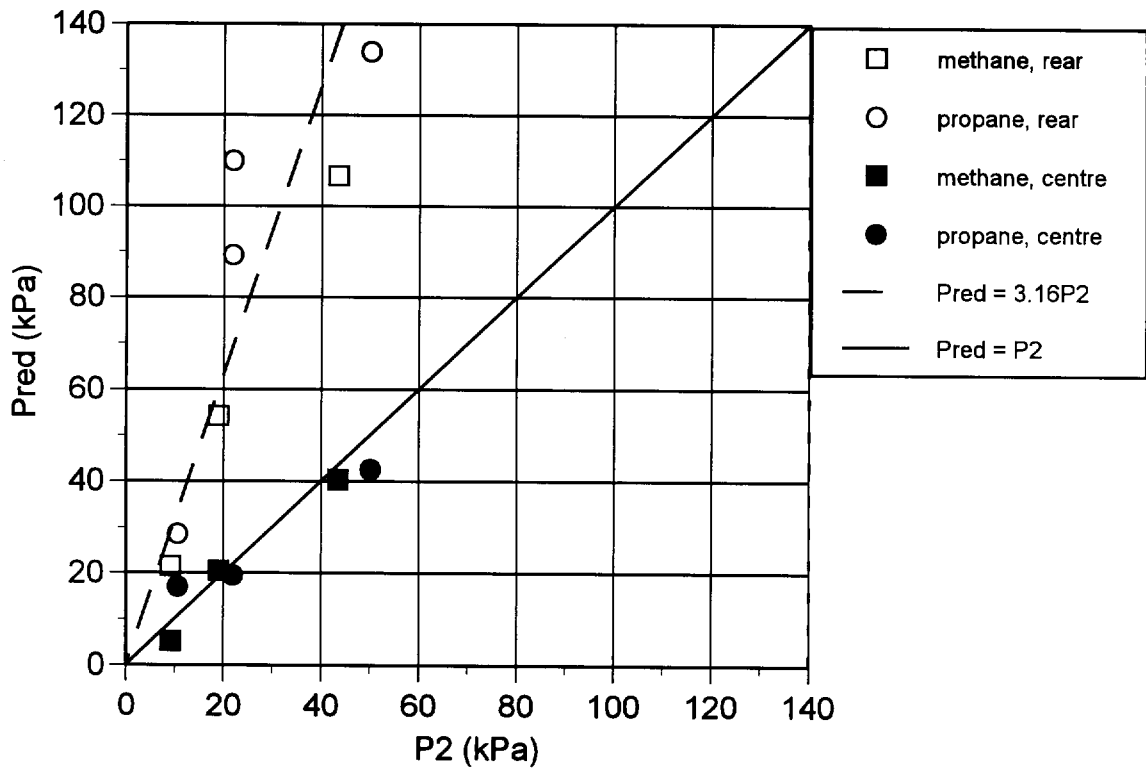
Figure 6.14. Experimental P_{red} (at rear) versus predicted P_2 internal peak pressures in the tests by Harrison & Eyre (1987).
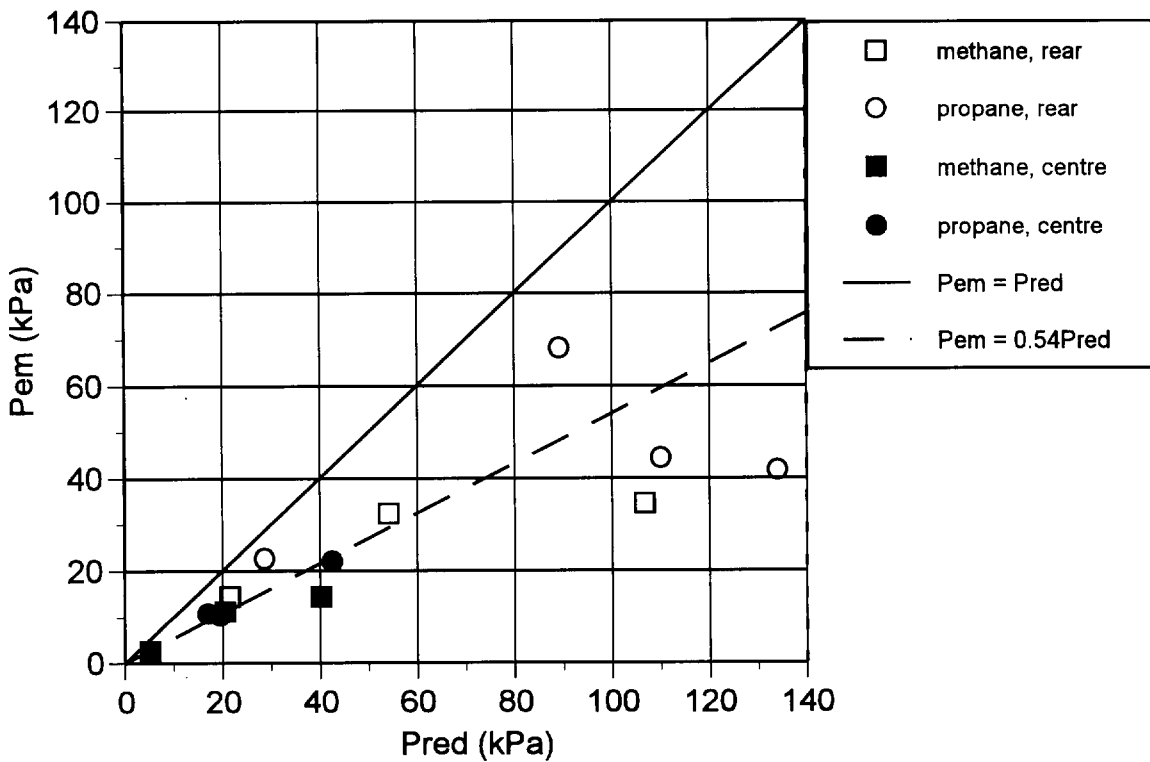
Figure 6.15. The external peak pressures P_{em} versus the internal peak pressures P_{red} measured in the explosion tests by Harrison & Eyre (1987).

Harrison and Eyre (1987) have calculated the flow velocities u at the vent from the measured pressure differences ΔP. Figure 6.16 shows the maximum external pressure P_{em} as a function of the flow velocity. As concluded by Harrison and Eyre (1987), the external peak pressure increases with the flow velocity. In Fig. 6.16, a power function has been fitted to the experimental points from tests with central ignition and rear ignition.

The remarkable thing about Fig. 6.16 is that the external peak pressures P_{em} measured in both central and rear ignition tests are described by the same correlation. High internal pressures in tests with rear ignition result in high flow velocities, causing high external pressures. Unfortunately, the flow velocity u is determined by the pressure difference across the vent ΔP which is the result of a complex interaction of the external and internal explosion. Thus, it is not possible to predict u based on a venting guideline.

$$P_{em} = 0{,}021 \, u^{1,28}$$
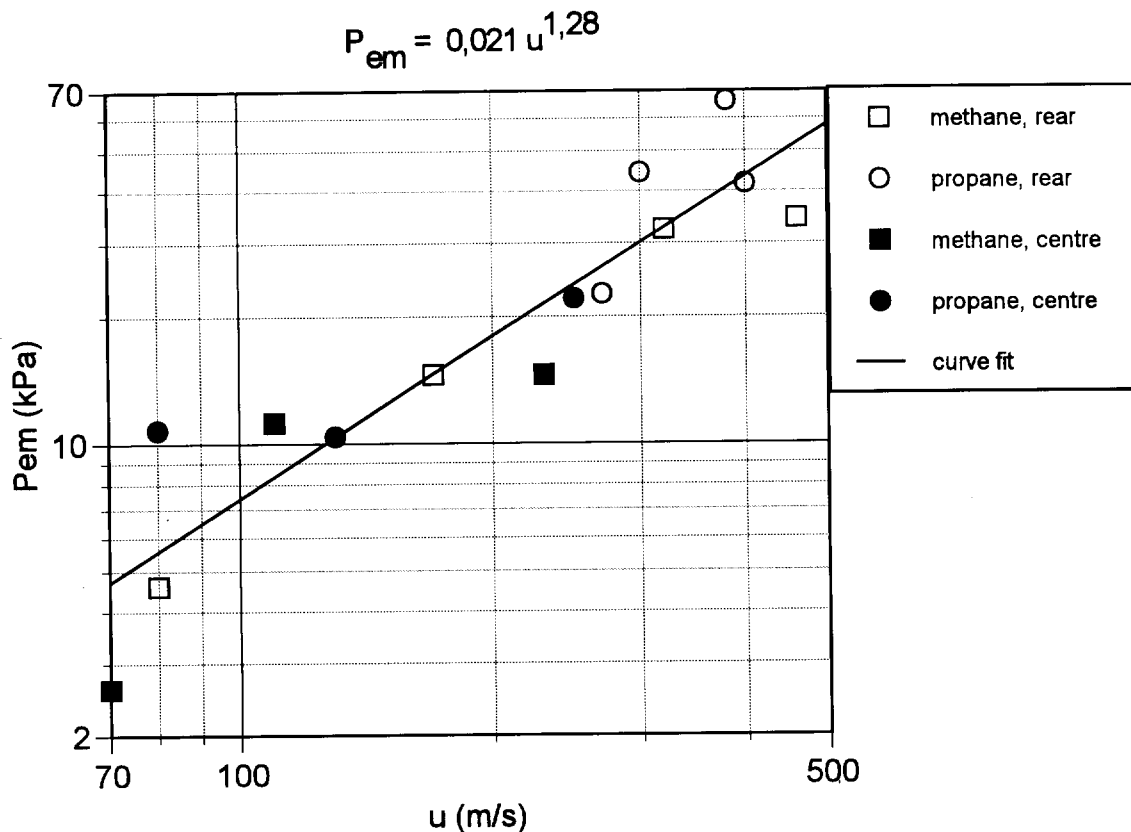
Figure 6.16. The external peak pressures P_{em} measured in the explosion tests by Harrison & Eyre (1987) versus the flow velocity at the vent.

Fig. 6.17 shows the external peak pressures P_{em} versus predicted internal peak pressures P_2. As in Fig. 6.14, the experimental points for central and rear ignition show different behaviour. Two lines have been fitted to the data sets. For rear ignition, P_{em} is about 1.7 times P_2. The scatter of data points, however, is large for large values of P_2. For central ignition, P_{em} is about 0.5 times P_2. These multipliers can also be derived on the basis of the line fits in Figs. 6.14 and 6.15.
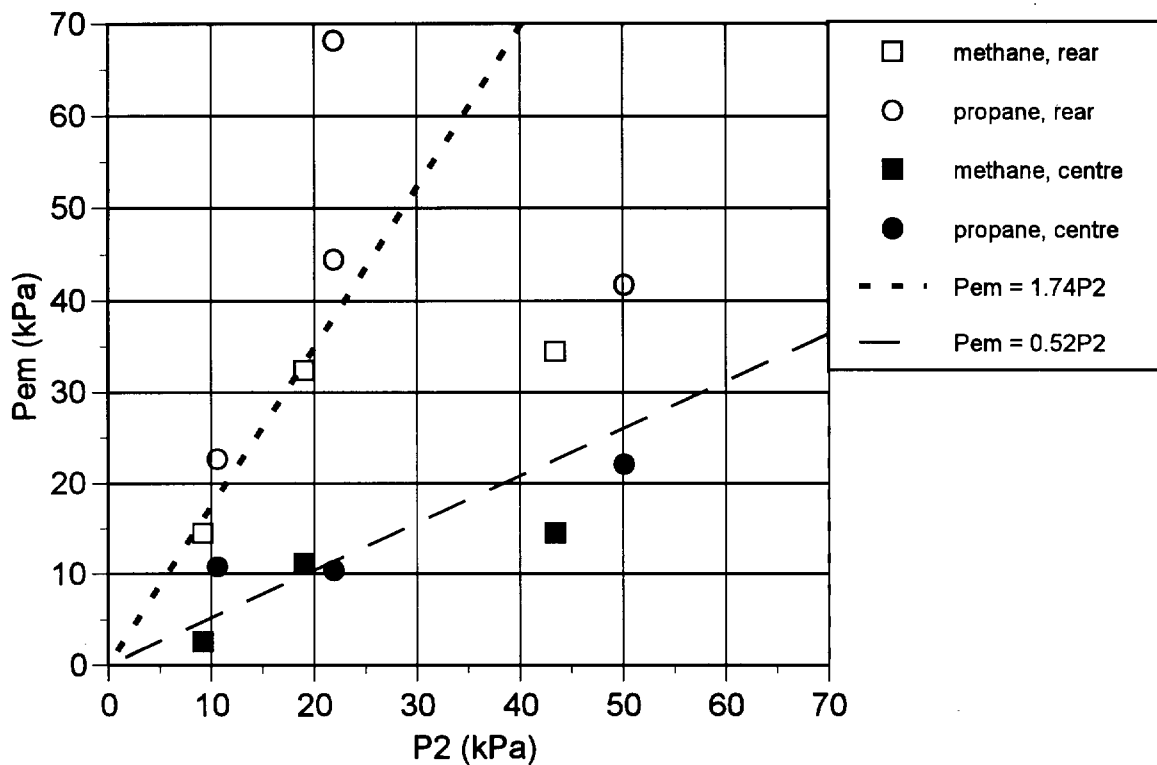
Figure 6.17. The external peak pressures P_{em} versus the predicted internal peak pressures P_2 in the tests by Harrison & Eyre (1987).

When the geometry and volume of the room are such that the venting guideline for P_2, Eq. (26), can be used, and are not too different from those of the test chamber used by Harrison and Eyre (1987), the correlations in Figs. 6.14 and 6.17 could be used to get an indication of the magnitude of P_{em}:

- for central ignition: $P_{red} = P_2$, $P_{cm} = 0.5P_2$
- for rear ignition: $P_{red} = 3P_2$, $P_{em} = 1.7P_2$.

In the explosion tests by Bimson et al. (1993), low peak pressures were measured both inside and outside the 550 m³ chamber. In Sec. 6.2 it was shown that the internal peak pressures are much better predicted by the original Cubbage and Simmonds formula, Eq. (25), than the modified one, Eq. (26). When the experimental peak pressures are compared with the predictions of Eq. (25) one finds

- methane: $P_{red} = 0.8P_2$, $P_{em} = 1.4P_2$
- propane: $P_{red} = 1.5P_2$, $P_{em} = 1.4P_2$.

This looks similar to the correlations derived above from the tests by Harrison and Eyre (1987), but is not because P_2 has been predicted with a different formula. Actually the peak pressures measured in the tests by Bimson et al. (1993) were much lower than predicted by a number of numerical models.

If Eq. (42) is seen as a correlation of two experimental quantities it can be verified with the results of the gas explosion tests. For the tests by Harrison and Eyre (1987), the predicted value of the ratio P_{em}/P_{red} ranges 0.36 - 0.41, depending on the vent size

A_v. This is not too different from the experimental value 0.54 (Fig. 6.15). For the tests of Bimson et al. (1993), the predicted value is $P_{em}/P_{red} = 0.87$ and the experimental one is 1.8 (methane) and 0.93 (propane). In these cases, Eq. (42) is seen to give satisfactory predictions for the ratio P_{em}/P_{red}, but the problem of predicting P_2 remains.

A method that has sometimes been used to predict P_{ext} of a vented explosion is the Multi-Energy Method (van den Berg 1985). This is currently the standard method to estimate all the necessary blast wave parameters of a vapour cloud explosion. In the method, the partially confined volume congested with obstacles and filled by a flammable mixture is replaced with a hemisphere of stoichiometric mixture of equal volume (the **equivalent hemisphere** with a radius of R_0 [m]).

The peak pressure generated in the congested volume ΔP_s [bar] is a parameter of the model. The main difficulty is in the selection of this parameter on the basis of the obstacle configuration, location of ignition source and reactivity of mixture. After the value of the parameter ΔP_s has been selected, the blast wave parameters can be read from Fig. 6.18.

Except for the strongest explosion, the blast waves obey the acoustic decay law ie. P_{ext} $\propto R_f/r$ where R_f [m] is the final radius of the hemisphere ($R_f = (E - 1)R_0$).

van Wingerden (1993) has compared the predictions of the Multi-Energy Method and the empirical method of Wirkner-Bott et al. (1992), Eqs. (40), (41) and (42), with values of P_{ext} measured in dust explosion tests (Fig. 6.19). It is quite natural to select the P_{red} measured in the test as the parameter ΔP_s of the Multi-Energy Method. It is not so easy to select a value for the volume of the equivalent hemisphere. An upper limit to P_{ext} can be had by setting this parameter equal to the vessel volume. This selection, however, leads to an overestimation of the measured P_{ext} in Fig. 6.19.

Another selection is to put the bottom area of the equivalent hemisphere (πR_0^2) equal to the vent size A_v. This selection leads to an underestimation of the test data in Fig. 6.19. These two selections, differing by a factor 5 - 10, give respectively an upper and a lower estimate for P_{ext}. The experimental points correspond to an intermediate value of the equivalent hemisphere volume which has no obvious equivalent in the test chamber.
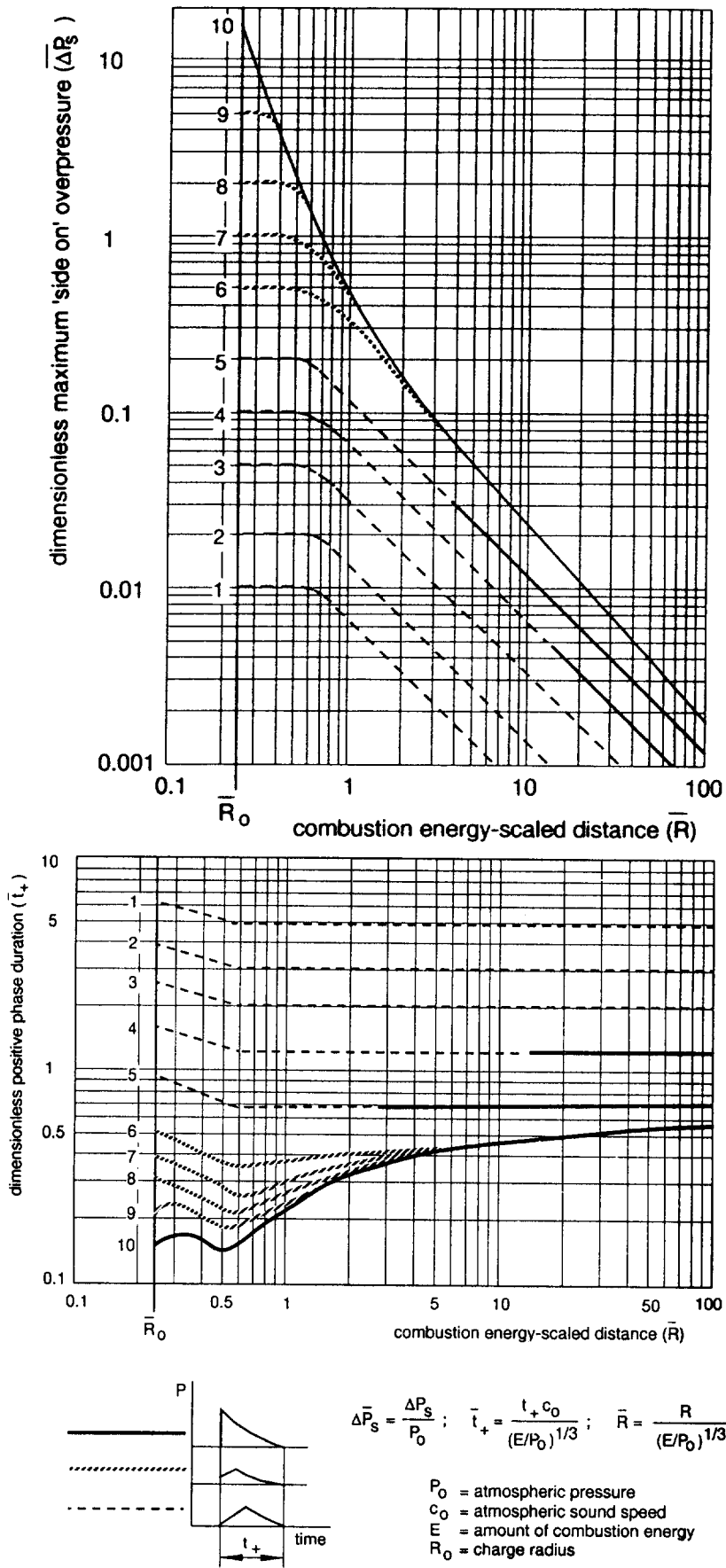
Figure 6.18. The Multi-Energy Method (AIChE 1994).
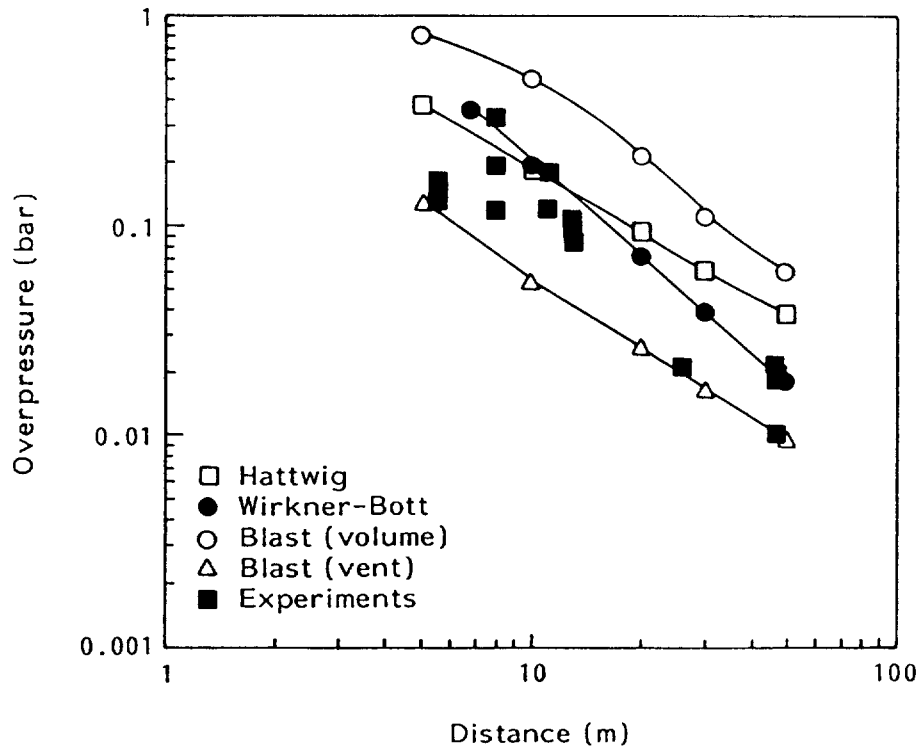
Figure 6.19. Comparison of prediction methods for P_{ext} with experimental data of dust explosions (van Wingerden 1993).

6.9 OTHER PREDICTIVE METHODS

The following presentation of predictive methods for gas explosion hazard assessment is based mainly on the review by Gardner and Hulme (1995). Their report is an update of the previous review of methods by British Gas (1990). The earlier report provided a state-of-the-art review on the modelling approaches and models that could be used for the prediction of gas explosion overpressures in offshore modules. The later report concentrates only on those models that are known to be available for use in offshore explosion hazard assessments.

Gardner and Hulme (1995) divide the models and methods into four general categories:

1. **Empirical models:** venting guidelines, small-scale experiments involving congested volumes, methods for estimating explosion duration and complex empirical models for offshore application.
2. **Physically-based models:** confined explosion type and high turbulence type.
3. **Numerical models.**
4. **Physical scale modelling.**

Venting guidelines are based mainly on tests in small-scale empty chambers with initially quiescent gas-air mixtures. The effect of flow turbulence on flame speed has been included in the venting guidelines by a number of authors who recommend a "turbulence factor". According to Rasbash et al. (1976) the burning velocity S_0 is to be multiplied by 1.5 for furniture in the room, 5 for obstacles distributed throughout a

89

volume and 8 - 10 for turbulence following a high-pressure leakage.

The concept of a turbulence factor is attractive and knowing the value of turbulence factor for a given configuration would indeed save a lot of work. Unfortunately, gas explosion tests performed in congested volumes over the last ten years do not support the concept of a turbulence factor. These experiments have been mainly carried out
- to assist in the development of complex empirical models and physically-based models and
- to test the accuracy of numerical models.

Hjertager et al. (1988) have performed explosion tests in two 1:5 scale (50 m^3, 2 m x 2.5 m x 8 m) models of offshore modules. The separator module was characterized by seven large cylindrical vessels (four on the upper deck and three on the lower deck) aligned along the module length (Fig. 6.20). In addition, the module also contained a lot of small pipes. The separator module had an overall volume blockage ratio of 0.3.
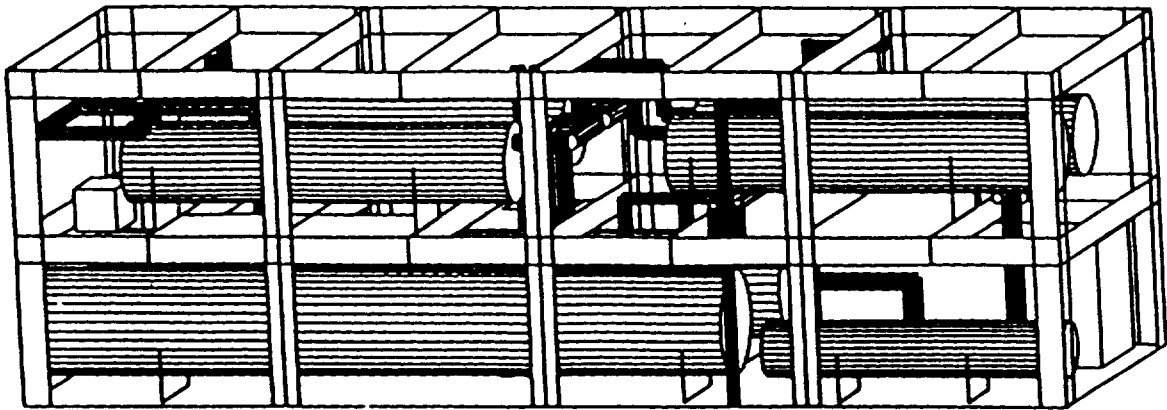
Figure 6.20. Internal layout of a 1:5 separator module (Hjertager et al. 1992).

The compressor module was characterized by two compressor trains, two large box-shaped rooms, and four box-shaped and two cylindrical objects (Fig. 6.21). The volume blockage ratio for the compressor module was 0.13.
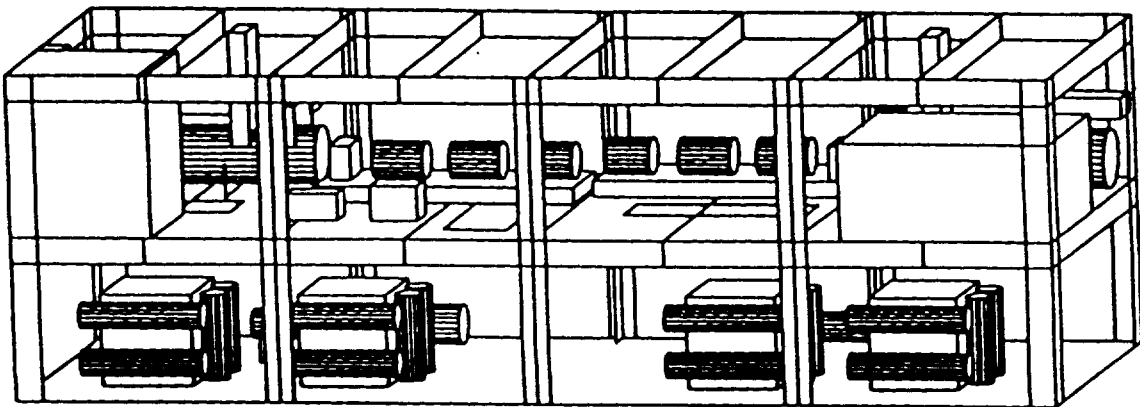
Figure 6.21. Internal layout of a 1:5 compressor module (Hjertager et al. 1992).

The modules were filled with slightly fuel rich methane and propane mixtures. Different venting arrangements were used:

1. Venting through louvres at the two ends, K = 2.2.
2. Venting through the open ends, K = 1.1.
3. Venting through louvres at the two ends and front wall, K = 0.7.
4. Venting through the open ends and half the front wall, K = 0.5.
5. Venting through the open ends and front wall, K = 0.35.
6. Venting through the open ends as well as the front and back wall, K = 0.21.

The measured peak pressures for central ignition are plotted in Figs. 6.22 and 6.23 as a function of the "vent parameter" $A_v/V^{2/3}$ which is just the inverse (1/K) of the vent coefficient K. (Note that K can be smaller than 1 when there are several open walls.) Figs. 6.22 and 6.23 include the results of laboratory tests with a 1:33 scale (0.14 m^3, 0.33 m x 0.35 m x 1.25 m) model which were performed with methane only.

Eg. the following conclusions can be drawn from Figs. 6.22 and 6.23 (Hjertager et al. 1988):

1. The internal peak pressure shows strong dependence on the venting arrangement. The highest peak pressure was 1.9 bar for propane and venting arrangement 1 (K = 2.2). The lowest peak pressure was 1 kPa for methane and venting arrangement 6 (K = 0.21).
2. For most cases, the peak pressures in the 1:5 scale modules were higher by factors 5 - 10 compared with the 1:33 scale tests.
3. For venting through three louvred walls (venting arrangement 3, K = 0.70) the peak pressure amounted to about 10 kPa. This is lower by the factor 2.5 compared to the value found by interpolating between the other arrangements.
4. The peak pressures in the congested modules were higher by factors 7 - 17 (methane) and 3 - 5 (propane) compared with empty modules.
5. The peak pressures for propane were higher by factors 3.7 (empty modules) and 2 - 3 (congested modules) compared to methane. This cannot be explained by the increase in burning velocity S_0 which is only 15 %.

Gardner and Hulme (1995) used the modified Cubbage and Simmonds guideline Eq. (26) to predict the peak pressures measured in the tests. For vent coefficients K and volume V applicable to the tests by Hjertager et al. (1988), the Cubbage and Simmonds formulas predict that P_2 will be larger than P_1.

The test results for propane were used to derive the corresponding values of the turbulence factor. The derived turbulence factors ranged 0.95 - 8.3 for the separator module and 2 - 5.6 for the compressor module for the different venting arrangements. This shows that it is difficult or impossible to choose a turbulence factor representative of such obstacle configurations.

Figs. 6.22 and 6.23 have been used to provide order of magnitude estimates of explosion overpressure at a conceptual design stage, when information of equipment layout within an offshore module is very limited or not available (Gardner and Hulme 1995). However, because the overpressure is due to flame acceleration by obstacles

Figs. 6.22 and 6.23 cannot be applied to different types of equipment layout than those in Figs. 6.20 and 6.21. Even if the peak overpressures in Figs. 6.22 and 6.23 are plotted as a function of 1/K the curves cannot be used as venting guidelines (Kees van Wingerden, Christian Michelsen Research, private communication).
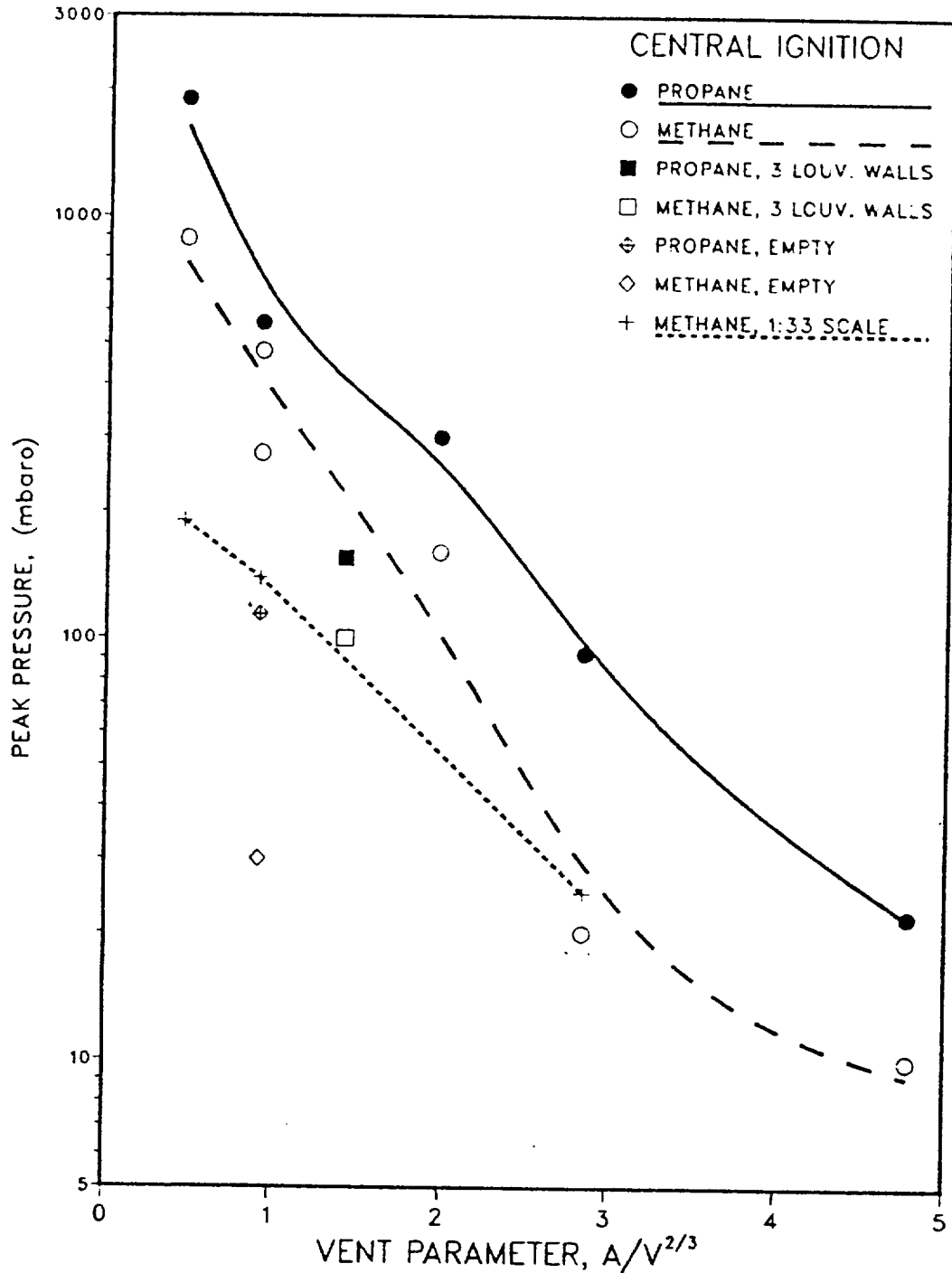
Figure 6.22. Peak pressures as function of 1/K for the explosions in the 1:5 scale separator module (Hjertager et al. 1988).

CENTRAL IGNITION

- ● PROPANE
- ○ METHANE
- ■ PROPANE, 3 LOUV. WALLS
- □ METHANE, 3 LOUV. WALLS
- ⊕ PROPANE, EMPTY
- ◇ METHANE, EMPTY
- + METHANE, 1:33 SCALE

PEAK PRESSURE, (mbaro)

3000

1000

100

10

5

0   1   2   3   4   5

VENT PARAMETER, $A/V^{2/3}$
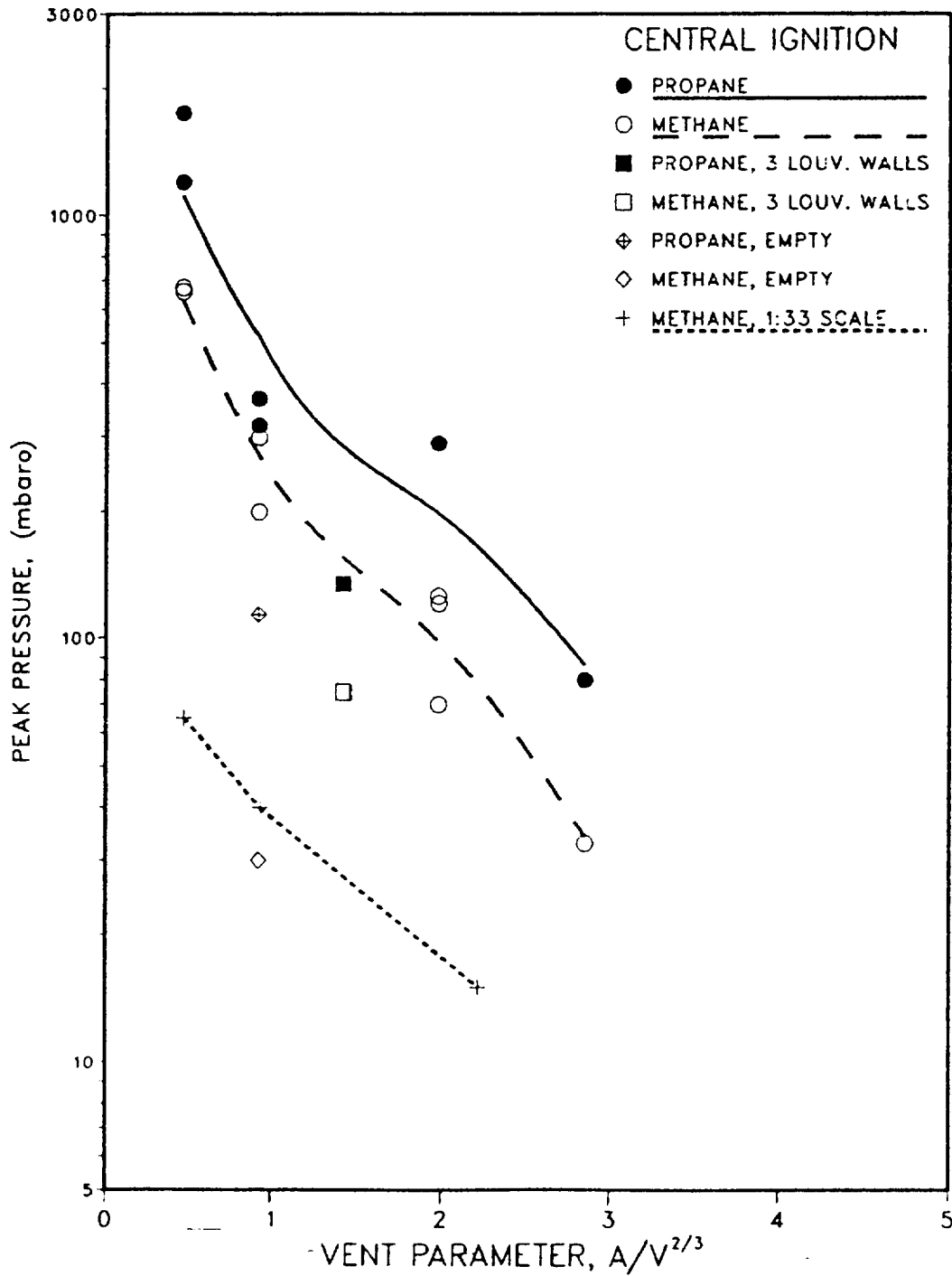
Figure 6.23. Peak pressures as function of 1/K for the explosions in the 1:5 scale compressor module (Hjertager et al. 1988).

Published venting guidelines do not give information on the duration or time dependence of the explosion overpressure. This information is potentially important for the structural analysis of the room which experiences a gas explosion. The duration of explosion can be estimated approximately from the flame travel time between the ignition location and vent. The flame travel time is estimated from the flame speed (calculated from S_0, E and turbulence factor) and the distance. The usual approximation for the form of the pressure pulse is an isosceles triangle. The alternative method is to

review information on published pressure-time curves. This is the recommended method for congested volumes where significant flame acceleration will occur.

Complex empirical models have been derived by the offshore industry over the past ten years to represent explosions in highly congested volumes. They can be regarded as complex venting guidelines which take account of a large number of parameters which contribute to explosion overpressure, including details of obstacle layout. The methods tend to be computer-based because of the number of parameters involved in the calculations. Extrapolation to different situations than were covered in the test work will be limited.

Physically-based models are simplified models which are usually computer-based and which represent the major physical processes in the overall explosion process. The physical processes may be described either theoretically or based on information derived from experiments. These models are more complicated than empirical models but not as complicated as numerical models. The use of physically-based models is well established in other subjects related to combustion modelling eg. room fires.

The two types of physically-based models are:

1. **Confined explosion type.** These models can only represent low levels of turbulence and provide a theoretically based alternative to venting guidelines for empty rooms.

2. **High turbulence type.** These models can represent high levels of turbulence generated by obstacles and so could be used to model explosions in congested volumes.

Confined explosion type models have been developed to assist in the understanding of vented gas explosions in the situations normally covered by venting guidelines. These models provide a more theoretically based alternative to venting guidelines. They do not suffer from the limitations on V (except possibly in the scale-dependency of flame wrinkling), L_{max}/L_{min}, K and P_v which apply to venting guidelines. The models cannot be used for congested volumes.

High turbulence type models have been developed to model explosions in congested volumes typical of offshore platforms. Theoretical models and experimental correlations are used to describe the different physical processes. The models have been validated with data from explosion tests involving repeated obstacles.

Physically-based models provide a quick and cost effective hazard assessment tools for studying the effects of different equipment layouts and different venting arrangements on the development of explosion overpressures. The simplifications present in some physically-based models are more generally consistent with some of the major simplifying assumptions used in structural analysis for explosion pressure loading.

Idealization of equipment layout into obstacle grids generally requires substantial judgement. The models may have a restricted capacity for multiple venting path, whereas provision of such paths is desirable for reduction of explosion overpressure.

The models cannot describe explosions where the flame speed is accelerated to values in excess of 150 m/s.

Numerical modelling methods involve the direct evaluation of the fundamental partial differential equations governing explosion processes. The motivation for using them is that they could, in principle, offer a means of obtaining more accurate predictions over a wide range of conditions and geometrical arrangements (Gardner and Hulme 1995). Thus, numerical models are used for design purposes while empirical and physically-based models can only be used as screening tools to study the effects of venting arrangements, obstacle layout etc. (Kees van Wingerden, Christian Michelsen Research, private communication).

Numerical models are based on the subdivision of the domain of interest into a large number of small cells in which the conservation equations of mass, momentum and energy are solved. This approach has two major limitations:

1. It is impractical to represent some of the processes involved in explosions (especially turbulence and combustion) by the fundamental differential equations. This necessitates the use of modelling approximations and a reliance on experimental data for the calibration of models.
2. The development of explosions depend on fine-scale processes such as flames and flow around small objects. Thus, an accurate prediction would require a large number of cells. In practice, solutions of differing degrees of approximation are obtained.

Results of explosion tests have extensively used to develop and validate the numerical models. The development of the most validated and applied models is still ongoing. Generally, the models have been found to predict the correct trends of the experimental peak pressures. Errors of the order of ±40 % are claimed. The models can be applied with confidence to compare different equipment layouts and venting arrangements. Some models are available to outside organizations through consultancy by the developing organization.

Physical scale modelling uses methods by which the effects of lower flame speeds and explosion overpressures, which are associated with the small scale tests relative to full scale, are directly compensated for. This is achieved by modification of the gas-air mixture by either using a more reactive gas (eg. ethylene instead of methane) or oxygen-enriched air. This enables the high costs of the full scale testing to be avoided. However, the methods are feasible only for organizations with extensive research and development capabilities.

The main advantage of physical scale modelling over mathematical models is that the physical processes are correctly represented rather than approximated. In the construction of test rigs, it is possible to handle a finer resolution of equipment and piping layout geometries than can be covered with current numerical models. It is possible to make tests with any layout geometry without idealization of obstacle arrangements and geometries. A disadvantage is the cost of constructing the small-scale test rig and conducting the tests.

7 REDUCTION OF EXPLOSION CONSEQUENCES BY DESIGN

7.1 EXPLOSION RELIEF PANEL DESIGN

Ideally, it would be desirable to have any vent opening always uncovered. However, in most industrial situations an uncovered vent opening would be impractical. A vent cover is, therefore, used to seal the room or vessel, but is designed to open at a low pressure and allow an outflow of gases to be established at an early stage.

Because any explosion relief cover has mass it will also have inertia. A finite time is therefore required, after the opening pressure P_v has been reached, to move the vent cover a sufficient distance to allow the full flow of gas out of the enclosure. Until this time has elapsed the internal pressure will continue to rise, although at a reduced rate. It follows that the first pressure peak P_1 will be somewhat larger than P_v. To restrict P_1, the explosion relief should be as light as possible (ie. have low inertia) so that the delay in establishing the outflow of gas is minimized (Harris 1983).

The most common types of vent covers used for different applications are
- windows with glass panes which shatter
- explosion relief panels which fly away
- explosion relief doors which open
- rupture diaphragms which rupture.

Glass windows, whose primary purpose is to let light into the room and which may be opened for airing, are sometimes used in the industry as explosion relief vents. The drawbacks of the use of glass panes as vent covers are the relatively high failure pressures and the generation of high-velocity glass fragments.

The thickness of a window pane is determined from the requirement that it must not be broken by wind loads. The design wind load in Finland ranges 0.5 - 1 kPa, depending on the location of the building and the height over grade of the window. The nominal thickness of a float glass pane is determined from the requirement that the bending stress corresponding to the design load must not exceed 30 MPa. This involves a safety factor of 1.5. Besides, the minimum thickness of a pane must be 3 mm; that of the panes of a double-glazed element 4 mm (RT 38-10316).

Methods used to estimate the pressure at which a window pane is broken by a blast wave cannot be used to estimate P_v in vented explosions. The strength of a glass pane decreases with increasing duration of applied load. Harris et al. (1977) have performed gas explosion tests to determine the failure pressures of window panes of different sizes and thicknesses. The average breaking pressure of single-glazed windows as a function of pane area is shown in Fig. 7.1.
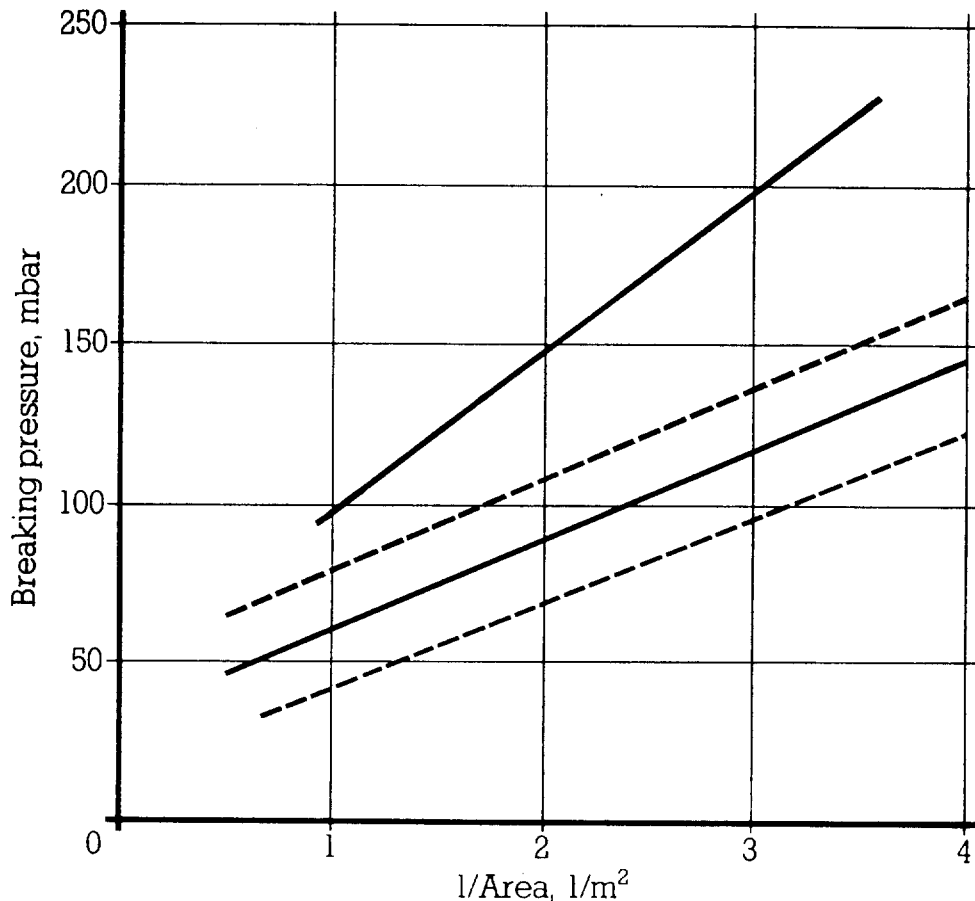
Figure 7.1. The breaking pressure of single-glazed glass windows as a function of pane area. The curves from top: 6.5 mm Georgian glass, 5 mm, 4 mm and 3 mm glass (Harris 1983).

It is seen from Fig. 7.1 that the breaking pressure increases with decreasing pane area. To get a low breaking pressure, the pane must be large. For example, the breaking pressure of a, say, 1 m² single-glazed window (whose thickness is 3 mm according to RT 38-10316) is 4 kPa, which is still an unnecessarily high value for an explosion relief vent. Increasing the pane area does not help since the glass thickness must be increased to prevent breakage due to wind loads.

If the windows have panes of different sizes the smaller ones will break at a later stage of an explosion, or may not break at all. This means that only part of the total window area may act as pressure relief vent.

West (1973) has performed explosion tests to determine the breaking pressures of double glazed windows. A second pane was fixed to the wooden frame of a single-glazed window. The gap between the panes ranged 8 - 51 mm. Under these condition the double-glazed windows had breaking pressures up to only 30 % higher than single glazed ones of the same size and thickness. Failure pressures were found to be virtually independent of inter-pane spacing in the range studied.

The result of a failure of a glass window will often be the generation of a shower of high-velocity glass fragments. In some explosions, these fragments can travel further than the distance at which significant pressure effect occur.

However, experiments by Harris et al. (1977) demonstrate that the application of a shatter resistant film to glass panes effectively prevents the formation of glass fragments on window failure. In the tests, this kind of pane was found to be blown out in one piece. Besides, application of a shatter resistant film was found to have no significant effect on the breaking pressure of a glass pane.

Experiments by Harris et al. (1977) have also shown that the maximum distance travelled by a glass fragment, following failure of a window, is directly proportional to P_{red} (Fig. 7.2). The maximum distance to which a glass pane treated with shatter resistant film flies is seen to be significantly less than that of fragments from an untreated glass pane.

Figure 7.2. Distance of travel of glass window fragments as a function of maximum internal pressure P_{red}. Solid line = glass panes treated with shatter resistant film, dotted line = Georgian wired glass panes, dashed line = untreated plain/patterned glass panes (Harris 1983).

Howard and Karabinis (1980) present a list of important factors that should be considered when designing explosion relief panels:

1. Sufficient vent panel area A_v to prevent internal pressure P_{red} from exceeding the strength of the weakest part of the building desired not to vent.
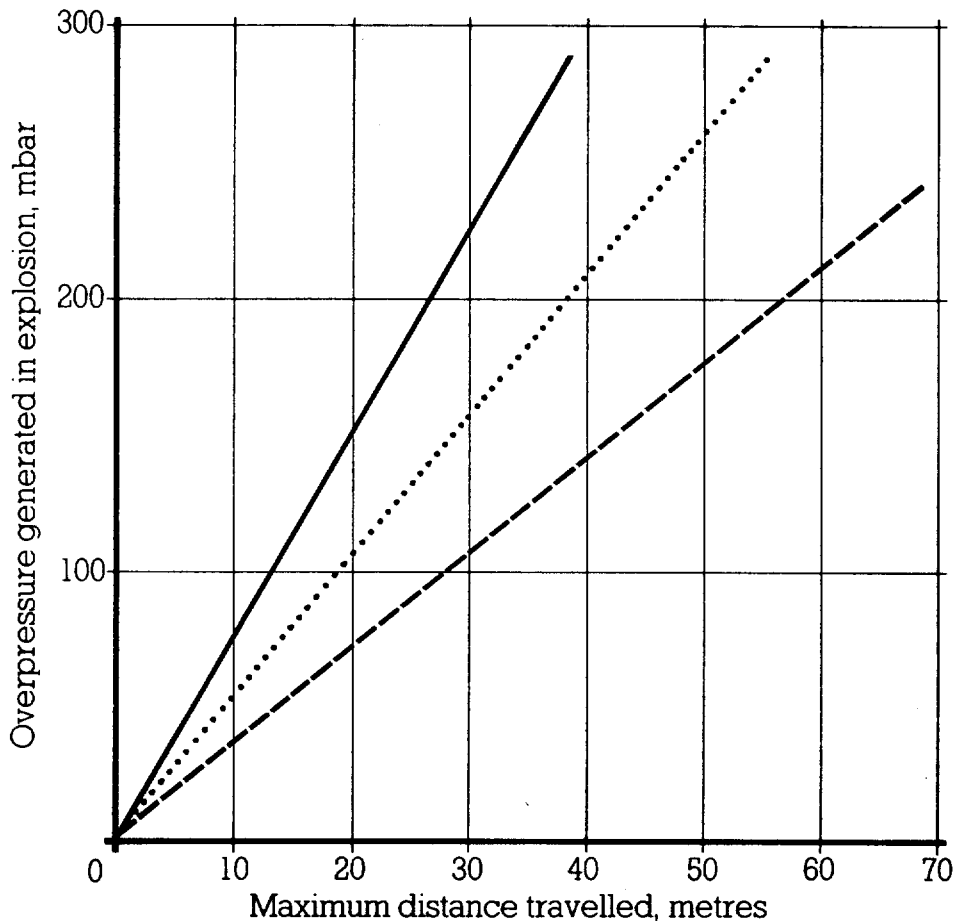
2. Sufficiently low mass/area ratio w for the explosion relief panel so that the panel is accelerated to the necessary high velocity for opening. Normally, w should not be larger than 10 kg/m^2.

3. Sufficient restraint of explosion relief panels to prevent the panels, once opened, from flying away from the building to cause damage elsewhere. This can be accomplished by fixing the panels to the building with tethers strong enough and incorporating some form of shock absorber.

4. The building member to which the tether is attached must be strong enough to withstand the force of the tether.

5. The explosion relief panel must not break into pieces during the venting sequence.

6. The explosion relief panel must withstand "wear and tear" in its normal service as a part of the building.

7. The explosion relief panel may need to incorporate thermal insulation. Again, the mass/area ratio w should be kept within the allowable limits.

8. The explosion relief panel opening pressure P_v should be as low as practicable. However, the strongest anticipated winds, producing negative pressures, should not cause the panel to open. In most cases, $P_v = 1$ kPa is acceptable (NFPA 68).

9. A railing may be necessary inside the building along the explosion relief panels to prevent people or equipment from falling against the panels, knocking them loose, and falling out of the building.

Howard and Karabinis (1980) used a test chamber of volume 81 m^3 (5.54 m x 4.43 m x 3.32 m), of which 40 m^3 was filled with 5 % propane-air mixture, to test different explosion relief panels. Three different types of conventional panels of corrugated construction were used made of:
1. fibre reinforced plastic, w = 1.8 kg/m^2
2. aluminium, w = 2.7 kg/m^2
3. galvanized steel, w = 6.2 kg/m^2.

Howard and Karabinis (1980) draw the following conclusions regarding the suitability of these materials:

1. The panels made of fibre reinforced plastic disintegrated into fragments, which were found as far as 15 m from the test chamber. This type of behaviour clearly demonstrated that only ductile materials should be employed for explosion relief panels.

2. The aluminium panels maintained their integrity in spite of the fact that many were greatly distorted. In some instances, tearing was observed near fasteners which, however, did not impair the integrity of the panel.

3. The galvanized steel panels maintained their integrity, exhibiting less average tearing and distortion than the aluminium panels.

The opening pressure P_v used in the tests was 1.4 kPa which is recommended by NFPA 68 for areas with severe windstorms. Three types of fasteners for explosion relief panels were tested.

1. The blind rivet available in a variety of lengths and rated by the manufacturer in both static shear and tension. The rivet was used either as a shear or tension fastener.
2. The standard stainless steel sheetmetal screw. The failure mechanism of this type of fastener involves a punching-tearing failure of the (aluminium) panel around the head of the screw, permitting the panel to pass over the head of each screw.
3. A stainless steel sheetmetal screw with a neoprene centring device and a stainless steel indented washer. This particular fastener was the only one marketed as an "explosion venting fastener". During installation, an oversized hole is drilled into the panel. In an explosion, the indented washer fails around the head of the screw permitting the panel to pass unobstructed.

The first type of fastener appeared to be the most reliable of the three in so far as the calculated and measured opening pressures P_v were compared. The total number of the second type of fasteners was determined on the basis of static pull-out tests conducted on individual fasteners, and the observation of tearing failures around such screws in previous tests. However, Howard and Karabinis (1980) considered it necessary to do a great deal more research before this fastener can be recommended for general use with aluminium panels.

The total number of fasteners of the third type was based upon the manufacturer's rated capacity. However, the measured opening pressure was 7 kPa instead of the calculated 1.4 kPa. This was thought to be attributable, in part, to the method used by the manufacturer to determine the capacity of the fastener: A container gradually filled with weights was suspended from a single fastener. The total weight causing failure of the indented washer was taken as the capacity of the fastener.

This technique involved very low strain rates and in no way simulated the actual strain rates in an explosion. It is well established that steel exhibits a dynamic increase in strength when loaded at high strain rates.

Harris (1983) comments this issue as follows. Experience suggests that the performance of an otherwise effective explosion relief panel can be reduced significantly in cases where the opening pressure P_v is actually determined by the type of fastener used. Commercially available fasteners - such as shear bolts, latches, spring clips etc. - rarely operate at the anticipated pressure. In most cases they fail at a pressure in excess that quoted by the manufacturer.

This discrepancy can be attributed largely to the methods used by manufacturers to "calibrate" the fasteners. Usually this is a simple dead weight determination of the force required to open the fastener. This makes no allowance for the dynamic response of the fastener under explosion conditions and, therefore, is likely to underestimate P_v under these conditions. The suitability of a fastener can only truly be judged through

observation of its performance under test explosion conditions.

Howard and Karabinis (1980) tested different restraint systems to prevent the explosion relief panels from flying away. The recommended restraint system of an insulated panel with w ≤ 12 kg/m² and A ≤ 3 m² is described as follows (NFPA 68):

1. A 6.5 mm diameter, 1.2 m long galvanized wire rope tether with three rope clips at each end where the wire rope is lapped.

2. The tether-to-panel anchorage shown in Fig. 7.3 with a forged 13 mm diameter eye bolt.

3. A "shock absorber" device with a fail-safe tether. The shock absorber is a 10 cm wide, 4.8 mm thick, L-shaped piece of steel plate to which the tether is attached (Fig. 7.3). During venting, the shock absorber will form a plastic hinge at the juncture in the "L" as the outstanding leg of the "L" rotates in an effort to follow the movement of the panel away from the structure. The rotation of this leg provides additional distance and time over which the panel is decelerated while simultaneously dissipating some of the panel's kinetic energy.
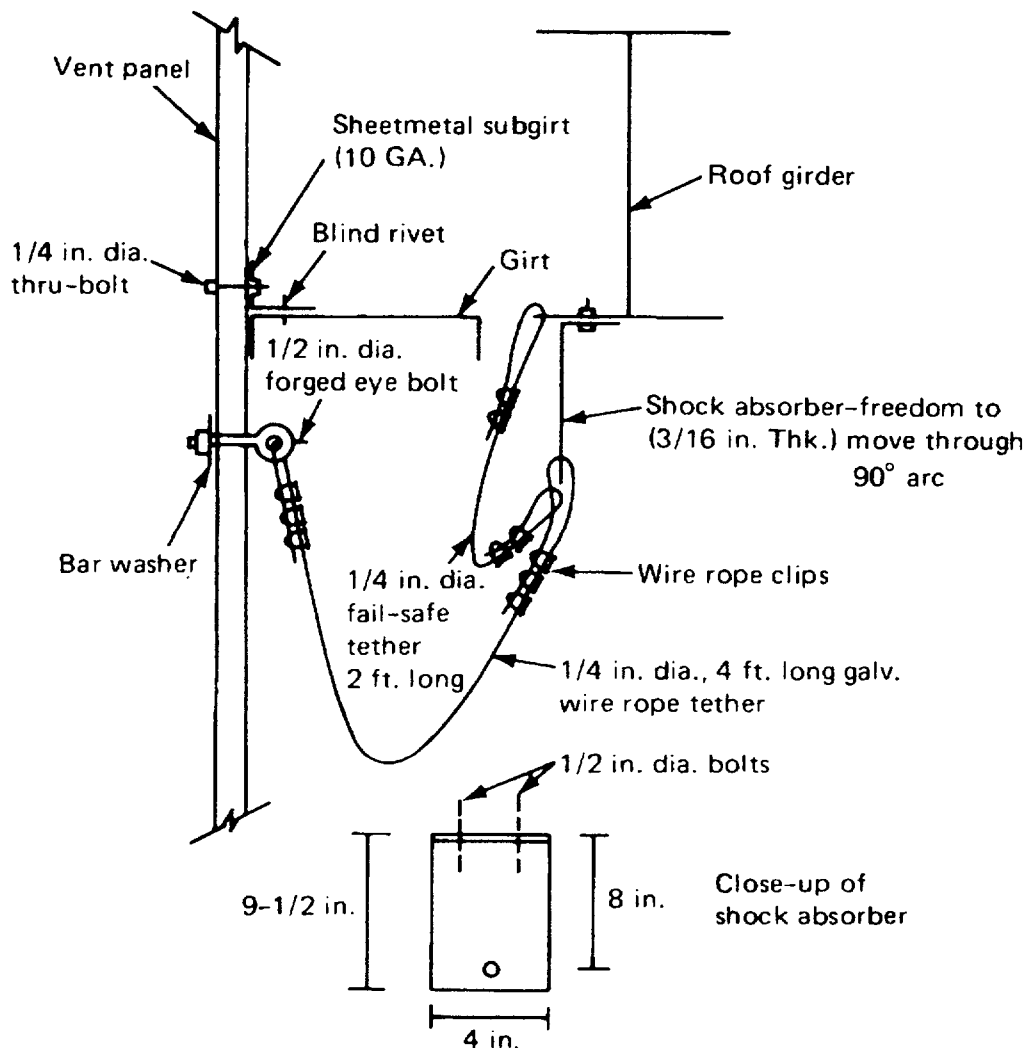

Figure 7.3. Restraint system with a "shock absorber" device (NFPA 68).

101

Dainty et al. (1990) have tested explosion relief doors developed by a Canadian manufacturer. The manufacturer used a calibrated magnetic latch mechanism to hold the door closed, also allowing it to open at a predetermined internal overpressure. The doors were fitted with a hold-open mechanism to prevent any damages to the building due to underpressure when the combustion products cool after the doors have closed. This was an option recommended by the manufacturer.

The explosion relief doors measured 0.76 m x 0.76 m and were hinged either at the top or the bottom. A shock absorption system was provided to absorb the kinetic energy of the door as it opens. The different door materials tested were
-       16 mm polycarbonate glazing
-       13 mm honeycomb paper core with a 0.8 mm thick aluminium skin on each side
-       51 mm honeycomb paper core with a 0.8 mm thick aluminium skin on each side
-       51 mm fibreglass insulated core with a 0.8 mm thick aluminium skin on each side.

The explosion relief door to be tested was mounted on a 1.9 m^3 cylindrical explosion chamber filled with 8 % methane-air mixture. The mixture was ignited at the centre and the internal pressure was measured at the rear of the chamber. Altogether 53 tests were performed.

In general, the explosion relief doors performed their intended task relieving the internal pressure. The maximum internal pressure P_{red} reached during any test was 3.9 kPa. When opening, the top hinged doors showed a tendency to bounce back and reclose from the fully open position. The hold-open mechanism had to be able to prevent the panel from reclosing in spite of this rebounding effect and the effect of the momentary underpressure in the chamber.

Some of the latch mechanisms tested were unable to resist these forces, and allowed the door to slam shut immediately after the explosion. In those cases, a significant underpressure was created in the chamber. Other latch mechanisms performed well, preventing the door from closing after the explosion.

The release mechanism was calibrated to release at a predetermined pressure P_v. The release pressure was checked by a portable hydraulic apparatus. The static release loads were set at ±10 % of their design values. The measured opening pressure was defined as the internal pressure at which the latch has just released and the door has began its outward swing. Test results indicated that the explosion relief doors opened generally at a lower pressure in an explosion situation than they did when checked statically. Additional tests would have been needed to find out the reason for this behaviour (Dainty et al. 1990).

Haaverstad (1992) presents typical design criteria for explosion relief doors for offshore platforms, and how they have been used to develop a system of relief doors. The system provides a large flexibility and can therefore meet the most relevant design criteria.

The explosion relief doors have to resist the external wind pressure (both pressure and suction) which is on the North Sea at most 2.5 kPa. This criterion implies that the opening pressure is to be approximately 50 - 100 % higher than the wind pressure because of dynamic effects. The typical design requirement is thus P_v = 5 kPa and the explosion relief door must be fully open after 40 ms.

To meet future requirements, the following additional criteria were stated:

-       the relief door system is to have full flexibility regarding dimensions, opening pressure and wind resistance
-       the relief door is to open as quick as possible (ie. have lowest possible weight)
-       the production method and design are to be cost-effective and the design is to ensure simple installation and repair methods
-       no fragmentation and permanent blockage of areas outside the relief area shall occur.

In order to fulfil the overall criterion regarding full design flexibility, a theoretical simulation method was used. The experimental work was therefore considered as a verification of this model. Due to the fact that it is relatively difficult to estimate the exact failure load of structural members exposed to dynamic loads, much effort was made to develop a simple, predictable and reliable design (Fig. 7.4).
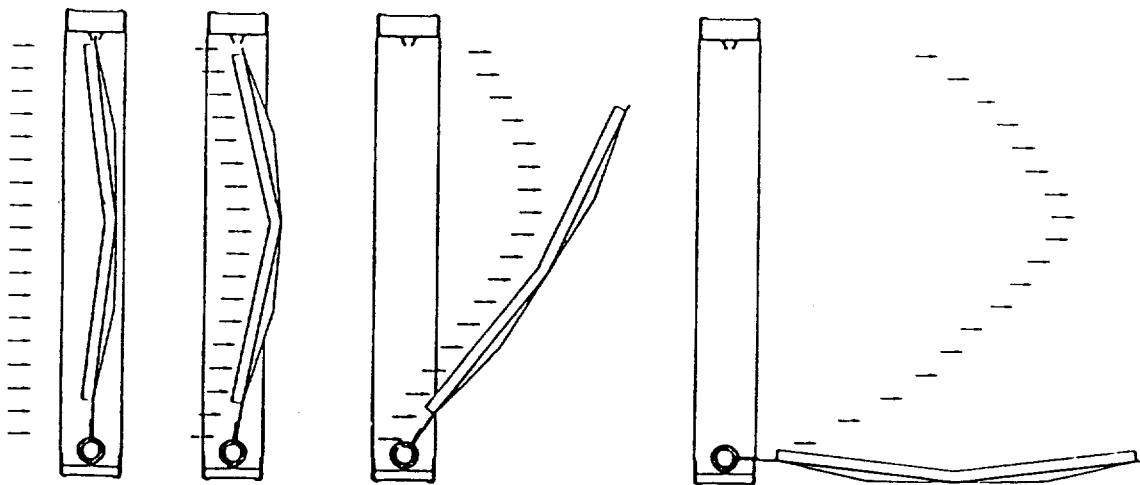
Figure 7.4. The design principle for the explosion relief door (Haaverstad 1992).

The behaviour of the explosion relief door during explosion is characterized by (Haaverstad 1992):

1.   During the initial part of the pressure build-up, the door will be displaced horizontally. The deformations will then pull the door out of the groove at the upper edge. There is no fixing at this edge. This provides small scatter since the door opening in controlled by bending and not by failure of any fixing component.
2.   When the vertical displacement at the groove edge pass the bottom of the groove, the door is free. It will then rotate around the hinge.

The development work started with simulation with a computer program based on the finite element method. The program included non-linear and static simulation routines. Several doors were designed. The dimensions, thickness, form etc. of the door were varied in order to achieve a best possible verification of the simulation method.

The test series consisted of ten different explosion relief doors which were subjected to various explosion loads. The detailed behaviour of the doors and the loads were recorded. Subsequently, the door behaviour was simulated again to compare the observed results with the simulated ones. The result was that the actual opening pressure was within 10 - 15 % of the simulated one. The opening times showed a somewhat higher scatter. The typical situation was that the actual opening time was 5 - 45 % longer than the simulated one.

7.2   WALL LINING

The oscillatory pressure peak P_4 is caused by the coupling of the pressure waves generated in the combustion of the remaining pockets of unburned mixture to the standing acoustic wave in the room. This pressure peak is increased by the following factors:

-       the room is cubic or nearly cubic in shape
-       the room has smooth walls
-       the room is empty or almost empty
-       the explosion relief vent is in the centre of a wall.

The presence of obstacles in the room can prevent the formation of the standing acoustic wave necessary for the generation of P_4. However, for a nearly cubic room with little internal obstacles it may be necessary to prevent the formation of the standing acoustic wave by other means. Lining the walls with a acoustically absorbing material is an easy and effective solution to this problem.

Fig. 7.5 shows the effect of lining the walls of a 2.55 m^3 cubic explosion chamber with a layer of mineral wool. Vent coefficient K is 5 and vent opening pressure P_v is 12 kPa. The value of the first pressure peak (which consists of the peaks P_1 and P_2 merged into a single peak as in Fig. 5.6) is 14 kPa. The value of the oscillatory peak P_4 (with the high frequency oscillations removed as in Fig. 6.1) is 42 kPa. With wall lining, the early part of the internal pressure is unchanged but no oscillatory peak is seen (Cooper et al. 1986).

van Wingerden and Zeeuwen (1983) have investigated the effect of different wall linings in a 5.2 m^3 explosion chamber. The chamber had a rectangular shape (height and width 2 m, length 1.2 m). One of the 2 m x 2 m walls was replaced by a curved wall with a vent opening whose size was either 1 or 2 m^2. The vent was covered with two layers of plastic sheeting which yielded at a static opening pressure of about 4.5 kPa. Five hydrocarbon gases were used in the different tests.

To test the effect of lining on the values of P_1, P_2 and P_4, tests were performed with propane-air mixture, using 50 mm glass wool and corrugated plates with two different

profiles as lining materials. The results are given in Table 7.1. It is seen that the lining of two internal surfaces is enough to make P_4 lower than P_1 and P_2. When three internal surfaces are lined the oscillatory peak disappears. In practical applications, one should line the side walls and the ceiling rather than the front and rear wall (Kees van Wingerden, Christian Michelsen Research, private communication).
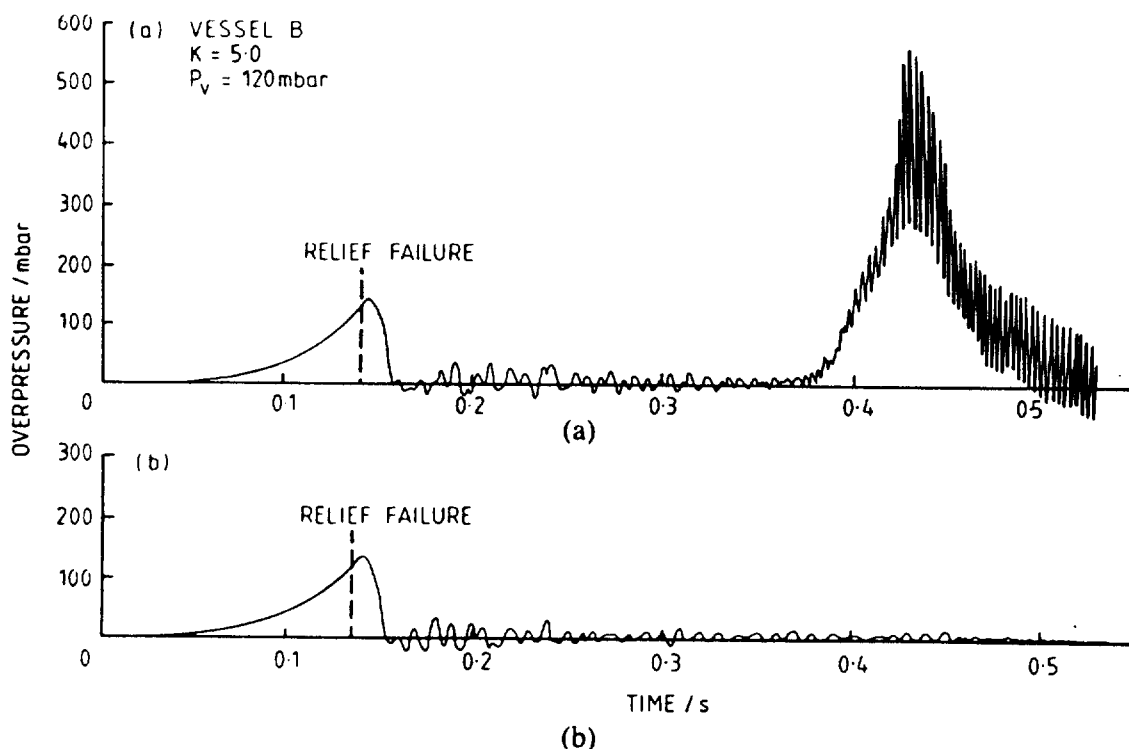
Figure 7.5. The effect of acoustically absorbing material on P_4. a) bare walls, b) walls lined with mineral wool (Cooper et al. 1986).

Table 7.1. Effect of lining on the pressure peaks.

lining material	lined walls	conc. %	P_1 kPa	P_2 kPa	P_4 kPa
none	none	5.6	4.2	5.2	34
glass wool	1 sidewall + floor	5.6	4.1	5.1	3.8
"	2 sidewalls	5.5	4.1	5.7	3.1
"	2 sidewalls + floor + ceiling	5.3 6.0	3.6 4.0	5.8 3.4	0 0
corrugated plate 1	2 sidewalls + ceiling	5.2	1.9	5.8	0
corrugated plate 2	2 sidewalls + ceiling	5.4	2.6	1.2	0

7.3 VENT LOCATION AND EQUIPMENT LAYOUT

The venting guidelines are usually based on tests with near-cubic empty chambers with a single square explosion relief vent centrally located at one side. A rectangular vent will be almost as effective as a square one with an equal area because the hydraulic diameter of the vent decreases only slowly with increasing ratio l_{max}/l_{min} of the vent (where l_{max} is the larger side and l_{min} the smaller side of the vent).

For large rooms, the vent size A_v given by the venting guidelines must be divided into a number of explosion relief vents. However, the pressure relief provided by multiple vents can be lower than that which will be obtained with a single vent of the same total area. This is particularly true for vent covers which must be shattered (eg. glass panes) to provide a vent opening, for which the breaking pressure is inversely proportional to the area. The relief venting will begin later and the resulting maximum internal pressure P_{red} will be higher.

If both the opening pressures P_v and masses per unit area w of the individual explosion relief panels/doors are the same, the effective overall vent coefficient K_{av} can be calculated from the formula

$$\frac{1}{K_{av}} = \sum_i \frac{1}{K_i} \tag{47}$$

where
K_i are the vent coefficients of the individual explosion vent panels/doors.

In practice this means that the opening pressures P_v must not vary by more than a factor of two. The tolerance of the mass per unit area w should be limited to a factor of no more than two (Harris 1983).

After the mechanism of flame acceleration was understood, it was possible to present guidelines for equipment layout and vent location to reduce the explosion overpressures. Such guidelines were presented by Pappas (1984) on the basis of the early explosion tests by Det norske Veritas. The guidelines cannot guarantee low explosion overpressures but will increase the likelihood of obtaining acceptable pressure loads. The following presentation is based mainly on a recent article by van Wingerden (1994).

The shape of the room and the location of the vent areas are closely linked and will therefore depend on each other. There are two main principles to apply when optimizing the shape of a room:

1. An ignition point anywhere in the room should be as close as possible to the major vent areas, so hot combustion products can be vented out at an early phase of the explosion.
2. Strong turbulence in the unburned mixture ahead of the flame front and long flame front travel distances should be avoided.

For a room with explosion vent areas on two opposite walls, the ideal shape is a cube (Fig. 7.6). The advantage of attaining cubic shape also depends on how densely packed with obstructing objects (ie. process equipment and piping) the room is. In such situations, the obstructing objects control the flame propagation and the shape of the compartment is less important.
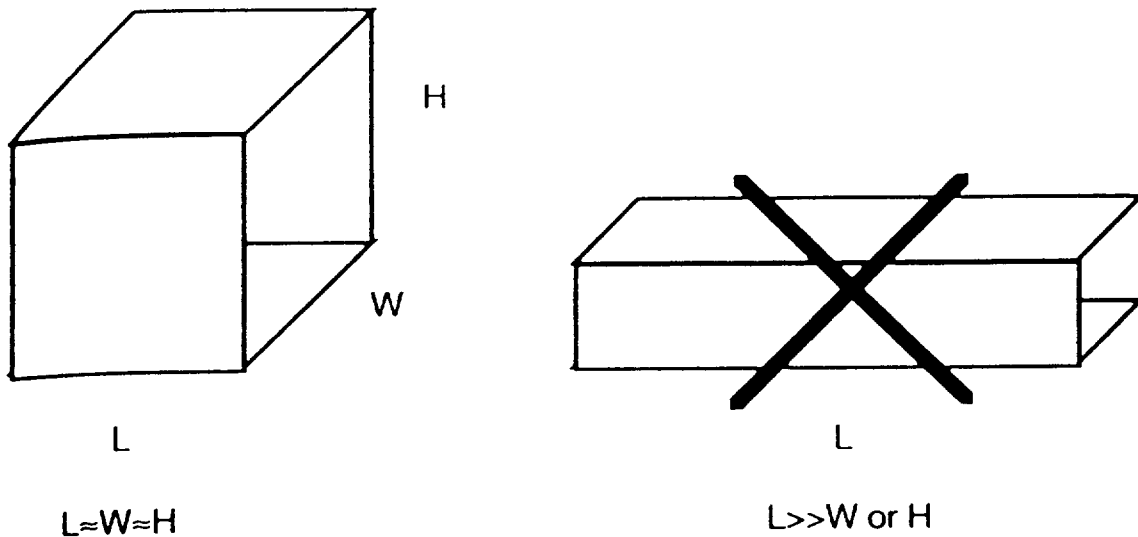
Figure 7.6. In the case of explosion vent areas on two opposite walls, a cubic shape gives the best explosion venting (van Wingerden 1994).

Most explosion scenarios will give higher pressures if the room is elongated and the vent areas are only located in the two end walls. In this case, the flame front can travel over a longer distance, and the conditions will support flame acceleration.

It is even more important to avoid an elongated shape if the room has vent area only in one of the end walls. In the case of ignition near the closed end wall, the flame can accelerate over a long distance and venting has no beneficial effect, since it only leads to flow past obstacles and hence to turbulence generation.

For an elongated room, it is necessary place the vent areas on at least one of the long side walls, instead of the end walls (Fig. 7.7). In this way, the distance from almost any ignition point to the nearest vent opening will be less (van Wingerden 1994).
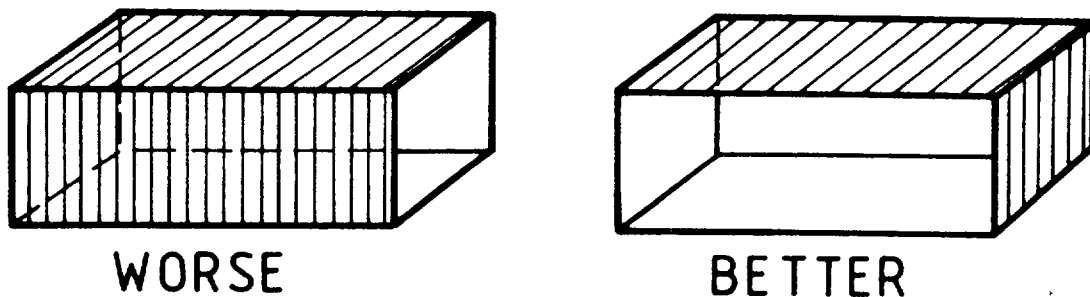
Figure 7.7. The recommended location of vent areas in an elongated room (Pappas 1984).

One of the most important factors governing the effect of obstacles on explosion overpressure is the direction of the flame propagation relative to the flow of the unburned mixture towards the vent. If the ignition point is remote from the vent significant flame acceleration can be expected to happen in the flow through the obstacle system. However, if the ignition point is close to the vent the flame front will propagate counter to the flow with significantly less flame acceleration (Fig. 7.8).
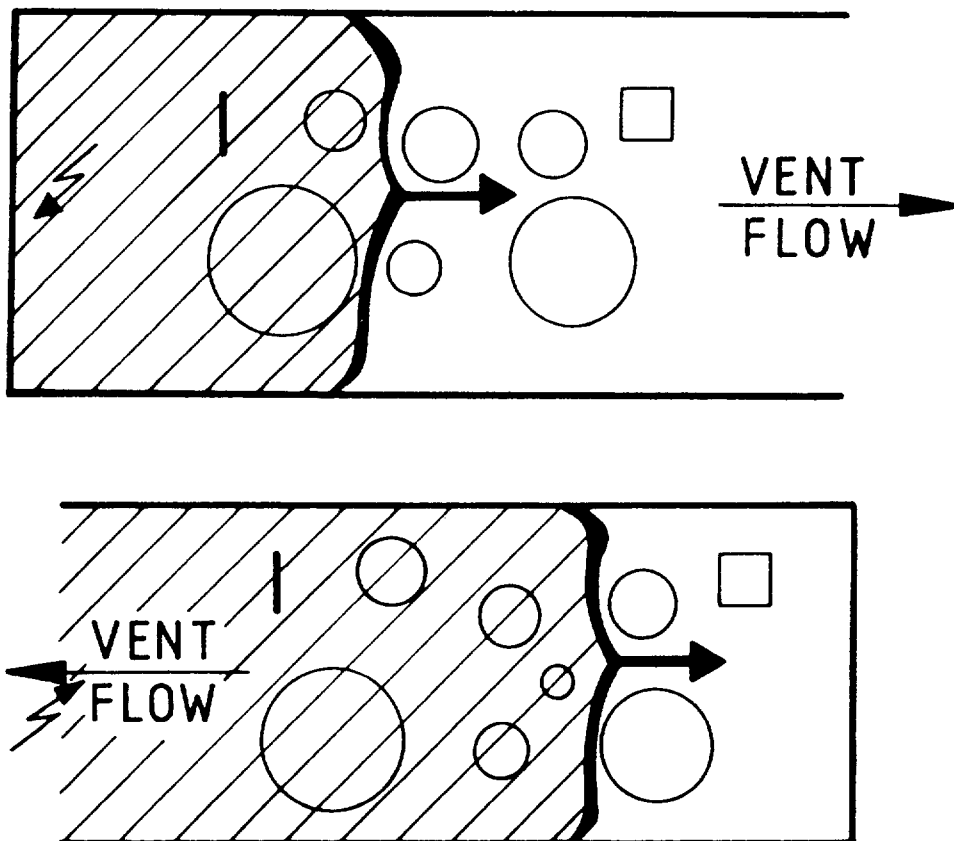
Figure 7.8. Effect of ignition location on flame propagation (Pappas 1984).

In practice, it is not usually possible to control the location of the ignition source. The conditions causing flame acceleration are determined by the relative location of obstacles, vent openings and the point of ignition. Generally, one should not locate obstacles in areas where high flow velocities can be expected, particularly close to vent openings (Kees van Wingerden, Christian Michelsen Research, private communication) (Fig. 7.9).

Positioning obstacles (pipes etc.) away from the vent also minimizes the drag forces (Sec. 7.4) on these obstacles caused by the high flow velocities. The obstacles will then be less liable to damage due to drag loading (Pappas 1984).

The main principles of the guidance in positioning obstacles (process equipment, pipework etc.) in the room are (van Wingerden 1994)
1.   minimize turbulence generation
2.   do not block explosion venting.

WORSE   BETTER
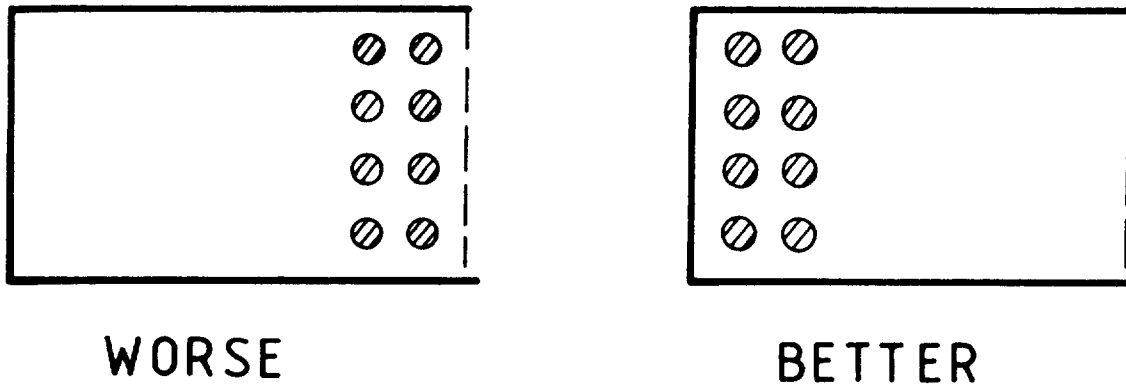
Figure 7.9. Preferable location of obstacles (Pappas 1984).

Fig. 7.10 shows the top view of two different layout arrangements in a room. The room has vent areas on the two end walls. The obstructing objects consist of two vessels and a small room. In the first layout, the room will block the main parts of the vent area on the right-hand side and the vessels in the left part of the room will cause reduced venting and (being repeated obstacles) flame acceleration.
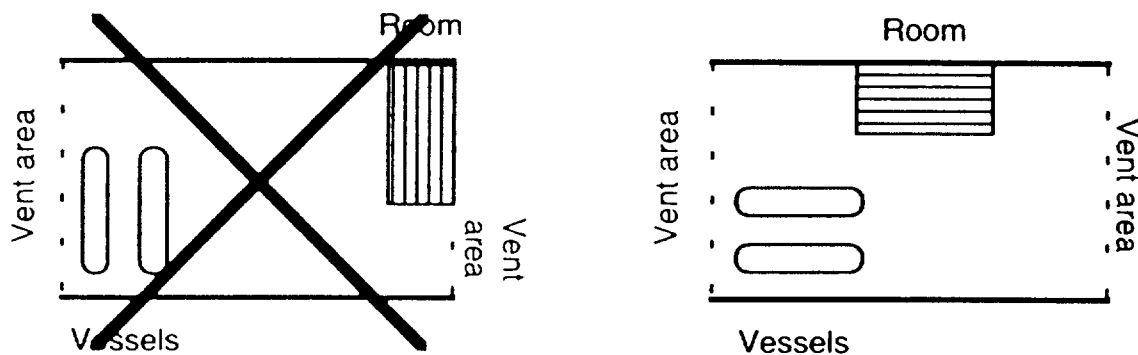
Figure 7.10. Two different layout arrangements in a room (van Wingerden 1994).

It is very important to arrange the equipment in such a way that minimum turbulence is generated during an explosion. This is normally obtained when the longest side/dimension of the equipment is parallel to the flow direction during an explosion ie. pointing in the direction of the vent area (as in the second layout in Fig. 7.10).

A room may contain repeated obstacles such as parallel pipes, vessels, girders, pillars etc., which cannot be aligned with the flow towards the vent area. For such cases, the following guidance can be given (Pappas 1984):

- avoid repeated obstacles in the direction of flow towards the vent area (Fig. 7.11)
- avoid obstacles with a sharp profile (at least the edges should be rounded) and prefer obstacles with a round profile
- try to keep the blockage ratio of a row of obstacles as low as possible.

WORSE   **BETTER**
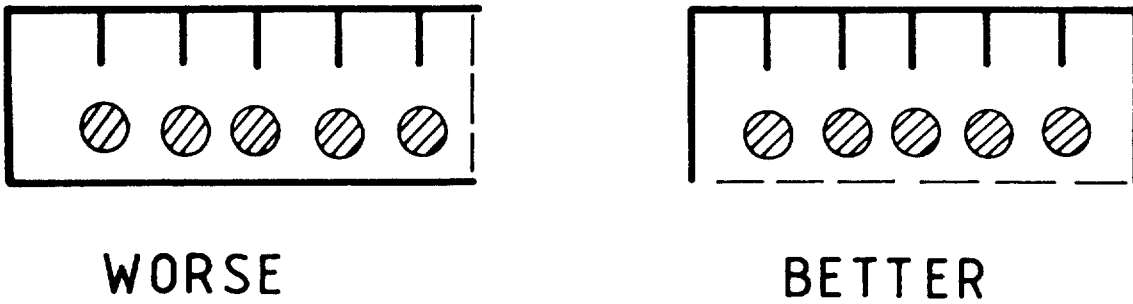
Figure 7.11. Avoid repeated obstacles in the direction of flow towards the vent area (Pappas 1984).

7.4 DIMENSIONING OF LOAD-BEARING WALLS

The aim of explosion venting is to reduce the maximum internal pressure P_{red} to a value which does not damage load-bearing walls and other primary structures. The following presentation on the response of structures to explosion overpressures is based mainly on the paper by Harris et al. (1985).

The response of even simple structural elements to real pressure loadings is extremely complex. However, by presenting a few idealized solutions for a simple system in which movement is allowed in only one direction, the basic effects produced by different overpressure/time loadings on structural elements of different resistance to loading can be demonstrated.

In Fig. 7.12, a structural element is represented by a simple forced spring and mass system. When it is subjected to an overpressure/time loading f(t) [N] and the resistance function describing the spring is R(y) [N] the equation of motion can be written as

$$m \frac{d^2y}{dt^2} = f(t) - R(y) \tag{48}$$

where
y   is the displacement of the centre of mass [m].
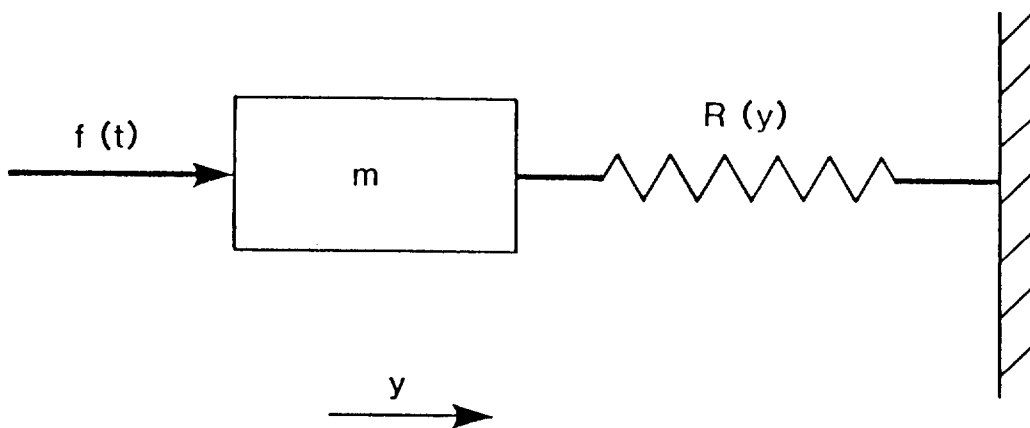
Figure 7.12. A simple forced spring and mass system (Harris et al. 1985).

For the case of a perfectly elastic system where the force required to cause displacement is directly proportional to the displacement, Eq. (48) becomes

$$m\frac{d^2y}{dt^2} = f(t) - ky \qquad\qquad (49)$$

where
k   is the stiffness constant of the spring [N/m].

The dynamic response of the perfectly elastic system under different applied loadings can be illustrated by solving Eq. (49) for the two types of pressure pulses shown in Fig. 2.3. The pulse of zero rise time (Fig. 2.3a) represents a blast wave from a detonation of high explosive. The pressure pulse of finite rise time (Fig. 2.3b) represents the internal or external overpressure of a vented gas explosion. The duration of the loading is denoted by t_d [s].

The solutions of Eq. (49) for maximum deflection y_{max} [m] are presented in Fig. 7.13. This Figure essentially shows the ratio of y_{max} to the static loading deflection f_{max}/k, as a function of the ratio of the duration of loading t_d to the natural period of vibration T_n [s] of the system. The ordinate of Fig. 7.13 is usually called the **dynamic load factor.**
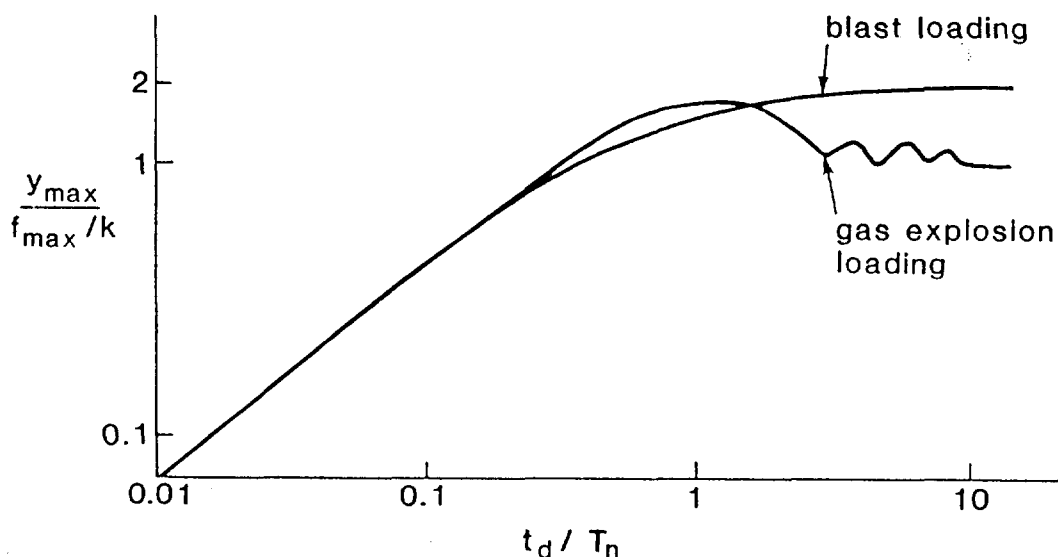
Figure 7.13. The dynamic load factor for a vented explosion and a blast wave from a detonation (Harris et al. 1985).

Figure 7.13 shows how this simple model illustrates that purely elastic structural response depends both on the peak pressure and on the ratio t_d/T_n. For the two pressure pulses in Fig. 2.3, three basic categories of response can be identified.

1. $t_d >> T_n$. The loading experienced will effectively be equivalent to a static load of a magnitude equal to either the peak overpressure (vented explosion) or twice the peak overpressure (blast wave from a detonation). This is because there is no dissipation of the load before maximum deformation is achieved.

2. $t_d < < T_n$. The loading experienced will effectively be equivalent to a static load lower than the peak overpressure. This is because the load is imparted to the structure and removed before the structure has adequate time to fully respond. This means that under these conditions a structure could withstand a higher dynamic pressure than the static load necessary to cause failure.

3. $t_d \approx T_n$. The loading experienced will effectively be equivalent to a static load greater than the peak overpressure. The equivalent static overpressure for a vented explosion can be up to a factor of almost twice the magnitude of the applied loading. This behaviour is produced by the resonance between the loading rate and the natural period of vibration T_n. For blast wave loading, there is a gradual transition region.

Most structures are not perfectly elastic but actually have resistance/displacement functions such as that shown in Fig. 7.14. This can be formalized into two parts in which the response is firstly perfectly elastic, and then perfectly plastic. Thus in Fig. 7.14, for displacements $y < y_{yield}$, $R(y) = ky$ and for $y_{yield} < y < y_{fail}$, $R(y) = ky_{yield}$ which is a constant.
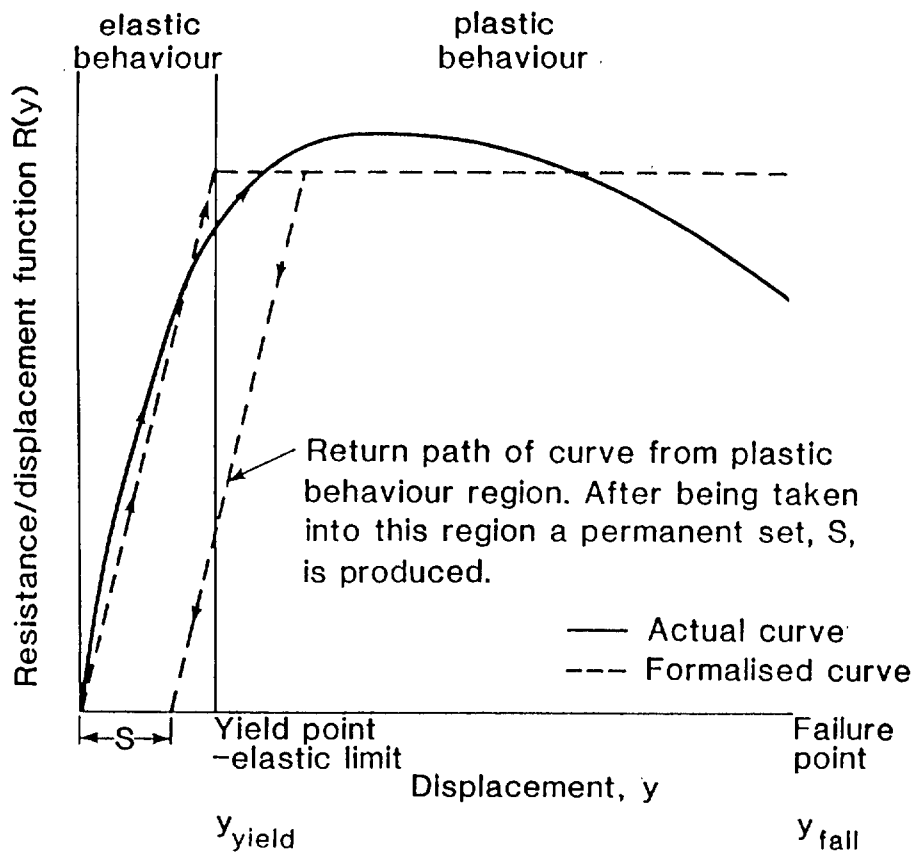
Figure 7.14. Resistance/displacements curves showing regions of elastic and plastic behaviour (Harris et al. 1985).

The effect of plasticity on structural response is illustrated in Fig. 7.15, which plots the dynamic load factor for vented explosion loading as a function of t_d/T_n. Fig. 7.15 reproduces the elastic response shown in Fig. 7.13 and also plots the responses to this

loading, of structures with ductility ratios μ of 3 and 10. The ductility ratio μ is the amount of total deformation that a material sustains compared to the limiting elastic (recoverable) deformation.

The effect of increasing plasticity in Fig. 7.15 is to damp out the resonant dynamic overshoot at $t_d \approx T_n$, and also to reduce the dynamic load factor for short duration loadings where $t_d < < T_n$. This is because more energy can be absorbed when the structure deforms plastically.
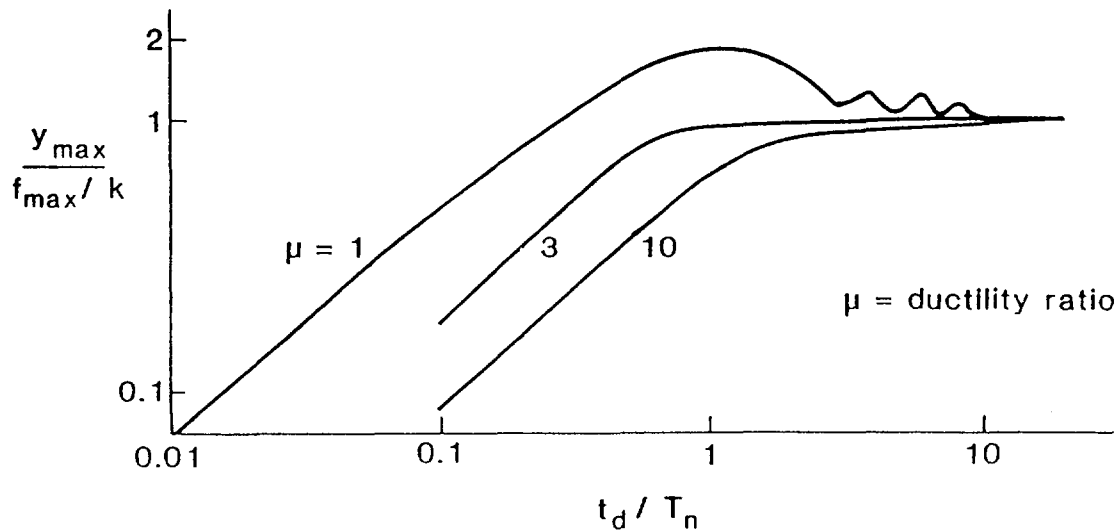
Figure 7.15. Effect of plasticity for vented explosion loadings (Harris et al. 1985).

Although the natural period of vibration T_n of a structural element will depend upon such factors as the actual method of construction, and the size of the components involved, some typical values of T_n for structural building components are given in Table 7.2.

Table 7.2. Typical values of t_d and T_n (ms).

blast wave from detonation of high explosive	1 - 10
concrete floors	10 - 30
concrete walls	10 - 15
brick walls	20 - 40
vented explosion	100 - 300

Also given are typical durations of pressure pulses t_d associated with detonations of high explosives and confined gas explosions. Typical pressure-time curves for these two cases are shown in Fig. 7.16. It is seen that the durations t_d are quite different, being typically 1 - 10 ms for detonation blast wave and 100 - 300 ms for a vented explosion.

113
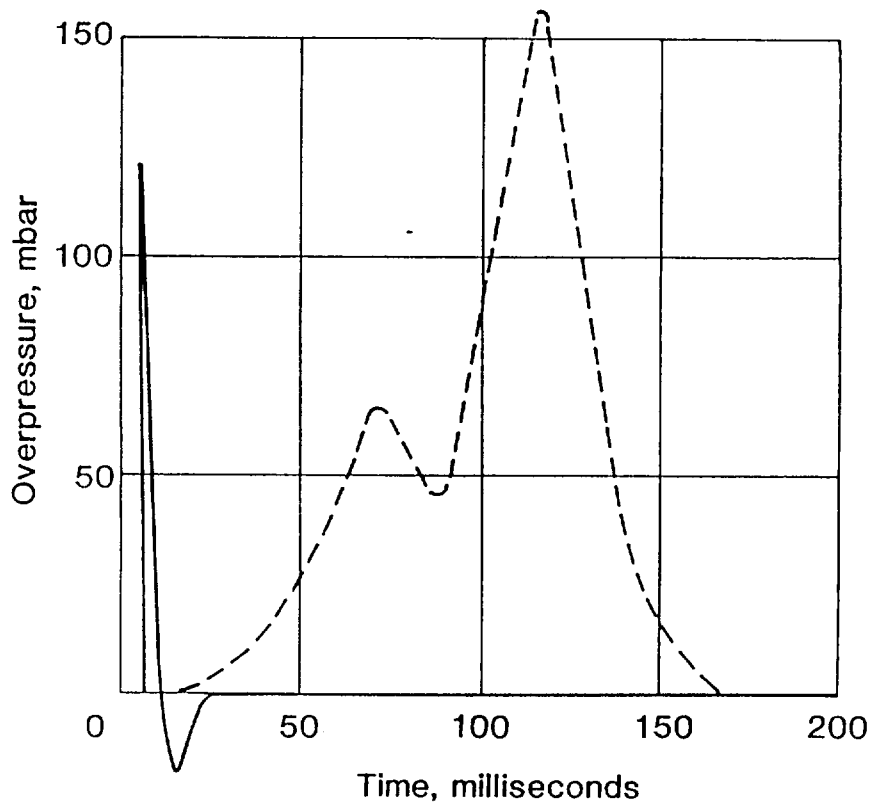
Figure 7.16. Typical pressure-time curves for a blast wave from a detonation (at 10 m distance from 1 kg TNT) and a vented explosion (natural gas-air in 1 m^3 cubic chamber, A_v = 0.2 m^2, P_v = 3.5 kPa, w = 3 kg/m^2) (Harris et al. 1985).

From data given in Table 7.2, it is apparent that vented explosions generate pressure loadings which produce a structural response equivalent to category 1, ie. t_d >> T_n. Thus, in terms of structural response, vented explosions may be considered (to a first approximation) as producing roughly the same effects as a static loading whose magnitude is equal to the peak overpressure P_{red}.

In contrast, the loading imposed by a blast wave from a detonation will, in general, fall into category 2, ie. t_d << T_n. The loading experienced will be equal to a static loading lower than the peak overpressure of the blast wave acting on the structure. This means that much of the experimental data available which relates to the failure pressure of structures, and which has been obtained under blast wave loading conditions, is not directly applicable to the case of a vented explosion.

The factor which determines whether or not failure of any structural element occurs as a result of an imposed loading is the displacement y of the element. For failure to occur maximum displacement y_{max} must not exceed y_{fail}. Knowledge of the resistance/displacement function R(y) is therefore very important.

For some structural elements R(y) can be calculated. In other cases R(y) can be obtained as an empirical relation between an applied static lateral load and the deflection produced. An example of such a static load/deflection curve for a brick wall is shown in Fig. 7.17.

114
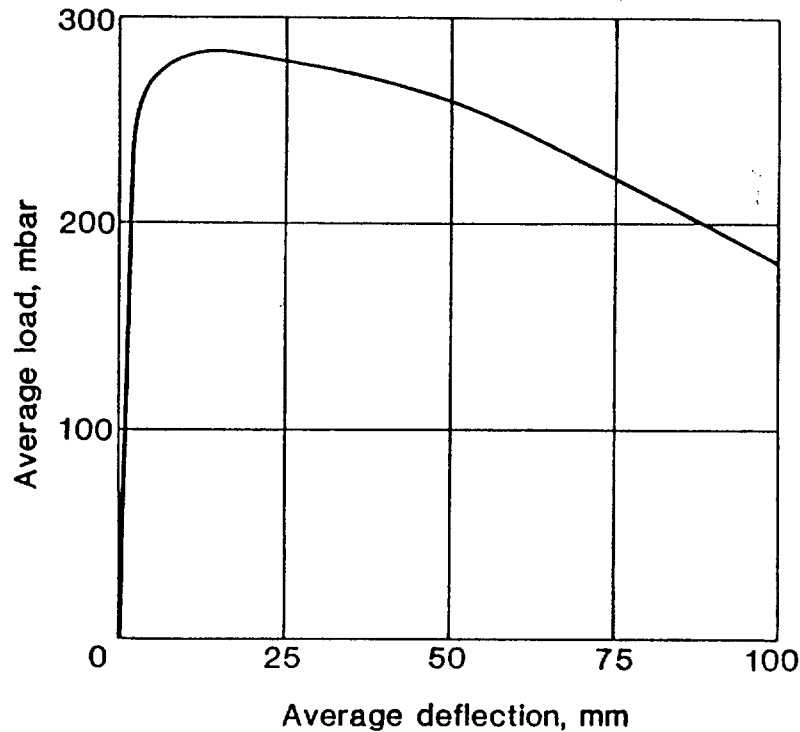
Figure 7.17. Example of a static load/deflection curve for a 114 mm thick brick wall of area 6.5 m² (Harris et al. 1985).

Different structural elements will obviously be able to withstand different amounts of displacement y before they fail. Ideally, in terms of pressure loading it would be desirable for construction materials to withstand large displacements, ie. have large ductility ratios.

Ductile materials, such as constructional steelwork, generally show high ductility ratios without fracture. In these cases plastic deformation which represents permanent damage, does not always mean total destruction. Brittle materials such as glass and brickwork show fracture and total failure at low ductility ratios.

Typical failure pressures of some structural building elements under vented explosion conditions are given in Table 7.3. For each component, a range of pressures is quoted since values will be dependent upon variation in construction and size (Harris et al. 1985).

Table 7.3. Failure pressures of structural building elements.

structural element	failure pressure (kPa)
room doors	2 - 3
light partition walls	2 - 5
glass windows	2 - 7
50 mm thick breeze block walls	4 - 5
unrestrained brick walls	7 - 15

For structural building elements such as walls, doors and windows the pressure loading is caused by the pressure difference across the element. Usually this is equal to the internal overpressure. This is not valid for small objects in the room or outside of an explosion relief vent. The explosion loading for such objects is caused by drag force F_D [N]

$$F_D = C_D A \frac{\rho u^2}{2}$$
(50)

where

C_D is the drag coefficient of the object
A   is the projected area of the object normal to the flow direction [m²]
ρ is the density of the flowing gas [kg/m³]
u   is the flow velocity [m/s].

Values of the drag coefficient C_D are given in standard reference works of hydrodynamics. Eg. for a long straight cylinder perpendicular to the direction of a flow with constant u, C_D is 1.20 (CPR 1989). For non-stationary loads from gas explosions, there are still uncertainties with regard to estimating drag load. The drag coefficient will probably be dependent on several factors such as turbulence levels, time, pressure rise time etc.

Fig. 7.18 shows some preliminary results of the drag load on a 168 mm diameter pipe placed in the exit of the wedge-shaped explosion vessel of Fig. 5.11 (Bjerketvedt et al. 1993).
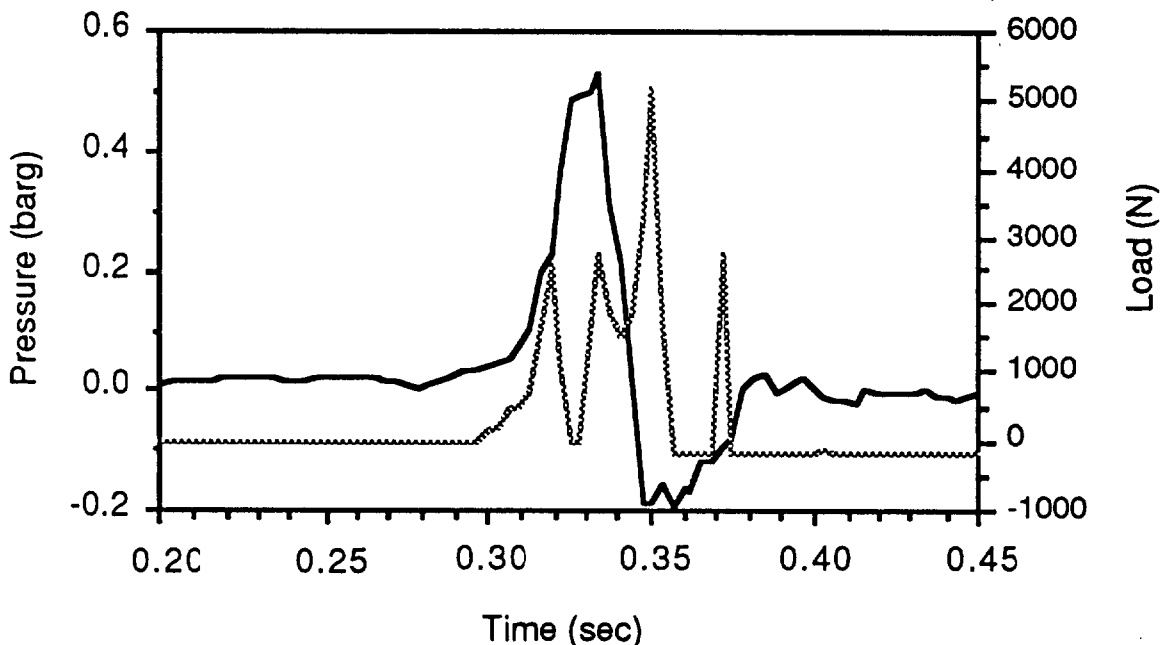

Figure 7.18. Experimental results of the drag load of a pipe. Solid line = overpressure (bar), dotted line = load (N) (Bjerketvedt et al. 1993).

7.5 EXPLOSION MITIGATION

Suppression of confined explosion in vessels by triggered extinguishers is an established technique developed in the 1950's. Although originally designed to protect from gas explosions, the technique is mainly used in plants handling combustible dusts. A triggered extinguisher consists of three components: the explosion detector, the power and control unit, and the suppressors.

In most cases, a membrane pressure detector is used to detect the rise of the internal pressure. The detection pressure is determined by the strength of the vessel and ranges 3.5 - 50 kPa. The detector responds in a very short time - of the order of 1 ms - to a rise of pressure providing a signal to the power and control unit. Optical detectors can be used to detect gas explosions.

The suppressors are cylinders containing a suppressant under a nitrogen pressure of at least 20 bar. The cylinders are equipped with pyrotechnic valves which is opened by the power and control unit. The suppressant is distributed into the vessel by means of a spraying system. Water, halogenated hydrocarbons and dry powders are used as suppressants (Pineau & Ronchail 1984).

The technique of explosion suppression can be applied to closed vessels, only. For vented gas explosions in congested rooms, the use of water spray systems has been investigated in the 1990's. This method seems a promising way to reduce explosion loads on offshore platforms where the other methods (rearrangement of equipment, increasing the size and possibly redistributing of the vent opening) involve high or even prohibitive costs.

Experiments have shown that the application of water spray may have a mitigating effect on explosion propagation. However, it may also increase the explosion overpressure. The mitigation effect is a result of evaporation of water droplets in the flame front. It has been established that the main reason for increased explosion overpressures is turbulence generation in the gas mixture by water sprays (van Wingerden & Wilkins 1995a).

Normal fire-protection water-spray systems generate droplets with a median diameter of 200 - 700 μm. However, to be able to evaporate, the droplets must be much smaller. Laboratory-scale tests show that droplets of the order 10 μm of diameter have the same ability to inert methane-air mixtures as water vapour. This indicates that the droplets are sufficiently small to evaporate completely in the flame front.

The same experiments show that the water vapour concentration of 31.5 % (234 g/m^3) is required to obtain a full quenching for a stoichiometric methane-air mixture. This concentration is of the same order of magnitude as the water volume fraction which can be produced by commercially available fire-protection nozzles (van Wingerden & Wilkins 1995b).

Droplet break-up is possible if the droplet is exposed to strong hydrodynamic forces due to strong flows around the droplet. Such flows are possible if an explosion occurs

in a highly congested area resulting in strong flame accelerations and hence a strongly accelerating flow field ahead of the flame front. In the absence of strong flame accelerations, water sprays will not mitigate the explosion. Due to the turbulence generated by the water sprays, the explosions are in fact made stronger (van Wingerden & Wilkins 1995a).

A theoretical analysis combined with a thorough analysis of experiments performed in the 1:5 scale compressor module (Fig. 6.15) shows that the most effective mitigation is accomplished with either very small ($<$ 10 μm) or large ($>$ 200 μm) droplets. Very small droplets will evaporate in the flame front directly. Nozzles generating droplets of diameters ranging 20 - 200 μm are the least effective. Droplets of this size will easily adapt to flow accelerations and, as a result, will not be exposed to strong hydrodynamic forces causing them to break up. Large droplets will not easily adapt to flow speed variations and break up more easily (van Wingerden & Wilkins 1995b).

Catlin et al. (1993) performed tests in a 180 m^3 (4.5 m x 4.5 m x 9 m) test chamber filled with stoichiometric methane-air mixture. The vent opening was located at one end. The vent coefficient K defined by Eq. (20) was either 9 or 1. Five base tests were performed without sprays and with different numbers (0 - 80) of 0.18 m horizontal pipes as obstacles. Two types of commercial fire deluge nozzles were used with three nozzle supply pressures and two nozzle separation distances.

With the small vent (K = 9) and no obstacles, the effect of the water sprays was to increase the internal peak pressure by a factor of 5. With 20 pipes the factor was 1.3 and with 40 pipes 1.2. With the large vent (K = 1) and 56 pipes, the internal peak pressure was decreased by the factor 0.8. With 80 pipes, the factor was 0.65. For both vent sizes, the external peak pressure was decreased on the average by the factor 0.55.

Catlin et al. (1993) conclude that with the small vent the turbulence generated by the sprays caused the observed higher internal peak pressure. Theoretical analysis suggests that the flame accelerations were generally insufficient to cause droplet break-up. Some break-up, however, may have occurred as the gas accelerated through the vent. In these conditions, the spray had a small limiting effect of the internal peak pressure, possible caused by the suppression of combustion occurring near the vent.

With the large vent, the use of water sprays significantly reduced both the internal and external overpressures. In this case, the theoretical analysis suggests that the droplet break-up occurred in all cases when a mitigative effect was observed as a result of the high flame acceleration. The implication is that a mitigative effect will only occur if the flame accelerations are sufficiently high (Catlin et al. 1993). Water spray systems must be activated early enough ie. already after a combustible gas detector has detected a gas leak.

8 SUMMARY AND CONCLUSIONS

A flammable mixture may be formed in a room as a consequence of a gas or liquid leak. A light gas will form an almost homogenous layer between the leak position and the ceiling. A dense gas or vapour will form a similar layer between the leak position and the floor.

The concentration in the layer will increase until it reaches a steady state value determined by the gas flow rate or liquid evaporation rate and the ventilation rate of the room. The steady state concentration is independent of the volume of the room. However, the latter affects the time required to reach the steady state concentration.

When a gas cloud consisting of stoichiometric mixture burns outdoors the volume increases during the combustion (flash fire) by the expansion factor whose value is close to 8. When a similar mixture fills a closed pressure vessel the absolute pressure in the vessel increases during the combustion (confined explosion) by a factor that is somewhat larger than the expansion factor.

The maximum overpressure generated in closed explosion vessels has little relevance to vented explosions in rooms. Windows, doors and walls fail already at pressures that are about 1 % of this overpressure. The maximum overpressure in rooms is thus determined primarily by the sizes and opening pressures of the vents. It has been known for decades that to relieve the explosion overpressure effectively, the vents must have a sufficient total area and as low an opening pressure as possible.

The vent opening pressure has a lower limit due to the requirement that the explosion relief panels or doors must not be opened by high winds. However, it cannot be usually assumed that the maximum pressure of a vented explosion will be approximately the opening pressure of the vents. The maximum pressure will be higher, but it must be limited to prevent the damage of the walls and other load-bearing structures.

Tests aimed at dimensioning the explosion vents correctly have been performed for decades, already. The test chambers were room-sized or smaller and the peak internal pressure was measured. Usually these correlations (called venting guidelines) are used to select the vent parameters starting from the parameters determined by the fuel and building, respectively.

The devastating vapour cloud explosions in Flixborough, UK in 1974 and Beek, the Netherlands in 1975 emphasized the need to understand how a blast wave is generated in a vapour cloud explosion, and to be able to predict the parameters of the blast wave. Experimental research leading to the unravelling of the mystery of the blast generation in vapour cloud explosions was performed in the early 1980's. The conclusion was that vapour cloud explosions were not "unconfined" but partially confined, and the additional factor needed to create a blast wave was repeated turbulence generating obstacles or jet ignition.

Another factor triggering research into gas explosions was the discovery of large gas and oil fields in the North Sea and the subsequent exploitation of the fields. Extensive research programs were started in Norway and in UK around 1980.

The research of British Gas produced a significant contribution to the understanding of vented gas explosions in empty rooms. It was shown in 1986 that the internal pressure as function of time can be described in terms of four distinct pressure peaks which can (but do not have to) occur (the four peak model). Each peak is produced by different physical processes at successive stages during a vented explosion.

The four peaks are:

P_1 which is associated with the pressure drop following the removal of the explosion relief vent and subsequent venting of unburned gas.

P_2 which is associated either with the pressure drop following venting of burned gas, or corresponds to the pressure pulse caused by a possible external explosion due to ignition of previously vented unburned gas by the flame emerging from the vent.

P_3 a long duration but generally small amplitude peak associated with the maximum rate of combustion within the room (this typically occurs when the flame front reaches the walls).

P_4 which is an oscillatory pressure peak attributed to excitation of acoustic resonances in the gaseous combustion products within the room. The resulting high combustion rate may cause a significant net overpressure to be developed in the room.

The results of earlier explosion tests had to be reassessed in the light of the four peak model. The critical review by British Gas recommended the use of the following venting guidelines:

-       The Cubbage and Simmonds formulas predicting P_1 and P_2. The formulas are applicable to situations in which the opening pressure of the vent is no larger than about 2 kPa.
-       The Cubbage and Marshall formula predicting P_1. The formula is applicable to situations in which the opening pressure of the vent is larger than about 2 kPa.

The third pressure peak only becomes of significant magnitude
-       with very small explosion vents and/or
-       in non-cubical, duct-like rooms or
-       under turbulent conditions.

The fourth pressure peak may be the largest one in a near-cubic empty room with a relatively small explosion vent. If necessary, this peak can be eliminated by lining the walls with a suitable sound absorbing material.

For vessels, British Gas recommended the Bartknecht method predicting peak overpressure. The method is applicable to situations in which the opening pressure of the vent is larger than 10 kPa. Due to the relatively high opening pressures, the method

is not applicable to normal buildings.

Two effects can be identified by the which the presence of obstacles could lead to an increase in flame speed. Firstly, the flame front is distorted as it flows around the obstacles leading to an increase in the flame area. Secondly, turbulence is generated in the unburned mixture as it flows over and around any obstacle.

When the flame front reaches the turbulent area (wake) behind the obstacles it is accelerated. The precise effect causing this depends on the intensity and scale of turbulence produced. The combined effect of flame folding and turbulence can cause a drastic increase of flame area and, consequently, flame speed.

The effect of repeated obstacles on flame speed is caused by the following positive feedback loop. Combustion of the unburned mixture is followed by expansion of the combustion products and increase of pressure. Assuming that the geometry is such that the combustion products are trapped behind the frame front, a flow of unburned mixture is created. The flow interacts with obstacles generating a turbulent flow field.

When the flame front propagates into the turbulent flow field the burning rate is increased significantly. This increased burning rate will further increase the flow velocity and turbulence at new obstructions ahead of the flame. This mechanism of flame acceleration due to repeated obstacles may result in very high overpressures (over 1 bar) within relatively short distances of flame propagation (less than 1 m).

The flame acceleration by repeated obstacles can to some extent be avoided by venting the hot combustion products at an early stage of the explosion. This can be achieved by using several suitably placed vents. Thanks to the vents, the hot combustion products will not be trapped behind the unburned gas. The flow velocity of unburned mixture and the resulting turbulence will be reduced. Early venting of hot combustion products is a very effective way of minimising the flame acceleration by repeated obstacles.

The effect of flow turbulence on flame speed has been included in the venting guidelines by a number of authors who recommend a "turbulence factor". Unfortunately, gas explosion tests performed in congested volumes over the last ten years do not support the concept of a turbulence factor.

Different empirical, numerical and experimental methods have been developed to predict the explosion overpressure in congested volumes. However, the empirical methods are limited to obstacle and venting arrangements similar to those used in the experiments. The numerical methods can be used over a wide range of conditions and geometrical arrangements, but require considerable expertise. They are used to design equipment layout in a way to minimize explosion overpressures.

The most reliable predictions can be had from explosion tests with scale models. However, explosion tests are feasible only for organizations with extensive research and development capabilities.

In 1987, it was shown that the blast wave from a vented gas explosion is caused by the external explosion. The strength of the external explosion is dependent on the amount of the unburned mixture released through the vent. The external explosion is particularly strong when the mixture is ignited near the rear wall of the chamber.

The external explosion of a vented dust explosion has been studied in the 1990's. The maximum pressure of the external explosion is generated at the blast centre and it can be related to the vent area, vessel volume and internal peak pressure by an empirical equation. The internal peak pressure is predicted by a venting guideline. The peak pressure of the blast wave decays inversely proportional to distance.

No such equation has been derived for gas explosions. In this report, the empirical equation for the ratio of the internal and external peak pressures in dust explosions is shown to give satisfactory predictions for gas explosion tests in 30 m^3 and 550 m^3 chambers. However, using a venting guideline for P_2, it not easy to predict the internal peak pressure for chambers with explosion relief vents opening at a low overpressure as in these tests.

Explosion relief panels or doors should have a sufficient total area, an opening pressure as low as practicable (say 1 kPa) and low inertia. The panels should be made of ductile materials to prevent the formation of flying fragments. Static loading sometimes used to "calibrate" the fasteners is likely to underestimate the opening pressure. The suitability of a fastener can only truly be judged through observation of its performance under test explosion conditions.

After the mechanism of flame acceleration was understood, it was possible to present guidelines for equipment layout and vent location to reduce the explosion overpressures. The guidelines cannot guarantee low explosion overpressures but will increase the likelihood of obtaining acceptable pressure loads.

The shape of the room and the location of the vent areas are closely linked and will therefore depend on each other. There are two main principles to apply when optimizing the shape of a room and location of vent areas:

1.   An ignition point anywhere in the room should be as close as possible to the major vent areas, so hot combustion products can be vented out at an early phase of the explosion.
2.   Strong turbulence in the unburned mixture ahead of the flame front and long flame front travel distances should be avoided.

The main principles of the guidance in positioning obstacles (process equipment, pipework etc.) in the room are

1.   minimize turbulence generation
2.   do not block explosion venting.

Load-bearing walls should be dimensioned to withstand the static load corresponding the predicted internal peak pressure. This is not valid for small objects in the room or

122

outside of an explosion relief vent. The explosion loading for such objects is caused by drag force.

Suppression of confined explosion in vessels by triggered extinguishers is an established technique developed in the 1950's. The technique of explosion suppression can be applied to closed vessels, only. For vented gas explosions in congested rooms, the use of water spray systems has been investigated in the 1990's.

Experiments have shown that the application of water spray may have a mitigating effect on explosion propagation. However, it may also increase the explosion overpressure. It has been established that the main reason for increased explosion overpressures is turbulence generation in the gas mixture by water sprays.

ACKNOWLEDGEMENT

REFERENCES

AIChE 1994. Guidelines for evaluating the characteristics of vapor cloud explosions, flash fires and BLEVEs. New York: American Institute of Chemical Engineers. 387 p. ISBN 0-9169-0474-X.

Bartknecht, W. 1981. Explosions, course, prevention, protection. Heidelberg: Springer-Verlag. 251 p. ISBN 3-540-10216-7.

Bartknecht, W. 1993. Explosionsschutz: Grundlagen and Anwendung. Berlin: Springer-Verlag. 891 p. ISBN 3-540-55464-5. (Referred to by Siwek (1996)).

van den Berg, A. C. 1985. The multi-energy method. A framework for vapour cloud explosion blast prediction. Journal of Hazardous Materials, vol. 12, p. 1 - 10.

Bimson, S. J. et al. 1993. An experimental study of the physics of gaseous deflagration in a very large vented enclosure. 14th International Colloquium on the Dynamics of Explosions and Reactive Systems, Coimbra, 1 - 6 Aug. 1993. 23 p.

Bjerketvedt, D., Bakke, J. R. & van Wingerden, K. 1993. Gas explosion handbook. Version 1.2. Bergen: Christian Michelsen Research. 225 p. (Report CMR-93-A25034).

Bradley, D. & Mitcheson, A. 1978a. The venting of gaseous explosions in spherical vessels. I - theory. Combustion and Flame, vol. 32, p. 221 - 236.

Bradley, D. & Mitcheson, A. 1978b. The venting of gaseous explosions in spherical vessels. II - theory and experiment. Combustion and Flame, vol. 32, p. 237 - 255.

British Gas 1990. Review of the applicability of predictive methods to gas explosions in offshore modules. London: Department of Energy. 175 p. (Offshore Technology Report OTH 89 312). ISBN 0-11-413314-X.

British Gas 1992. Explosions in highly congested volumes. London: Health and Safety Executive. 40 p. + app. 20 p. (Offshore Technology Information OTI 92 593). ISBN 0-11-882062-1.

Buckland, I. G. 1980. Explosions of gas layers in a room sized chamber. In: 7th International Symposium on Chemical Process Hazards with Special Reference to Plant Design. Rugby: The Institution of Chemical Engineers, Symposium Series 58. P. 289 - 304.

Catlin, C. A., Gregory, C. A. J., Johnson, D. M. & Walker, D. G. 1993. Explosion mitigation in offshore modules by general area deluge. Transactions of the Institution of Chemical Engineers, vol. 71, Part B, p. 101 - 111.

Cleaver, R.P., Humphreys, C. E. & Robinson, C. G. 1994. Accidental generation of gas clouds on offshore process installations. Journal of Loss Prevention in the Process Industries, vol. 7, no. 4, p. 273 - 280.

Cooper, M. G., Fairweather, M. & Tite, J. P. 1986. On the mechanisms of pressure generation in vented explosions. Combustion and Flame, vol. 65, no. 1, p. 1 - 14.

CPR 1989. The consequences of explosion effects on structures. Chapter 2. In: Methods for the determination of possible damage to people and objects resulting from releases of hazardous materials. Voorburg: Committee for the Prevention of Disasters, CPR 16E. 76 p.

Crowhurst, D., Colwell, S. A. & Hoare, D. P. 1995. The external explosion characteristics of vented dust explosions. In: Second 1995 Symposium on Major Hazards Onshore and Offshore. Rugby: The Institution of Chemical Engineers, Symposium Series 139. P. 79 - 96.

Cubbage, P. A. & Simmonds, W. A. 1955. An investigation of explosion reliefs for industrial drying ovens. I. Top reliefs in box ovens. Transactions of the Institute of Gas Engineers, vol. 105, p. 470 - 526.

Cubbage, P. A. & Simmonds, W. A. 1957. An investigation of explosion reliefs for industrial drying ovens. II. Back reliefs in box ovens, reliefs in conveyer ovens. Transactions of the Institute of Gas Engineers, vol. 107, p. 503 - 554.

Dainty, E. E., Hamel, D., Lobay, G, Olson, R. & Vincent, W. 1990. Performance testing of explosion relief panels manufactured by C/S Construction Specialties Limited. Ottawa: Canada Centre for Mineral and Energy Technology, Mining Research Laboratories. 13 p. + app. 28 p. (Divisional report MRL 90-20).

Decker, D. A. 1971. Explosion venting guide. Fire Technology, Vol. 7, p. 219 -. (Referred to by British Gas (1990)).

Dragosavić, M. 1973. Structural measures against natural-gas explosions in high-rise blocks of flats. Heron, vol. 19, no. 4, p. 1 - 51.

Gardner, D. J. & Hulme, G. 1995. A survey of current predictive methods for explosion hazard assessments in the UK offshore industry. London: Health and Safety Executive. 60 p. (Offshore Technology Report OTH 94 449). ISBN 0-7176-0969-3.

Haaverstad, T. A. 1992. Development and design of blast relief panels. In: 7th International Symposium on Loss Prevention and Safety Promotion in the Process Industries. Taormina, 4 - 8 May 1992. Rome. Italian Association of Chemical Engineering. Vol. 4. P. 117-1 - 117-12.

Harris, R. J. 1983. The investigation and control of gas explosions in buildings and heating plant. London: E & FN Spon. 194 p. ISBN 0-419-13220-1.

Harris, R. J., Marshall, M. R. & Moppet, D. J. 1977. The response of glass windows to explosion pressures. Institution of Chemical Engineers, Symposium Series 49. P. 83 - 97.

Harris, R. J., Wickens, M. J. & Johnson, D. M. 1985. The effect of explosion pressures on structures and structural components. In: A Practical Introduction to Gas and Dust Explosions, A Two Day European Seminar, Frankfurt, 3 - 4 June 1985. Hove: European Information Centre for Explosion Protection. Part 1. 15 p. + app. 7 p.

Harris, R. J. & Wickens, M. J. 1989. Understanding vapour cloud explosions - an experimental study. London: The Institution of Gas Engineers. 28 p. (Communication 1408).

Harrison, A. J. & Eyre, J. A. 1987. "External explosions" as a results of explosion venting. Combustion Science and Technology, vol. 52, p. 91 - 106.

Hjertager, B. H. 1991. Explosions in offshore modules. In: New Directions in Process Safety: Hazards XI. Rugby: The Institution of Chemical Engineers, Symposium Series 124. P. 19 - 35.

Hjertager, B. H., Fuhre, K. & Bjørkhaug, M. 1988. Gas explosion experiments in 1:33 and 1:5 scale offshore separator and compressor modules using stoichiometric homogeneous fuel/air clouds. Journal of Loss Prevention in the Process Industries, vol 1, October, p. 197 - 205.

Hjertager, B. H., Solberg, T. & Nymoen, K. O. 1992. Computer modelling of gas explosions in offshore modules. Journal of Loss Prevention in the Process Industries, vol. 5, no. 3, p. 165 - 174.

Howard, W. B. & Karabinis, A. H. 1980. Tests of explosion venting of buildings. In: 3rd International Symposium on Loss Prevention and Safety Promotion in the Process Industries. Basle, 15 - 19 Sept. 1980. Basle: Swiss Society of Chemical Industries. Vol. 3. P. 979 - 1019.

Lunn, G. 1985. Venting gas and dust explosions - a review. Rugby: The Institution of Chemical Engineers. 144 p. ISBN 0-85295-179-5.

Mahoney, D. G. 1991. Introduction to large property damage losses in the hydrocarbon-chemical industries: a thirty year review. Loss Prevention Bulletin, no. 99, June, p. 1 - 25.

Marshall, M. R. 1983. The effect of ventilation on the accumulation and dispersal of hazardous gases. 4th International Symposium on Loss Prevention and Safety Promotion in the Process Industries. Harrogate, 12 - 16 Sept. 1983. Rugby: The Institution of Chemical Engineers. Vol. 3. P. E11 - E22.

Marshall, M. R. & Stewart-Darling, F. L. 1986. Buoyancy-driven natural ventilation of enclosed spaces. In: Hazards in the Process Industries: Hazards IX. Manchester, 2 - 4 April 1986. Rugby: Institution of Chemical Engineers, Symposium Series 97. P. 7 - 18.

Mecklenburgh, J. C. 1986. Hazard zone sizes within buildings. In: 5th International Symposium "Loss Prevention and Safety Promotion in the Process Industries". Cannes, 12 - 16 Sept. 1986. Paris: Société de Chimie Industrielle. Vol. 2. P. 52-1 - 52-15.

Mercx, W. P. M. 1992. Large-scale experimental investigation into vapour cloud explosions. Comparison with the small scale DISCOE-trials. In: 7th International Symposium on Loss Prevention and Safety Promotion in the Process Industries. Taormina, 4 - 8 May 1992. Volume I. Rome: SRP Partners. P. 35-1 - 35-20.

Mercx, W. P. M. 1995, Modelling and experimental research into gas explosions. In: 8th International Symposium "Loss Prevention and Safety Promotion in the Process Industries". Antwerp, 6 - 9 June 1995. Volume I. Amsterdam: Elsevier. P. 333 - 347.

NFPA 68. Guide for venting of deflagrations. 1994 edition. Quincy, Mass: National Fire Protection Association, 1994. 58 p.

Pappas, J. A. 1984. Venting of large-scale volumes. In: The control and prevention of gas explosions. London, 1 Dec. 1983. London: Oyez Scientific and Technical Services Ltd. P. 157 - 181. ISBN 0-907822-38-X.

Palmer, K. N. & Tonkin, P. S. 1980. External pressures caused by venting gas explosion in a large chamber. In: 3rd International Symposium on Loss Prevention and Safety Promotion in the Process Industries. Basle, 15 - 19 Sept. 1980. Basle: Swiss Society of Chemical Industries. Vol. 3. P. 1274 - 1294.

Pineau, J. & Ronchail, G. 1984. Suppression of gas explosions. In: The control and prevention of gas explosions. London, 1 Dec 1983. London: Oyez Scientific and Technical Services Ltd. P. 205 - 240. ISBN 0-907822-38-X.

Rasbash, D. J. 1969. The relief of gas and vapour explosions in domestic structures. Fire Research Note, no. 759. (Referred to by British Gas (1990)).

Rasbash, D. J., Drysdale, D. D. & Kemp. N. 1976. Design of an explosion relief for a building handling liquefied fuel gas. In: Symposium on Process Industry Hazards. Rugby: The Institution of Chemical Engineers, Symposium Series 47. P. 145 - 156. (Referred to by British Gas (1990)).

Rasbash, D. J. & Rogowski, Z. W. 1960. Relief of explosions in duct systems. In: Symposium on Chemical Process Hazards. Rugby: The Institution of Chemical Engineers. (Referred to by British Gas (1990)).

Rasbash, D. J. & Rogowski, Z. W. 1963. Relief of explosions in propane-air mixtures moving in straight unobstructed ducts. In: 2nd Symposium on Chemical Process Hazards. Rugby: The Institution of Chemical Engineers. (Referred to by British Gas (1990)).

RT 38-10316. Lasilevyt, paksuuden mitoitus. (Glass sheets, dimensioning of thickness). Helsinki: Rakennustietosäätiö, 1986. 5 p. [In Finnish]

Runes, E. 1972. Explosion venting. Loss Prevention, vol. 6, p. 63 - 67. (Referred to by British Gas (1990)).

Siwek, R. 1996. Explosion venting technology. Journal of Loss Prevention in the Process Industries, vol. 9, no. 1, p. 81 - 90.

Solberg, D. M., Skramstad, E., & Pappas, J. A. 1979. Experimental investigation on partly confined gas explosions. Analysis of pressure loads, part I. Høvik: Det norske Veritas. 75 p. (Veritas report 79-0483).

Solberg, D. M., Pappas, J. A. & Skramstad, E. 1981. Observations of flame instabilities in large scale vented explosions. In: 18th Symposion (International) on Combustion. Pittsburg: The Combustion Institute. P. 1607 - 1614.

Tite, J. P., Binding, T. M. & Marshall, M. R. 1991. Explosion relief for long vessels. Br. Gas Res. Technol. (MRS E 634), p. 75 - 86.

West, H. W. H. 1973. A note on the resistance of glass windows to pressures generated by gaseous explosions. Proceedings of the British Ceramic Society, vol. 21, p. 213 -. (Referred to by Harris (1983)).

van Wingerden, C. J. M. 1989. Experimental investigation into the strenght of blast waves generated by vapour cloud explosions in congested areas. In: 6th International Symposium "Loss Prevention and Safety Promotion in the Process Industries". Oslo, 19 - 22 June 1989. Oslo: Norwegian Society of Chartered Engineers. Volume I. P. 26-1 - 26-16.

van Wingerden, K. 1993. Prediction of pressure and flame effects in the direct surroundings of installations protected by dust explosion venting. Journal of Loss Prevention in the Process Industries. Vol. 6, no. 4, p. 241 - 249.

van Wingerden, K. 1994. Course and strength of accidental explosions on offshore installations. Journal of Loss Prevention in the Process Industries. Vol. 7, no. 4, p. 295 - 304.

van Wingerden, K. 1995. Gas explosions in vented enclosures and in the open: mechanisms, prediction methods and mitigation. Bergen: University of Bergen. Dr. Philos. thesis. 48 p. + app. 200 p.

van Wingerden, K. & Wilkins, B. 1995a. The influence of water sprays on gas explosions. Part 1: water-spray-generated turbulence. Journal of Loss Prevention in the Process Industries. Vol. 8, no. 2, p. 53 - 59.

van Wingerden, K. & Wilkins, B. 1995b. The influence of water sprays on gas explosions. Part 2: mitigation. Journal of Loss Prevention in the Process Industries. Vol. 8, no. 2, p. 61 - 70.

van Wingerden, C. J. M. & Zeeuwen, J. P. 1983. Venting of gas explosions in large rooms. 4th International Symposium on Loss Prevention and Safety Promotion in the Process Industries. Harrogate, 12 - 16 Sept. 1983. Rugby: The Institution of Chemical Engineers. Vol. 3. P. F38 - F47.

van Wingerden, C. J. M. & Zeeuwen, J. P. 1986. Investigation of the explosion-enhancing properties of a pipe-rack-like obstacle array. Progress in Astronautics and Aeronautics, vol. 106, p. 53 - 65.

Wirkner-Bott, I., Schumann, S. & Stock, M. 1992. Dust explosion venting: investigation of the secondary explosion. In: 7th International Symposium on Loss Prevention and Safety Promotion in the Process Industries. Taormina, 4 - 8 May 1992. Rome: SRP Partners. Volume I. P. 58-1 - 58-20.

Zalosh, R. G. 1980. Gas explosion tests in room-sized vented enclosures. Loss Prevention, vol. 13, p. 98 - 110.

Zeeuwen, J. P. & van Wingerden, C. J. M. 1985. Pressure loading on control rooms resulting form gas explosions. 10. Internationales Kolloquium für die Verhütung von Arbeitsunfällen und Berufskrankheiten in der chemischen Industrie. Frankfurt am Main, 10 - 12 Juni 1985. 17 p.